

NEW GC SEPARATION APPROACHES AND ANALYSIS OF ANTIOXIDANTS FROM
ROSEMARY (*Rosmarinus Officinalis L.*) AND THEIR STABILITIES BY HPLC

by

YING ZHANG

Presented to the Faculty of the Graduate School of
The University of Texas at Arlington in Partial Fulfillment
of the Requirements
for the Degree of

DOCTOR OF PHILOSOPHY

THE UNIVERSITY OF TEXAS AT ARLINGTON

December 2011

Copyright © by Ying Zhang 2011

All Rights Reserved

This dissertation is dedicated to my dearest mother, Xiaoliu Yang, father, Guofeng Zhang and sister, Yan Zhang, who always accompany me, support me and believe in me in the long journey of pursuing happiness.

It is also dedicated to my husband, Yu Xiang, who let me understand the world better and know more about myself.

ACKNOWLEDGEMENTS

My first and deepest acknowledgement must go to my supervisor, Dr. Daniel W. Armstrong, who has been not only an erudite mentor in my research but also an inspiring teacher in so many aspects of my life. Without his guidance and persistent help this dissertation would not have been possible.

I would like to thank my committee members, Dr. Zoltan A. Schelly and Dr. Richard Guan. I am greatly honored to have them serve on my committee. I appreciate their precious time and research advice.

I would like to express my gratitude to the Department of Chemistry and Biochemistry for the financial aid and kind help. Also I thank the chemistry staff, especially Barbara for taking care of all my ordering and paperworks throughout the years, Debbie for dealing with all of my offer letters and financial problems, Jame and Jill for providing sufficient supplies for my research.

Also, I would like to thank all my friends and coworkers at UTA. I thank my best friend, Hien, who always give me a hand without hesitate when I need help since the first time we met in 2006. I thank the senior students, Ping, Chunlei, Koko, Violet, Xiaotong, Tharanga, Eranda, Yasith, Dilani and Zach for their guidance and advice in research. I thank Sirantha, Edra, Jonathan, Eva, Qing, Nilusha, Jason, Ross and Choyce for all the support in my projects.

At last, I thank my dear husband who always keeps me be aware of my situation and help me make important decisions. Also He is the one letting me understand who I am and what a family means to me.

November 10, 2011

ABSTRACT

NEW GC SEPARATION APPROACHES AND ANALYSIS OF ANTIOXIDANTS FROM ROSEMARY (*Rosmarinus Officinalis L.*) AND THEIR STABILITIES BY HPLC

Ying Zhang, PhD

The University of Texas at Arlington, 2011

Supervising Professor: Daniel W. Armstrong

Enantiomeric separations are of great interest in the pharmaceutical, biotechnology and agrochemical industries due to the different therapeutic effects of enantiomers. Because of the high efficiency, sensitivity and simplicity, chiral gas chromatography has been widely applied to separate enantiomers that are volatile and thermally stable. In this dissertation, a group of novel chiral selectors based on cyclofructans for gas chromatography is developed and their enantioselective properties are evaluated.

Room temperature ionic liquids (ILs) have been used as gas chromatographic stationary phase due to their unique physical properties in achiral separations. A series of trigonal tricationic ILs are synthesized, characterized and used as achiral gas chromatographic stationary phases. A rapid, efficient quantification method for water in solvents or solvents in water was developed using IL columns.

High performance liquid chromatography is another prevalently used technique for separations. In this dissertation, methods are developed to separate and identify antioxidants from rosemary. The stabilities of these antioxidants are investigated.

TABLE OF CONTENTS

ACKNOWLEDGEMENTS	iv
ABSTRACT	v
LIST OF ILLUSTRATIONS.....	viii
LIST OF TABLES	xi
Chapter	Page
PART ONE: ENANTIOSELECTIVE GAS CHROMATOGRAPHIC STATIONARY PHASES	
1. INTRODUCTION	2
1.1 Development of Cyclodextrin-based Chiral Stationary Phases	2
1.2 Mechanisms	7
1.3 Applications	14
1.4 Summary.....	18
1.5 Dissertation Organization.....	19
2. PERMETHYLATED CYCLOFRUCTAN CHIRAL SELECTORS.....	20
2.1 Introduction	20
2.2 Experimental	22
2.3 Results and Discussion.....	24
2.4 Conclusions.....	34
3. 4,6-DI-O-PHENYL-3-O-TRIFLUOROACETYL/PROPIONYL CYCLOFRUCTAN CHIRAL SELECTORS.....	36
3.1 Introduction	36
3.2 Experimental	38
3.3 Results and Discussion.....	40
3.4 Conclusions.....	55

PART TWO: IONIC LIQUID BASED GAS CHROMATOGRAPHIC STATIONARY PHASES

4. OVERVIEW OF IONIC LIQUIDS IN GC SEPARATIONS.....	57
5. TRIGONAL TRICATIONIC IONIC LIQUID STATIONARY PHASES.....	61
5.1 Introduction	63
5.2 Experimental	66
5.3 Results and Discussion.....	69
5.4 Conclusions.....	86
6. RAPID, EFFICIENT QUANTIFICATION OF WATER IN SOLVENTS AND SOLVENTS IN WATER USING AN IONIC LIQUID-BASED GC COLUMN.....	88
6.1 Introduction	89
6.2 Experimental	92
6.3 Results and Discussion.....	94
6.4 Conclusions.....	104

PART THREE: ANALYSIS OF ANTIOXIDANTS FROM ROSEMARY BY HPLC

7. DEGRADATION STUDY ON CARNOSIC ACID, CARNOSOL, ROSMARINIC ACID AND ROSEMARY EXTRACT.....	105
7.1 Introduction	105
7.2 Experimental	108
7.3 Results and Discussion.....	110
7.4 Conclusions.....	127
8. GENERAL CONCLUSIONS.....	128

APPENDIX

A. PUBLICATION INFORMATION.....	131
---------------------------------	-----

REFERENCES.....	133
-----------------	-----

BIOGRAPHICAL INFORMATION	149
--------------------------------	-----

LIST OF ILLUSTRATIONS

Figure	Page
1.1 Different types of CD based CSPs.....	3
1.2 Complementary behavior of DP-TFA α -, β - and γ -CD CSPs.....	8
1.3 Structures of crocetane (A) and phytane (B)	16
1.4 Gas chromatographic enantioseparation of hydrocarbons on Chirasil- β -Dex.....	17
1.5 Separation of the enantiomers of Tröger's base by gas chromatography on immobilised Chirasil- β -Dex under various experimental conditions.....	18
2.1 (a) structure of cyclofructan and (b) 3D view of fructose moiety in cyclofructan.....	21
2.2 Crystal structure of CF6 and space-filling image.	22
2.3 Modeling results of derived cyclofructans	25
2.4 Chiral separations obtained by PM-CF6 and PM-CF7.....	30
3.1 Structure of native cyclofructan (a) and 3D view of native CF6 (b)	37
3.2 Enantiomeric separations on DP-TA-CF6 and DP-PN-CF6 CSPs	45
3.3 Enantiomeric separations of a series of homologous on DP-TA-CF6 stationary phase at 70°C	47
3.4 Enantiomeric separations of a series of structurely related analytes on DP-TA-CF6 stationary phase	50
3.5 Enantiomeric separations three different derivatives of isoleucine methyl ester on DP-TA-CF6 stationary phase	51
4.1 Common cations and anions of room temperature ionic liquids	58
4.2 Structures of cations with multiple charges.....	59
5.1 Structures of trigonal tricationic ionic liquids	62
5.2 Temperature profile for column bleeding in gas chromatography due to thermal decomposition or volatilization.....	71

5.3 X-ray crystallographic data of $C_3(\text{mim})_2 2\text{Br}^-$ showing stacks along short a – axis and H-bonding	74
5.4 Separation of Grob test mixture in trigonal tricationic IL columns and commercial columns with varying degrees of polarity.....	78
5.5 Separation of homologous alkane and alcohol mixture	81
5.6 Comparison of separation of homologous alkane and alcohol mixture using different ionic liquid columns.....	82
5.7 Separation of flavor and fragrance mixture.....	84
5.8 Separation of a mixture of methyl oleate and methyl elaidate	85
6.1 Ionic liquid GC stationary phases used.....	91
6.2 Chromatograms illustrating the relative retention orders of water and different organic solvents	95
6.3 Example of improved resolution and peak symmetry using an ionic liquid based stationary phase (A) versus a commercial PEG column (B).....	96
6.4 Plot of normalized response versus amount of spiked water injected onto column	97
6.5 Illustration showing the number of successful water separations on each of the three IL based columns	102
6.6 Example of the separation of organic solvents in water using ionic liquid based stationary phase	103
7.1 Structures of antioxidants.....	107
7.2 Degradation profiles of the ethanolic solutions	112
7.3. HPLC chromatograms of carnosol ethanol solutions stored under different conditions after 14 days	114
7.4 The peak areas of the degradation products of carnosol vs. time	115
7.5. HPLC chromatograms of carnosic acid ethanol solutions stored under different conditions after 14 days.....	117
7.6 The degradation pathway of carnosic acid in ethanol solution.	120
7.7 HPLC chromatograms of mixed standards stored under different conditions after 14 days	122

7.8 HPLC chromatograms A) methanolic rosemary extract,
B) fish oil diluted with methanol and C) rosemary extract
in fish oil diluted with methanol 125

LIST OF TABLES

Table	Page
1.1 Thermodynamic parameters measured by GC on DP-TFA- γ -CS CSP	10
1.2. ChiralDex series columns	11
2.1 Chiral analytes separated by PM-CF6	27
2.2 Chiral analytes separated by PM-CF7	28
2.3 Chiral analytes separated by DP-CF6.....	29
2.4 Comparison of some enantiomeric separations on PM-CF6 CSP and Chiralsil-man-18C6-25 phase	32
3.1 Separations on DP-TA-CF6 and DP-PN-CF6.....	41
3.2 Retention and enantioselectivity of three homologous seires on DP-TA-CF6 and DP-PN-CF6.....	48
3.3 Thermodynamic parameters measured by GC on DP-TA-CF6 CSP	52
3.4 Thermodynamic parameters measured by GC on DP-PN-CF6 CSP	53
5.1 Solute descriptor values for all the probe molecules	66
5.2 Physical properties of the trigonal tricationic ILs used as stationary phases	70
5.3 Variation of retention factors (k_{naph}) with thermal treatment of D core trigonal tricationic IL columns	73
5.4 Interaction parameters obtained for trigonal tricationic IL stationary phases	79
5.5 Comparison of the interaction parameters of monocationic and dicationic RTILs with trigonal tricationic ionic liquids	80
6.1 Comparison of the ionic liquid GC results with the best results from the Karl Fischer Titration (KFT) and the use of a commercial PEG GC column	98

6.2 Detection of water in 50 solvents	99
7.1 The peak areas of epirosmanol ethyl ether and carnosol in carnosol, carnosic acid and mixture solutions.....	123
7.2 Mass spectra and UV spectra data for degradation products and components in rosemary extracts	126

PART ONE: ENANTIOSELECTIVE GAS CHROMATOGRAPHIC STATIONARY PHASES

CHAPTER 1

INTRODUCTION

Since the first direct enantiomeric separations in gas chromatography (GC) was achieved in 1966¹, chiral gas chromatography has become widely applied to the separation of enantiomers that are volatile and thermally stable. GC is highly efficient, sensitive and simple. In the last two decades, over 24,000 separations of more than 8,000 enantiomers have been reported on gas chromatography chiral stationary phases (CSPs).² Three classes of chiral stationary phases are used for enantiomeric separations: 1) chiral amino acid derivatives, 2) chiral metal coordination compounds and 3) cyclodextrin (CD) derivatives. Of these, the CD based chiral selectors dominate the field.

1.1 Development of Cyclodextrin-based Chiral Stationary Phases

The first reported cyclodextrin based stationary phase in GC was developed by Schlenk and coworkers in 1962 for separating achiral polar compounds.³ However, CD based GC stationary phases did not attract much attention until the late 1970s when dissolved and bonded CDs were utilized in liquid chromatography. Smolkova-Keulemansova, et al. experimented with native and methylated CDs as GC stationary phases by dissolving them in solvents such as dimethylformamide and coating the solution on the stationary phase support.^{4,5} It was found that the CD-based stationary phases provided interesting selectivity and that an inclusion complex mechanism was very likely involved.⁴⁻¹⁰ The first GC enantiomeric separation of terpenoid hydrocarbons (α - or β -pinene, cis- and trans-pinane) on a CD based chiral stationary phase was reported by Koscielski, et al in 1983.¹¹ The glass column was packed with celite coated with formamide solution of native α - or β -CD hydrate. Those CD based stationary phases were largely solid because of the evaporation of the coating solvents. Thus the peak efficiency and

thermal stability of those columns were low and the enantiomeric separations obtained were limited.

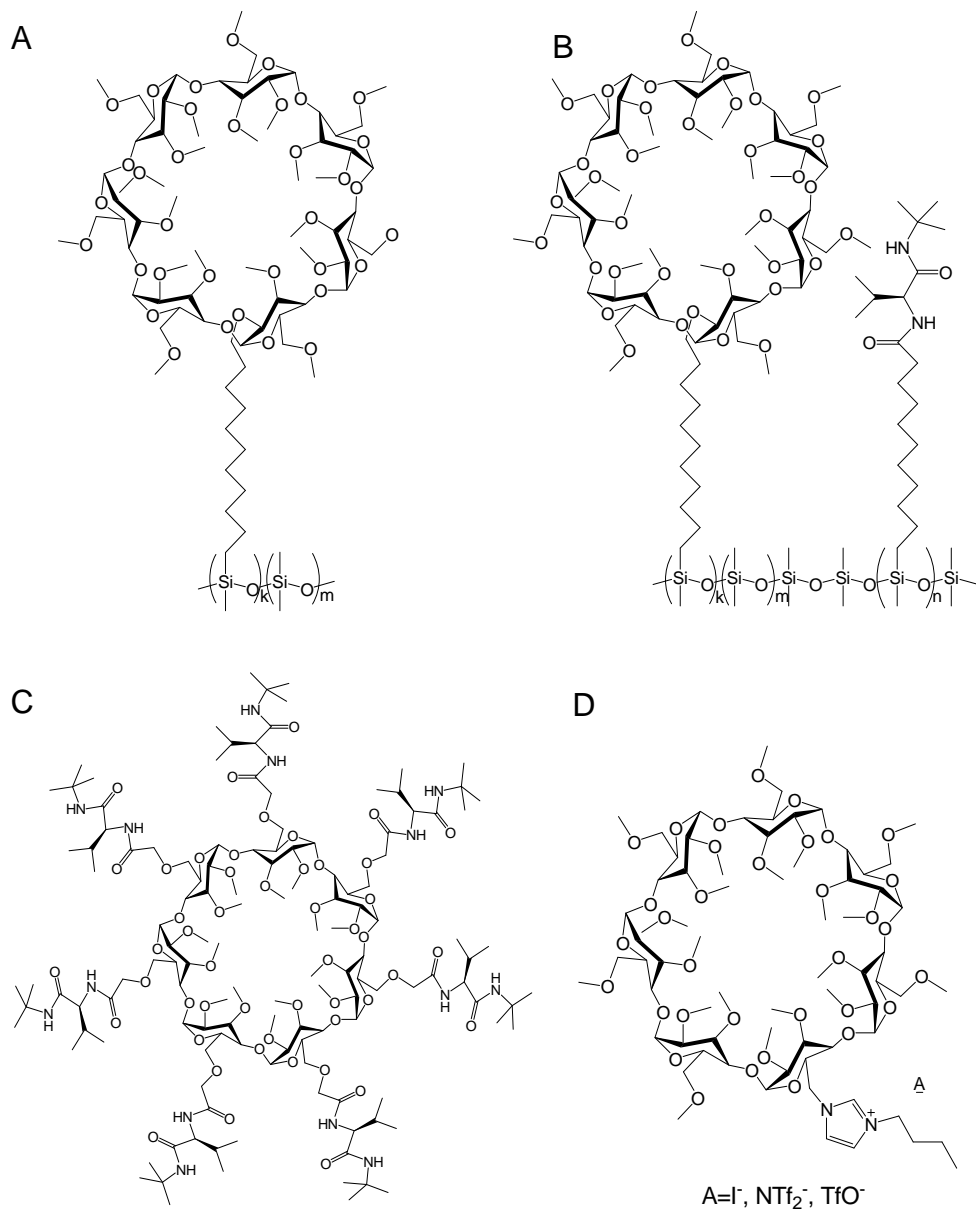


Figure 1.1 Different types of CD based CSPs: A) Chirasil- β -Dex²³; B) Chirasil-DexVal-C₁₁²⁹; C) heptakis[6-O-(N-acetyl-L-valine-tert-butylamide)-2,3-O-methyl]- β -CD^{31, 32}; D) ionic permethylated β -CD²¹.

From the late 1980s to the early 1990s, a great number of CD based GC chiral selectors were developed by varying the alkylation or acylation substituents on the 2-, 3-, and 6-hydroxyl groups of the CD glucose units. These groups can be alkylated and acylated regioselectively. As will be discussed, cyclodextrins with various derivatization groups provided different types of interactions and have substantially different enantioselectivities toward chiral molecules. Capillary columns (made of glass and later with fused silica) were used instead of packed columns to increase the column efficiency. Permethyated β -CD was the first reported CD derivative which was used as a chiral stationary phase in capillary GC. In 1987, Juvancz et al. coated permethylated β -CD on Pyrex borosilicate glass capillary (deactivated with Carbowax 20M).¹² The enantiomers, (+)- and (-)-*cis*-permetrinic acid methyl esters were separated on this CSP at 130°C in 15 min. However, liquid stationary phases are preferable to solid stationary phases in open tubular capillary GC. There were several approaches to obtain liquid stationary phases with CD based selectors.

1.1.1 Undiluted selectors

One approach to obtain liquid CD based stationary phases is to make amorphous derivatives of CD with low melting points. When the hydroxyl groups of CDs are partially or fully etherified with *n*-pentyl groups, the pentylated CD derivatives are viscous liquids and show good wetting ability when coated on glass or fused silica capillaries. The partially pentylated CDs are actually mixtures of homologues and isomers. This heterogeneity creates low melting points.¹³ For fully pentylated CD derivatives, the liquefaction is likely due to the functionalization of the hydroxyl groups with non-polar, non-hydrogen-bonding and sterically bulky pentyl groups which seems to inhibit the crystallization.¹³ In this approach the CD selectors were undiluted. This method was first reported by König et al.¹⁴⁻¹⁶ Per-*O*-pentylated α -CD, and heptakis(3-*O*-acetyl-2,6-di-*O*-pentyl)- α/β -CDs were directly coated on Pyrex glass capillaries and showed enantioselectivity to trifluoroacetylated chiral amines, amino alcohols, α - and β -amino acid esters, and cyclic trans-diols. Those undiluted CSPs exhibited a wide range of operating

temperature and were thermally stable above 200°C. In 1990, 2,6-di-pentyl-3-O-trifluoroacetyl α -, β - and γ -CDs (DP-TFA α -, β - and γ -CD, respectively) were synthesized and evaluated as undiluted GC CSPs by Armstrong and coworkers.¹⁷ More than 150 pairs of enantiomers were separated by those CSPs. The enantiomers separated included derivatized chiral alcohols, diols, polyols, amines, amino alcohols, halohydrocarbons, lactones, α -halocarboxylic acid esters, carbohydrates, epoxides, nicotine compounds, pyrans, furans, etc. Nowadays, DP-TFA γ -CD (Chiraldex GTA) is the most broadly applicable CSP in GC enantioseparations.

1.1.2 Diluted selectors

The approach advanced by Schurig and Nowotny was to dissolve permethylated CDs in a moderately polar polysiloxane stationary phase (e.g. OV-1701) and coat the mixture on capillary columns.^{18, 19} The inherent enantioselectivity of the diluted, derivatized CDs and the unique properties of polysiloxanes were combined in this GC CSP. The good coating properties of polysiloxanes produced high efficiency, high resolution and thermal stability.

Besides polysiloxanes, ionic liquids (ILs) were employed as the matrix for CD based CSPs in GC whereas ILs showed excellent chromatographic properties in GC. In 2001, Berthod et al. developed a new type of IL-based CSPs by dissolving permethylated β -CD and dimethylated β -CD in 1-butyl-3-methylimidazolium chloride and compared their chromatographic performance and enantioselectivity to the polysiloxane diluted permethylated and dimethylated β -CD columns (Chiraldex BPM and Chiraldex BDM, respectively).²⁰ The IL-based column efficiencies were up to 10 times higher than the polysiloxane-based columns. However, only about one third of the racemic analytes that could be separated on the commercial columns were separated on the IL-based columns. This was thought to be due to the inclusion of the IL cation in the cyclodextrin cavity. In order to improve the enantioselectivity of the IL based CD columns while retaining their extraordinary efficiency, ionic CD derivatives were synthesized and used as GC CSPs by dissolving them in ILs.²¹ Butylimidazolium or tripropylphosphonium groups were attached to permethylated β -CD to introduce positive charges to the derivatized

CDs (Figure 1.1D). The ionic CD derivatives were more soluble in ionic liquids and exhibited broader enantioselectivities and greater thermal stabilities than neutral cyclodextrin chiral selectors. When compared to the analogous commercial column with a polysiloxane matrix (ChiralDex BPM), it exhibited different enantioselectivities, more symmetric peak shapes and some complementary enantioseparations.

1.1.3 Grafted chiral selectors

Besides the two approaches mentioned above, grafting derivatized CD to polysiloxane was another path to obtain liquid CD based GC CSPs. Permethylated β -CD was grafted to polydimethylsiloxane and tested as GC stationary phase by several research groups independently.²²⁻²⁴ The structure of CD grafted stationary phase (Chirasil- β -Dex) is shown in Figure 1.1A. There were several advantages to this approach: 1) compared to the method of diluting permethylated CDs in semipolar polysiloxanes, apolar polysiloxanes can be used as the backbone of the stationary phase, thus the analysis time for polar analytes were shortened; 2) The concentration of chiral selectors was not restricted by their solubility in the polysiloxanes; 3) The thermal stability was enhanced and operating temperature can vary in the wide range (-25°C -250°C). This type of CD based CSPs was able to be immobilized on the fused silica surface by thermal treatment.^{24,25}

1.1.4 Mixed binary selectors

In enantioselective GC, enantiomers were separated via hydrogen bonding interactions on stationary phases consisting of amino acid derivatives (e.g. Chirasil-Val), via coordination on metal complexes or via inclusion or external interactions on CD derivatives. Each of the three main types of chiral selectors provided different or unique interactions in enantiomeric separations. In order to combine the individual enantioselectivities of different types of chiral selectors, either tandem-column arrangement (coupling two columns with different selectors) in the system or mixing different types of chiral selectors in one stationary phase was required. In the late 1990s, the thought of binary selectors in one stationary phase was reported.²⁶ Three

methods were used to produce CSPs with binary selectors: 1) simultaneously bonding two chiral selectors to polysiloxane backbone (e.g. Chirasil-Calival-Dex^{27, 28} or Chirasil-DexVal-C₁₁,²⁹ Figure 1.1B), 2) doping one chiral selector in the second (Chirasil-Val(γ -Dex)³⁰), 3) Directly linking one chiral selector to the other (e.g. heptakis[6-O-(N-acetyl-L-valine-tert-butylamide)-2,3-O-methyl]- β -CD,^{31,32} Figure 1.1C). Considering the individual contribution of the two chiral selectors to the enantiomeric separation, the chiral recognition ability of the binary CSPs may be enhanced ("matched case") or compensated ("mismatched case"). The separation of enantiomers by enantioselective GC on CSPs with binary chiral selectors was governed by many different factors such as the combination, the concentration, the enantiomeric purity of the chiral selectors and the choice of the matrix.³³

1.2 Mechanisms

Discussions on the chiral recognition mechanism of cyclodextrin-based CSPs quickly followed their development and extensive utilization. However, rationalization of chiral recognition involving CD derivatives is difficult since almost all classes of chiral compounds, ranging from apolar to highly polar are often separated on the same CD-based CSPs. Apparently multimodel recognition processes, which may involve inclusion complex formation, hydrogen-bonding, dispersion forces, dipole-dipole and steric interactions, are important.³⁴

1.2.1 Cavity size of CD derivatives

The macrocyclic α -, β - and γ -cyclodextrins contain 6, 7 and 8 glucose moieties respectively. Consequently the internal diameters of their cavities vary as well (~6.5, 7.0 and 8.5Å respectively).³⁵ Conversely, the depths of their cavities are all ~7Å. As will be discussed, different size cyclodextrins with exactly the same functionality have different selectivities. Indeed there seems to be no logical or predictive relationship between size and selectivity in GC. In HPLC, β -CD was the most frequently used homologue while α - and γ -CD were less useful.³⁶ In a 1990 paper about DP-TFA α -, β - and γ -CDs, the enantioselectivity data of more than 150 pairs of enantiomers on the three CSPs were reported. The size of the chiral selectors showed

significant influence on the enantioselectivity of the CSPs. In fact 116 racemates were separated on the DP-TFA γ -CD, 81 on DP-TFA β -CD and 36 on DP-TFA α -CD.¹⁷ The complementary separation behavior of these related chiral selectors is shown in Figure 1.2. It was the first reported γ -CD stationary phase that was more widely useful than the β -CD analogue. In 1991, Bicchi et al. compared the enantioselectivities of permethylated α -, β - and γ -CD CSPs in GC. These permethylated CDs of different sizes also showed complementary behavior.³⁷ In some cases, reversals of elution orders were observed on CD derivatives with the same substituents but different cavity sizes.^{37, 38}

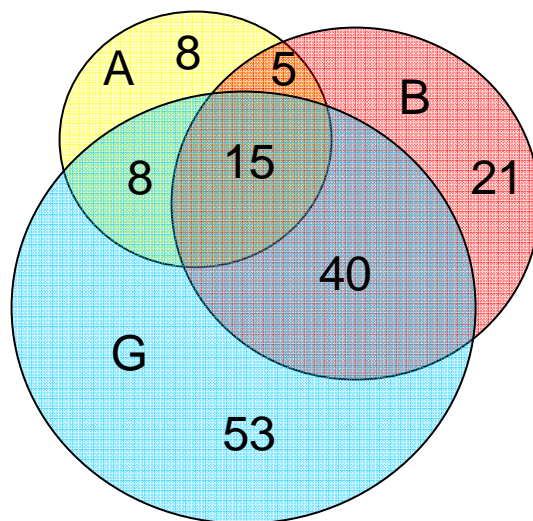


Figure 1.2 Complementary behavior of DP-TFA α -, β - and γ -CD CSPs (A, B and G, respectively)¹⁷

1.2.2 Inclusion complex formation

Due to the truncated hollow cup shape of CD molecules, a hypothesis was advanced in reversed phase liquid chromatography that CD could form hydrophobic inclusion complexes with certain types of molecules. Enantiomeric separations could be achieved if one enantiomer could fit into the hydrophobic cavity differently than the other. Even though there is no water and

no hydrophobic inclusion in GC, it is interesting to examine whether or not inclusion complex formation contributes to the chiral recognition ability of CD derivatives when used as GC CSPs. Thermodynamic analysis and column overloading experiments were two of the more useful approaches for studying separation behaviors on CD-based CSPs.³⁹

When a pair of enantiomers is separated by a CSP, the difference in the Gibbs free energy of association, $\Delta(\Delta G^\circ)$, can be estimated from the selectivity factor, α , by

$$-\Delta(\Delta G^\circ) = RT \ln \alpha \quad (1)$$

Where R is the gas constant and T is the temperature in degrees Kelvin. $\Delta(\Delta G^\circ)$ is related to enthalpy $\Delta(\Delta H^\circ)$ and entropy $\Delta(\Delta S^\circ)$ by the following relationship:

$$-\Delta(\Delta G^\circ) = -\Delta(\Delta H^\circ) + T\Delta(\Delta S^\circ) \quad (2)$$

Thus the relationship between α , $\Delta(\Delta H^\circ)$ and $\Delta(\Delta S^\circ)$ can be rewritten as the van't Hoff equation:

$$\ln \alpha = -\Delta(\Delta H^\circ)/RT + \Delta(\Delta S^\circ)/R \quad (3)$$

The $\Delta(\Delta H^\circ)$ and $\Delta(\Delta S^\circ)$ values for a pair of enantiomers on a certain CSP can be obtained by measuring the α values at different temperatures and plotting $\ln \alpha$ versus $1/T$. In 1992, Armstrong and co-workers studied the enantioselective retention mechanisms on two CD-based CSPs (DP-TFA- β -CD and DP-TFA- γ -CD).³⁹ They postulated two different enantioselective retention mechanisms. One involved enantioselective inclusion complex formation. The other mechanism was a much looser, external association of multiple analytes per cyclodextrin molecule. In this study, the racemic analytes were able to be categorized into two groups according to the values of their thermodynamic parameters. The analytes thought to be separated via inclusion complex formation showed high values for $-\Delta(\Delta H^\circ)$ and $-\Delta(\Delta S^\circ)$ whereas the analytes separated through an external interaction mechanism had relatively lower $-\Delta(\Delta H^\circ)$ and $-\Delta(\Delta S^\circ)$ values (as shown in Table 1.1).

Table 1.1 Thermodynamic parameters measured by GC on DP-TFA- γ -CS CSP^a. Reproduced with permission.³⁹

racemic compound ^b	temp range, °C ^c		$-\Delta(\Delta G^\circ)$, °C cal/mol		$-\Delta H^\circ_{R_1}$	$-\Delta H^\circ_{S_1}$	$-\Delta(\Delta H^\circ)$	$-\Delta(\Delta S^\circ)$	T_{iso}^d
	min	max	min	max	kcal/mol	kcal/mol	kcal/mol	cal/(mol·K)	°C
Group I									
trans-2,5-dimethoxytetrahydrofuran	50	90	530	210	12.0	16.0	3.1	8.0	110
methyl 2-chloropropanoate	60	100	550	300	14.7	17.4	2.7	6.2	160
1,3-dibromobutane	60	100	430	180	14.2	16.7	2.5	6.3	120
styrene oxide	70	110	380	160	16.4	17.7	2.3	6.4	140
methyl 2-bromopropanoate	60	100	360	180			1.8	4.4	140
1,2-hexanediol	60	100	210	43	16.1	17.8	1.7	4.3	120
1,2-pentanediol	60	110	220	43	16.2	16.9	1.4	4.5	100
3-chloro-2-butanone	50	90	360	210	12.5	14.0	1.5	3.6	140
2-chlorocyclopentanone	80	110	300	200	16.5	16.9	1.4	3.2	160
2-hexanol	40	80	210	67			1.4	3.7	110
Group II									
1,2-dibromobutane	60	100	90	30	13.5	14.4	0.9	2.4	100
2-pentanol	40	80	160	60			0.9	2.4	100
2-heptanol	50	90	120	35	12.4	13.1	0.8	2.2	90
2-bromoheptane	50	90	120	36			0.77	2.1	90
2-methylcyclohexanone	60	100	120	36	14.0	14.7	0.8	1.8	120
3-butyrolactone	60	100	150	110	16.2	16.8	0.6	1.3	190
2-chlorocyclohexanone	80	110	120	72	16.6	17.2	0.6	1.4	160
n-butyl 2-bromobutanoate	80	120	60	0	16.8	16.3	0.5	1.4	80
2-octanol	50	90	80	30	13.3	13.8	0.5	1.3	110
n-hexyl 2-bromobutanoate	80	120	54	0	16.8	17.3	0.5	1.3	110
n-pentyl 2-bromobutanoate	80	120	54	0	16.4	16.9	0.5	1.3	110
sec-butyl 2-bromobutanoate	60	100	39	0			0.45	1.3	70
n-hexyl 2-bromopropanoate	70	100	59	36			0.3	0.7	160
n-pentyl 2-bromopropanoate	60	100	39	29			0.15	0.4	100

^a20-m wall-coated fused silica capillary columns, carrier gas nitrogen at 10-15cm/s velocity, injection volume 0.5 μ L with a 100/1 split ratio. The $-\Delta H^\circ_{S_1}$ were used with the corresponding $\ln k'$ values for enthalpy-entropy compensation studies. ^bAll amines and alcohol were resolved after trifluoroacetylation. ^cRetention and α values were measured at 10°C intervals. Hence every van't Hoff plot contained at least five data points. ^dTemperatures reported to the nearest 10°C.

Table 1.2. ChiralDex series columns^a

Derivative	Feature ^b	Mechanism observations
2,6-di-O-pentyl-3-trifluoroacetyl (TA)	<ul style="list-style-type: none"> •Separate the widest variety and the greatest number of enantiomers •G-TA more selective than B-TA •Useful for homologous series of: amino acids (primary, secondary, aliphatic, and aromatic), amines (primary, secondary, cyclic, aromatic, and halogenated), amino alcohols, alkanes, hydrogenated alkanes, alcohols (aliphatic and aromatic), acids (halogenated and hydroxy), esters (aliphatic, aromatic, hydroxy, and di-ester), diols, lactones, ketones, phthalides, sulphoxides 	<ul style="list-style-type: none"> •Strong dipole-dipole interactions •Longer alkyl chain, greater retention •Halogens known to favor cavity interaction
2,3-di-O-methyl-6-t-butyl silyl (DM)	<ul style="list-style-type: none"> •Broad chiral selectivity •Combine selectivity of the PM and PH phases •Short retention, high resolution •B-DM broadly applicable •Resolve aliphatic, olefinic and aromatic enantiomers 	<ul style="list-style-type: none"> •Size selectivity present but not dominant as in the DA phases •Fewer structural requirements •Characteristic temperature selectivity
2,6-di-O-pentyl-3-propionyl (PN)	<ul style="list-style-type: none"> •Suitable for epoxide separations •High selectivity for lactones •High selectivity for aromatic amines •More stable to moisture than the TA phases 	<p>There is little evidence of inclusion formation. Retention increases with increased chain length of analyte. This allows for efficient separation of a series of homologues.</p>
2,6-di-O-pentyl-3-butyryl (BP)	<ul style="list-style-type: none"> •High selectivity for amino acids, amines, and furans •Thermally stable 	<ul style="list-style-type: none"> •Alkyl chain on analyte contributes to chiral recognition •High sample capacity, therefore, primary surface interactions

Table 1.2-continued

<p>2,3-di-<i>O</i>-propionyl-6-<i>t</i>-butyl silyl (DP)</p>	<ul style="list-style-type: none"> •Broad chiral selectivity •Good hydrolytic stability •Excellent for aliphatic and aromatic amines •Good for many aliphatic and some aromatic esters •High efficiency and resolution at low retention times for polar racemates 	<ul style="list-style-type: none"> •Mostly surface interactions •Fused ring structures exhibit better selectivity on the G-DP •Acids have better selectivity as methyl esters rather than ethyl esters
<p>2,6-di-<i>O</i>-pentyl-3-methoxyl (DA)</p>	<ul style="list-style-type: none"> •Hydrophobic surface •Pronounced selectivity differences based on analyte size, shape and functionality •Separate heterocyclic amines •Selectivity priorities: A-DA: simple epoxides, cyclic ethers, and linear substituted alkanes; B-DA: heterocyclic amines; G-DA: naphthyl analogs 	<ul style="list-style-type: none"> •Strongest mechanism is inclusion, therefore, size selectivity is important •Critical temperature dependence for enantioselectivity, above this temperature no separation occurs
<p>(<i>S</i>)-2-hydroxy propyl methyl ether (PH)</p>	<ul style="list-style-type: none"> •Hydrophilic surface •Separate a wide variety of enantiomers •Resolve aliphatic, olefinic, and aromatic enantiomers •Good general purpose chiral columns 	<ul style="list-style-type: none"> •Reduced influence of inclusion complexing •Less size selectivity than the DA phases •Characteristic temperature selectivity on a given column for a given class of compounds •Fewer functional requirements for analyte than LC
<p>2,3,6-tri-<i>O</i>-methyl (PM)</p>	<ul style="list-style-type: none"> •Broad chiral selectivity •Strong inclusion/size selectivity 	<ul style="list-style-type: none"> •Inclusion is the dominant mechanism •Along with the DM phases, has the highest temperature stability of the Astec CHIRALDEX line

^aInformation obtained from <http://www.sigmaaldrich.com/analytical-chromatography/gas-chromatography/columns/astec-chiraldex.html>

^bUsing the prefix A, B and G describes the cyclodextrins, α , β and γ , respectively.

It had been shown that native CDs form inclusion complexes with certain types of molecules in a definable host-guest molecular ratio.⁴⁰ From this point of view, for the enantiomers separated via inclusion complex formation, the column capacity was determined by the number of CD molecules within the stationary phase. Thus the column capacity towards these types of enantiomers would be lower than those of enantiomers separated via multiple external interactions. The results of column loading experiments were in good agreement with the results of the thermodynamic analysis.³⁹ The enantiomers which had lower $-\Delta(\Delta H^\circ)$ and $-\Delta(\Delta S^\circ)$ values showed much higher column capacities than the enantiomers which had relatively higher $-\Delta(\Delta H^\circ)$ and $-\Delta(\Delta S^\circ)$ values. The highest column capacity obtained with trifluoroacetylated 2-heptanol was 50-fold greater than that of methyl-2-chloropropanoate which had the lowest capacity.³⁹ It should be noted that the enantioselective retention mechanism of some compounds may be temperature dependent.

1.2.3 Substituents

The functionality and the geometric distribution of the substituents on the 2-, 3- and 6-hydroxyl groups also show a substantial influence on the enantioselectivity of CD derivatives. For example, 2,6-di-O-pentyl-3-trifluoroacetyl CDs had much wider enantioselectivity compared to 2,6-di-O-pentyl CDs.^{13, 17} The trifluoroacetyl substituents at the 3-hydroxyl functions eliminated the hydrogen donor capabilities of the hydroxyl groups but provided strong dipole-dipole interactions which appeared to provide a vital contribution to the enantioselectivity. The nature of the substituents may also effect the elution order of the enantiomers. For example, the enantiomers of some trifluoroacetylated amines, alcohols and monosaccharides showed the opposite elution order on permethyl-O-((S)-2-hydroxypropyl)- β -CD and 2,6-di-O-pentyl-3-trifluoroacetyl β -CD CSPs.⁴¹

In 1993, König compiled a useful collection of enantioselectivity factors of racemates observed on octakis(6-O-methyl-2,3-di-O-pentyl)- γ -CD, octakis(2,6-di-O-methyl-3-O-pentyl)- γ -CD and octakis(3-O-butanoyl-2,6-di-O-pentyl)- γ -CD.^{42, 43} Among all the CSPs compared,

octakis(3-*O*-butanoyl-2,6-di-*O*-pentyl)- γ -CD (Lipodex E) showed exceptionally broad enantioselectivity. At present, it is one of the more useful CSPs in enantioselective GC.

Two other effective CD based CSPs are the heptakis(2,3-di-*O*-acetyl-6-*O*-tert-butylmethylsilyl)- β -CD and heptakis(2,3-di-*O*-methyl-6-*O*-tert-butylmethylsilyl)- β -CD derivatives. The presence of a bulky substituent at the primary 6-hydroxyl function blocks the entrance to the cavity from the narrower rim which might have a negative impact on enantioselectivity.^{44, 45}

Sicoli et al. investigated the enantiomeric separation ability of linear dextrans as CSPs for GC.⁴⁶ A comparison of acyclic and cyclic dextrans for their ability to enantioseparate racemates was made as another approach to probe the role of external interactions versus molecular inclusion by CD derivatives in the enantiorecognition process. The observation that acyclic counterparts of cyclodextrins were able to separate racemates demonstrated the important role of polar substituents (i.e. acetyl/TBDMS functional groups) in both acyclic and cyclodextrin selectors. However, the enantioselectivity of the linear dextrans was much more limited than was found for similarly functionalized cyclodextrins. More details about the effects of cavity size and substituents of CD based CSPs are given in Table 1.2.

1.3 Applications

GC capillary columns coated with CD based CSPs were widely employed for enantiomeric analysis in many fields, including clinical and pharmaceutical chemistry, enzymatic reactions, authenticity control of essential oils, flavors and fragrances, forensics and environmental matrixes.²

1.3.1 Commercial CD columns and database

Different types of capillary columns coated with CD derivatives are commercially available under the name of Lipodex and Hydrodex (distributed by Macherey Nagel, Düren, Germany), obtained according to procedures from König et al. and Schurig-Nowotny, respectively. ChiralDEX is the trademark for the series of stationary phases (listed in Table 1.2) developed by Armstrong et al. and produced by Astec, Supelco/Aldrich/Sigma (Bellefonte, PA, USA). The group of Koppenhoefer et al. at the University of Tübingen, Germany, developed a

database, “ChirBase/GC”, for GC enantioseparations (http://www.acdlabs.com/products/chrom_lab/chirbase/gc.html). Information is compiled for over 24,000 separations of more than 8,000 chiral molecules. The database provides experimental conditions along with structural details.

1.3.2 Enantiomeric separation of chiral hydrocarbons

Hydrocarbons exist widely in living organisms and are particularly prevalent in geological deposits of biological origin. The structures of some hydrocarbons in geological deposits can be related to functionalized precursors in the source material. Many of the functional groups of those precursor molecules were removed by biological, chemical and physical processes over time (i.e., diagenesis). The source material usually was buried and often subject to high temperature and pressure environments conducive to the formation of a multitude of hydrocarbon products.^{47, 48} Some chiral hydrocarbons have a high resistance to enantiomerization and have pronounced enantiomeric or diastereomeric excesses despite the fact that they are tens of millions of years old.⁴⁹ Because of the biological origin of these geochemical molecules, they are referred to as biomarkers. The stereochemical analysis of biomarkers may provide information on the time of deposition, the maturity, diagenetic history, and so forth. Also, in astrobiology, the stereochemical analysis of chiral hydrocarbons is of particular interest in a search for extraterrestrial homochirality. To answer the question of whether chiral specimens in space exist as racemates or are stereochemically enriched, the chromatographic separation of the chiral components of carbonaceous material obtained from outer-space is required.⁵⁰

The enantiomeric separation of compounds possessing no “nonhydrocarbon” functional groups is a significant challenge in separation science. Because of the lack of functional groups, chiral recognition by a chiral selector is based largely on weak van der Waals forces. Due to the high efficiency of enantioselective GC and the particular cavity structure of CD derivatives, enantioseparation of chiral hydrocarbons often can be achieved on CD based CSPs in GC.

The first set of successful direct separations of hydrocarbon biomarker enantiomers was obtained on the permethyl-*O*-((*S*)-2-hydroxypropyl)- α - and β -CD CSPs (Chiraldex APH and BPH) in 1991.⁴⁷ The enantiomerically separated hydrocarbons included saturated isoprenoids and hydroaromatics, which were of geochemical importance. At present, the Chiraldex BPH appears to be a powerful CSP for the GC enantioseparation of chiral hydrocarbons. Crocetane and phytane are two isoprenoids widely detected in crude oil, microbial colonies and sediments containing archaea. They are structural isomers as shown in Figure 1.3. The first fast and effective baseline separation of crocetane from phytane, as well as separation of their stereoisomers was achieved using CD based GC CSPs. The best separations were obtained on Chiraldex BPH CSP.⁵¹

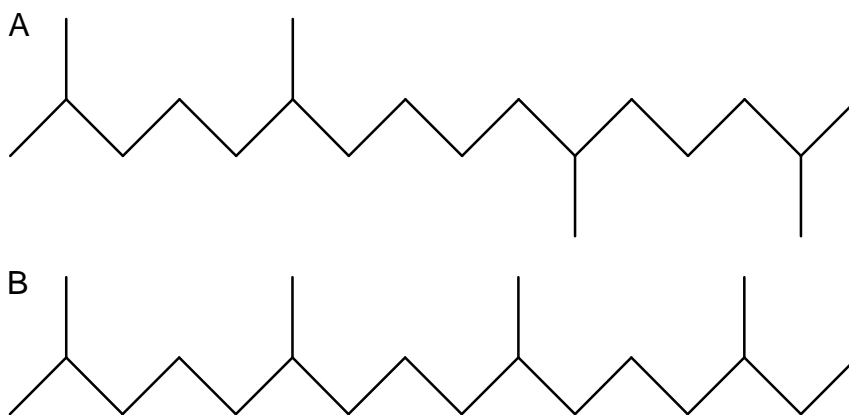


Figure 1.3 Structures of crocetane (A) and phytane (B).

The enantiomeric separation of racemic alkanes containing seven and eight carbon atoms has been reported (see Figure 1.4 for some of the results).⁵² The substitution pattern and cavity size of the cyclodextrin based chiral selectors had a substantial effect on the observed chiral recognition ability. The possible role of molecular inclusion was indicated by the complete loss of enantioselectivity when the CDs are replaced by the corresponding chain-length linear dextrins.

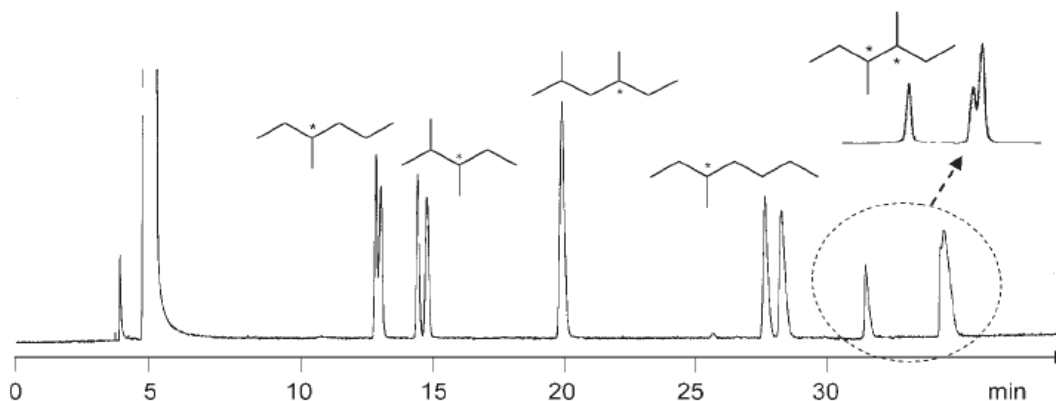


Figure 1.4 Gas chromatographic enantioseparation of racemic 3-methylhexane, 2,3-dimethylpentane, 2,4-dimethylhexane (not resolved), 3-methylheptane, and 3,4-dimethylhexane (including the meso-diastereomer) on Chirasil- β -Dex. Column: 25 m \times 0.25 mm i.d. fused silica capillary, film thickness 0.25 μ m, T = 30°C, carrier gas: 30 kPa H₂. The insertion on top, right, refers to a 50 m \times 0.25 mm i.d. capillary. Reproduced with permission.⁵²

1.3.3 Miniaturization of the enantioseparation system

For simple binary separations where only one enantiomeric pair is considered the whole separation window offered by long columns (typically 10 – 40m \times 0.25 mm I.D. glass or fused-silica capillaries coated with a CSP) is not required. By using short columns, the loss in efficiency can be compensated for by lowering the separation temperature. In most cases the speed of analysis is improved with short columns and the sharp peaks obtained improve detectability. The first use of short columns in enantioselective gas chromatography involving CD derivatives was reported by Lindström.⁵³ The enantiomers were separated on a 2m \times 0.25mm I.D. column coated with permethylated- β -CD CSP. The fastest separation of enantiomers reported by GC, namely that of enflurane on immobilised Chirasil- γ -Dex, required only few seconds.⁵⁴ The influence of column length and column diameter on the resolution factor is demonstrated in Figure 1.5 for the separation of enantiomers of Tröger's base on Chirasil- β -Dex.³⁴ Compared to the 20m \times 0.25mm I.D. \times 140nm(stationary phase thickness) column, a faster analysis time was achieved on the short column(2m \times 0.25mm I.D. \times 140nm) at a

lower temperature. When a capillary of smaller inner diameter was used, the length of the column can be further reduced without losing enantioselectivity.³⁴

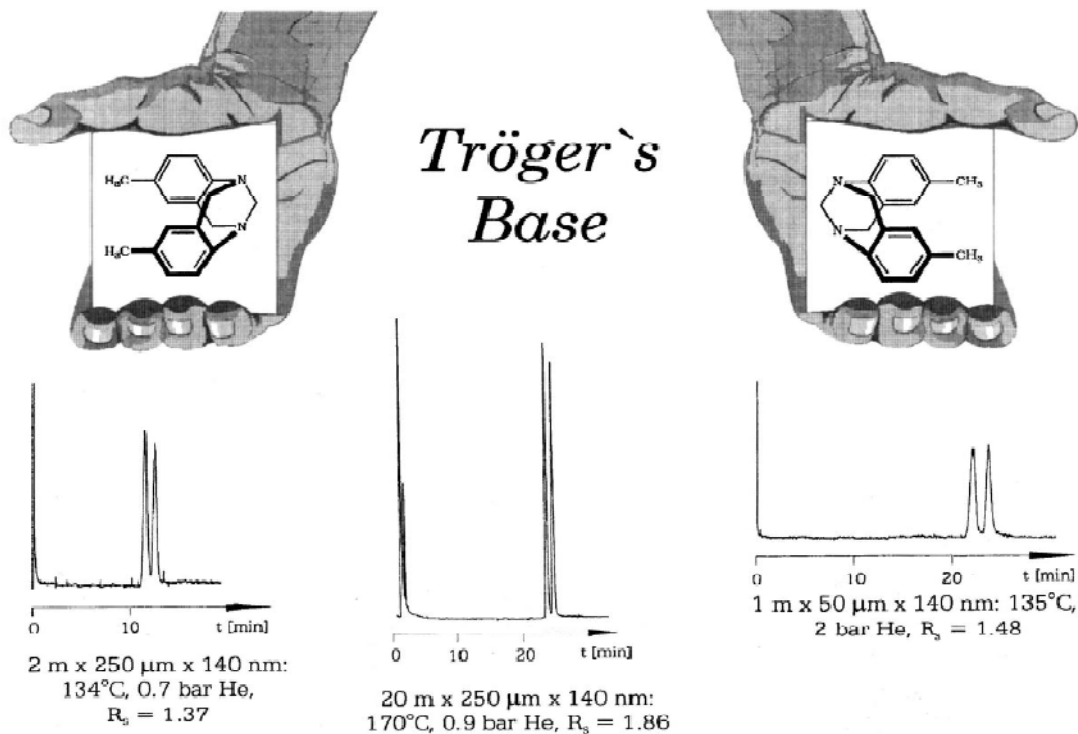


Figure 1.5 Separation of the enantiomers of Tröger's base by gas chromatography on immobilised Chiral- β -Dex under various experimental conditions. Reproduced with permission.³⁴

1.4 Summary

Enantioselective GC is quite complementary to enantioselective HPLC. Analytes that have smaller molecular weight and limited functionality can sometimes be difficult to separate by HPLC. Also chiral analytes that react with protic solvents and/or have no UV chromophore can be problematic with HPLC. Fortunately these types of analytes are usually amenable to GC enantiomeric separations. Some racemates can be separated both by GC and HPLC. In general, enantioselective HPLC is preferred for thermally labile molecules, nonvolatile molecules and preparative separations. Conversely, enantioselective GC is preferable for quantitative analysis, quality control and volatile molecules. An extensive series of studies has

been published on the enantiomeric purity of commercial chiral synthons, catalysts, auxiliaries and resolving agents used in asymmetric synthesis.⁵⁵⁻⁵⁷ Apparently two thirds of the preferred assays for these chiral starting materials utilized cyclodextrin based GC while one third required HPLC.

1.5 Dissertation Organization

This manuscript presents research in three areas: 1) development of novel cyclofructan-based chiral selectors for enantioselective GC separations; 2) development, characterization and evaluation of trigonal tricationic ionic liquids as GC stationary phases, and application of ionic liquid stationary phase for quantification of water in solvents and solvents in water; 3) analysis of antioxidants from rosemary and their stabilities in ethanol solution and fish oil by HPLC.

CHAPTER 2

PERMETHYLATED CYCLOFRUCTAN CHIRAL SELECTORS

Cyclofructans can not be used as chiral stationary phases for GLC in their native states. This is due to their high melting points and their inability to be solubilized in other liquid stationary phases. However, when cyclofructans are derivatized (via the 3-, 4-, or 6-hydroxyl groups) they can then be dissolved in an achiral matrix and the mixture is suitable as a GLC chiral stationary phase. In this study, per-*O*-methylated cycloinulohexaose (PM-CF6), per-*O*-methylated cycloinuloheptose (PM-CF7) and 4, 6-di-*O*-pentyl cycloinulohexaose (DP-CF6) were tested as new chiral selectors for GLC. Enantiomeric separations of several different compounds were observed when using the derivatized cyclofructans as chiral selectors. The enantiomers separated include esters, β -lactams, alcohols, and amino acid derivatives. Differences in the enantiomeric separations obtained by using PM-CF6, PM-CF7 and DP-CF6 as the chiral selector were observed. These differences gave some insight as to the mechanism of enantioselectivity for permethylated cyclofructans as GLC chiral selectors.

2.1 Introduction

Cyclofructans are a family of cyclic oligosaccharides which are obtained by fermentation of inulin with *Bacillus circulans* or by incubation of inulin with the derived fructosyltransferase.⁵⁸ Cyclofructans consist of 6 to 8 fructose units connected by β -(1 \rightarrow 2) linkages. They have a crown ether core and the fructose units in the macrocycle are alternately staggered above and below the crown ether ring, as shown in Figures 2.1 and 2.2.

As seen from the crystal structure of CF6 in Figure 2.2, the 1-O, 3-O and 4-O atoms are all located on one side of the molecule while 1-CH₂ and 6-CH₂ groups are on the opposite side. Consequently one side of cyclofructans is hydrophilic and the other side is hydrophobic.

According to computational modeling studies, there are no accessible cavities at the center of the CF6 and CF7 molecules.⁵⁹ This is significantly different from the molecular structures of cyclodextrins which have the shapes of hollow truncated cones, with nonpolar cavities at the center of the macrocycle.⁶⁰⁻⁶³ Both crystal structure and computational modeling studies of native CF6 show that the 3-OH groups in 1, 3-related fructose moieties form stable intramolecular hydrogen bonds. The hydrogen bonded 3-OH groups block the core crown ether structure of the cyclofructans. When all the 3-OH groups are methylated, these intramolecular hydrogen bonding interactions are disrupted, essentially “relaxing” the structure and exposing the central crown ether core. However, it should be noted that the 3-OMe groups still can act as lone electron pair donors. It was reported that when permethylated cyclofructans form complexes with metal cations, the binding points included the oxygens in the crown ether ring and the oxygens in the 3-OMe groups.⁶⁴⁻⁶⁶

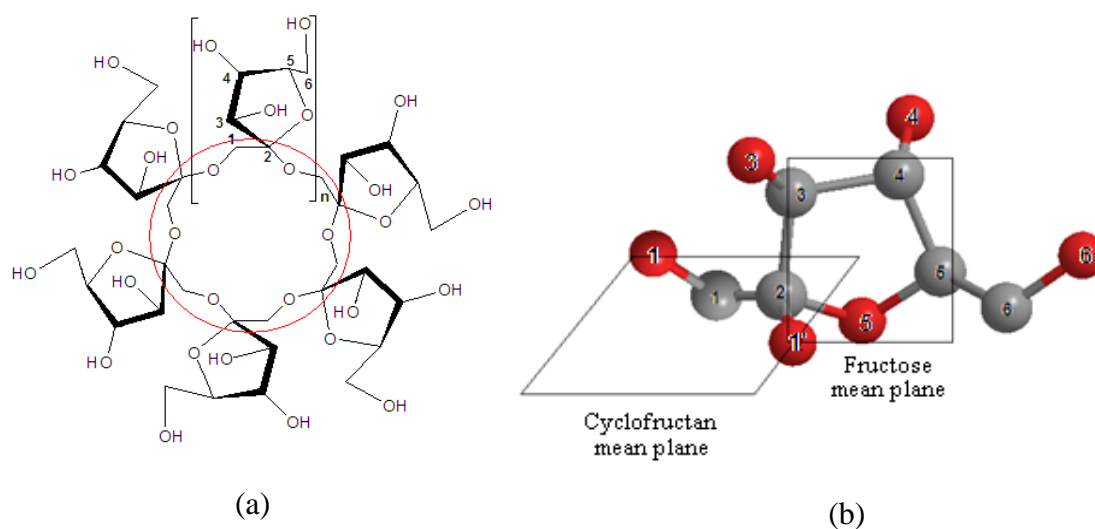


Figure 2.1 (a) structure of cyclofructan and (b) 3D view of fructose moiety in cyclofructan, gray spheres: carbon, red spheres: oxygen. The crown ether ring skeleton is circled in (a).

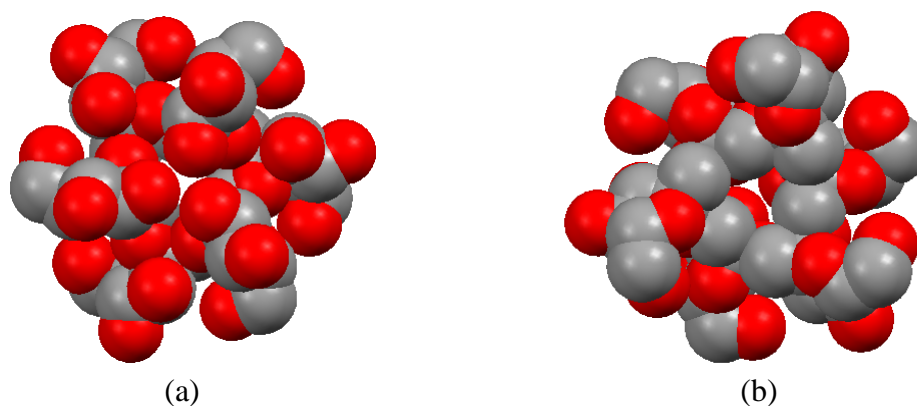


Figure 2.2 Crystal structure of CF6, space-filling image. Gray spheres: carbon, red spheres: oxygen. Structures are shown perpendicular to the cyclofructan mean plan, (a) the hydrophilic side points towards the viewer, the 1-O, 3-O and 4-O atoms are located on this side; (b) the hydrophobic side points towards the viewer, the 1-CH₂ and 6-CH₂ groups are located on this side.

The gas phase chiral discrimination ability of permethylated cyclofructans towards amino acid isopropyl ester ammonium salts has been studied in FAB mass spectrometry.⁶⁷⁻⁶⁹ The ion-dipole interaction between the ammonium groups and the crown ether ring was proposed to be the driving force for the complexation of cyclofructans with amino acid isopropyl ester ammonium salts. Interestingly, it was reported that PM-CF6 showed smaller chiral recognition ability than permethylated linear fructo-oligosaccharides.⁶⁹

To the date, no reports on the enantioselectivity of cyclofructans or their derivatives in GLC have appeared. In this paper, we first report the use of cyclofructan-based chiral selectors in GLC and propose a possible mechanism for chiral recognition.

2.2 Experimental

2.2.1 Materials

NaH, dimethyl sulfoxide and methyl iodide were purchased from Sigma-Aldrich (Milwaukee, WI, USA). Untreated fused silica capillary (I.D. 0.25mm) was purchased from Supelco (Bellefonte, PA, USA). The cyclofructans were the gift of Dr. Mari Yasuda at the Mitsubishi Chemical Group (Tokyo, Japan). The racemic β -lactams were prepared by cycloaddition of chlorosulfonyl isocyanate to the corresponding cycloalkenes and

cycloalkadienes.⁷⁰ All the other analytes were purchased from Sigma-Aldrich (Milwaukee, WI, USA).

2.2.2 Permethylation of Cyclofructans

NaH (12mmol) was added to anhydrous DMSO (1.5mL) and stirred at room temperature for 8 hrs under Argon protection until the mixture became light gray. Next, cyclofructan (0.25mmol) was dissolved in anhydrous DMSO (1mL), and the solution was added to the NaH and DMSO mixture. This mixture was stirred for 30 min, then cooled by ice bath, so that CH₃I (2.7mL) could be added to the mixture. The mixture was stirred for 4 hrs under Argon protection. Subsequently, CH₂Cl₂ (10mL) was added to the solution. The DMSO was removed with water. And the organic layer was collected. After evaporating the solvent, the product was kept in the vacuum over night.

PM-CF6: A white powder (Yield over 85%) was obtained. ¹H NMR (300MHz, DMSO-d₆): δ(ppm) 3.94(6H, d, H-3), 3.86(6H, q, H-5), 3.78(6H, d, H-1), 3.75(6H, t, H-4), 3.60(6H, d, H-1'), 3.50(12H, m, H-6), 3.50(18H, s, CH₃), 3.41(18H, s, CH₃), 3.38(18H, s, CH₃). ESI-MS (m/z) 1247.83 [M+Na]⁺.

PM-CF7: A clear yellow viscous liquid (Yield 53%) was obtained. ¹H NMR (300MHz, DMSO-d₆): δ(ppm) 3.89(7H, d, H-3), 3.80(7H, q, H-5), 3.73(7H, d, H-1), 3.64(7H, t, H-4), 3.57(7H, d, H-1'), 3.45(14H, m, H-6), 3.36(21H, s, CH₃), 3.32(21H, s, CH₃), 3.29(21H, s, CH₃). ESI-MS (m/z) 1451.83 [M+Na]⁺.

2.2.3 Pentylation of cyclofructan

The 4, 6-di-O-pentyl CF6 was synthesized following the procedure for pentylation of cyclodextrin.¹⁷ ESI-MS (m/z) 1837.42 [M+Na]⁺.

2.2.4 Column Preparation

The chiral selector was dissolved in polysiloxane (PM-CF6 and PM-CF7 in polysiloxane OV-1701 (15% by weight), DP-CF6 in polysiloxane OV-17 (15% by weight)). This is much the same as was originally used for permethylated cyclodextrins.¹⁸ The mixture was dissolved in dichloromethane (0.25% w/v). The solution was injected to 10m fused silica capillary which was

set in a water bath at 40°C. One end of the column was sealed while the other end was connected to an adjustable vacuum in order to evaporate the solvent at constant speed. After all the solvent was evaporated the column was conditioned while flushed with helium. The temperature program for conditioning was: from 30 to 150°C at 1°C/min, 150°C for 2 hours and cooled to 100°C over night. The efficiency was tested by injecting naphthalene at 100°C. All columns had efficiency over 3000 plates/m.

2.2.5 Sample Preparation

All the amino acid analytes were derivatized. The carboxylic acid groups were converted to methyl esters by reacting with methanolic HCl. The amino group was trifluoroacetylated according to a literature procedure.⁷¹ The hydroxyl groups of all tartrates were trifluoroacetylated. All chiral analytes were dissolved in dichloromethane as 1mg/mL. An Agilent model 6890N network gas chromatograph system was used for all the separations. Split ratio at the injector was 1:100. A FID detector was employed for all the detections. The temperatures for the injector and the detector were both 250°C.

2.2.6 Modeling

Modeling studies used the published crystal structure of native CF6 and the crystal structure of the complex of PM-CF6 and barium as the point of departure.^{72,73} The structure of PM-CF6 and DP-CF6 were optimized by using Hartree-Fock theory with 6-31g basis set in Gaussian 03.

2.3 Results and Discussion

2.3.1 Modeling Studies

The results of the modeling studies are shown in Figure 2.3. Compared to the crystal structure of native CF6, the structure of PM-CF6 is more flexible and open due to the elimination of the intramolecular hydrogen bonds by the per-O-methylation. The fructose units in the macrocycle are no longer alternately staggered above and below the crown ether ring. The distances between the 3-O atoms increase to about 5Å. Consequently, the crown ether core is more exposed from the hydrophilic side.

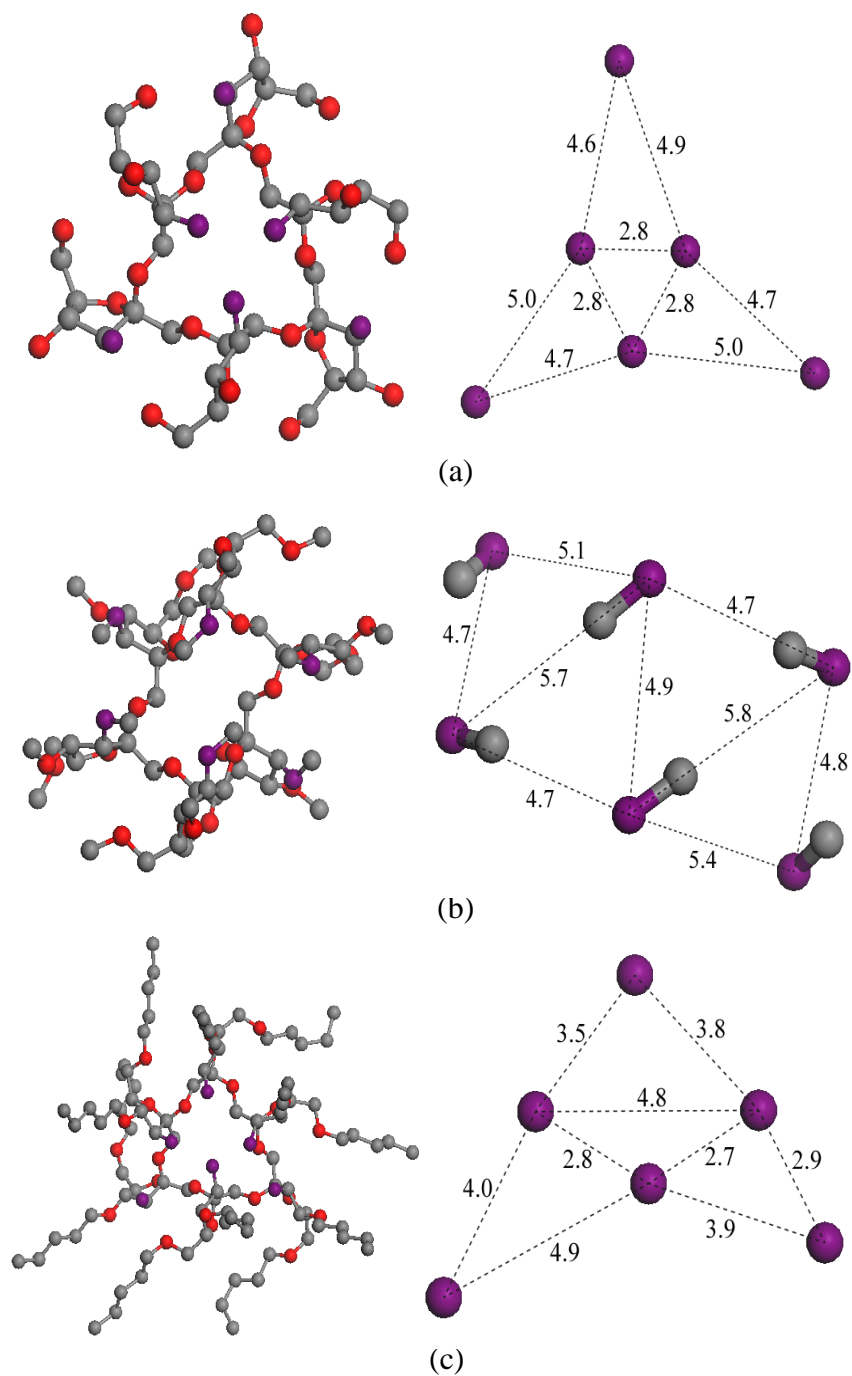


Figure 2.3 Modeling results of derived cyclofructans. Red sphere: oxygen; gray sphere: carbon; purple sphere: 3-O oxygen atom. Structures are shown perpendicular to the cyclofructan mean plane and the 3-O/4-O side points towards the viewer. On the left are (a) the crystal structure of native CF6, (b) the optimized structures of PM-CF6 and (c) the optimized structure of DF-CF6. On the right are the distributions of the 3-O atoms in the corresponding molecule. The numbers are the distances (\AA) between the 3-O atoms.

The spatial arrangement of the DP-CF6 fructose units also are changed due to the steric effects of the 4- and 6-OC₅H₁₁ groups and the disruption of the hydrogen bonds between the 4- and 6-OH groups. Although the 3-OH groups remain underivatized, the distance between two 3-O atoms in 1, 3-related fructose units increases to 4.8Å. Thus the crown ether core is again more exposed from the hydrophilic side.

2.3.2 Influence of Cyclofructan Ring

When PM-CF6 and PM-CF7 were used as GLC chiral selectors, they showed enantioselectivity for at least four classes of compounds, including alcohols, esters, β -lactams and amino acid derivatives. The separation data for PM-CF6 and PM-CF7 chiral stationary phases (CSPs) are given in Tables 2.1 and 2.2. Some data for unseparated analytes are also listed for comparison. Figure 4 shows chromatograms for several separations obtained on PM-CF6 and PM-CF7 CSPs.

One chiral alcohol, 4 β -lactams and 2 amino acid derivatives were separated by both PM-CF6 and PM-CF7. For all of the 7 compounds, the retention factors (k_1) obtained on PM-CF7 were larger than on PM-CF6. PM-CF7 showed slightly larger selectivity factors (α) for the β -lactams analytes, while PM-CF6 had slightly larger selectivity factors for the amino acid derivatives. Also there were several compounds which were separated only on one of the CSPs. Seven more amino acid derivatives were separated on PM-CF6 while PM-CF7 separated four more of the β -lactam analytes. Only PM-CF6 showed enantioselectivities towards the derivatives of tartaric acid. It is obvious that the difference between the structures of PM-CF6 and PM-CF7 have certain influences on their enantioselectivities. However, there are no reported crystal structures of CF7 or PM-CF7. The spatial geometry of the PM-CF7 is unknown. Thus, further study on the structure of PM-CF7 is needed in order to reveal the effect of the ring size on the chiral recognition by PM-CF6 and PM-CF7.

Table 2.1 Chiral analytes separated by PM-CF6

No.	Compound	Structure	T/°C	k1	α	Rs	No.	Compound	Structure	T/°C	k1	α	Rs
1	(±)- α -(Trifluoromethyl)benzyl alcohol		50	93.2	1.05	1.4	13	D-O-trifluoroacetyl di-t-butyl DL-tartrate		70	69.0	1.03	1.1
2	cis-6-azabicyclo[3.2.0]heptan-7-one		80	34.2	1.02	0.6	14	N-trifluoroacetyl leucine methyl ester		60	55.7	1.05	1.5
3	cis-7-azabicyclo[4.2.0]oct-3-en-8-one		100	34.8	1.05	1.4	15	N-trifluoroacetyl isoleucine methyl ester		50	75.8	1.13	2.7
4	cis-7-azabicyclo[4.2.0]oct-4-en-8-one		90	34.7	1.02	0.8	16	N-acetyl isoleucine methyl ester		50	27.9	1.01	0.6
5	cis-3,4-benzo-6-azabicyclo[3.2.0]heptan-7-one		135	34.6	1.02	0.8	17	N-trifluoroacetyl alanine methyl ester		50	19.5	1.03	0.9
6	Di-O-trifluoroacetyl dimethyl DL-tartrate		65	26.9	1.03	0.9	18	N-trifluoroacetyl valine methyl ester		60	20.4	1.03	1.1
7	Mono-O-trifluoroacetylated dimethyl DL-tartrate		65	84.3	1.03	1.0	19	N-trifluoroacetyl methionine methyl ester		100	40.2	1.02	0.8
8	Di-O-trifluoroacetyl diethyl DL-tartrate		70	40.0	1.03	1.4	20	N-trifluoroacetyl aspartic acid methyl ester		70	94.3	1.02	0.6
9	Mono-O-trifluoroacetylated diethyl DL-tartrate		70	121.7	1.02	0.9	21	N-trifluoroacetyl phenylalanine isopropyl ester		100	98.4	1.02	0.7
10	Di-O-trifluoroacetyl diisopropyl DL-tartrate		70	51.1	1.02	0.9	22	N-trifluoroacetyl phenylalanine methyl ester		100	65.7	1.01	0.5
11	Mono-O-trifluoroacetyl diisopropyl DL-tartrate		70	153.0	1.01	0.6	23	1-Phenylethanol		50	34.4	1.00	-
12	Diisopropyl DL-tartrate		70	243.5	1.03	1.3	24	Trifluoroacetyl (±)- α -(trifluoromethyl)benzyl alcohol		50	4.2	1.00	-

Table 2.2 Chiral analytes separated by PM-CF7

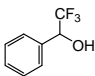
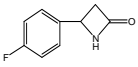
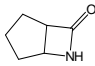
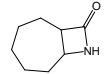
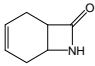
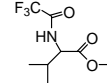
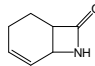
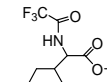
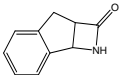
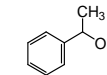
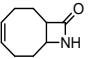
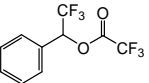
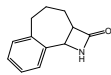
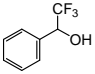
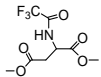
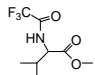
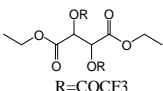
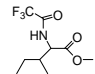
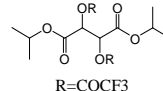
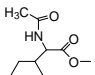
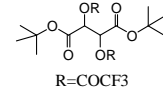
No.	Compound	Structure	T/°C	k1	α	Rs	No.	Compound	Structure	T/°C	k1	α	Rs
1	(±)- α -(Trifluoromethyl)benzyl alcohol		50	126.2	1.04	0.8	8	4-(p-fluorophenyl)-2-azetidinone		120	69.2	1.01	0.6
2	cis-6-azabicyclo[3.2.0]heptan-7-one		80	42.0	1.03	0.8	9	cis-8-azabicyclo[5.2.0]nonan-9-one		110	39.2	1.02	1.0
3	cis-7-azabicyclo[4.2.0]oct-3-en-8-one		100	40.5	1.07	2.1	10	N-trifluoroacetyl leucine methyl ester		60	64.6	1.03	0.8
4	cis-7-azabicyclo[4.2.0]oct-4-en-8-one		90	45.4	1.03	0.9	11	N-trifluoroacetyl isoleucine methyl ester		50	78.3	1.10	1.9
5	cis-3,4-benzo-6-azabicyclo[3.2.0]heptan-7-one		135	42.2	1.02	0.8	12	1-Phenylethanol		50	43.1	1.00	-
6	cis-3,4-benzo-6-azabicyclo[3.2.0]heptan-7-one		125	43.8	1.02	0.6	13	Trifluoroacetyl (±)- α -(trifluoromethyl)benzyl alcohol		50	4.4	1.00	-
7	cis-5,6-benzo-8-azabicyclo[5.2.0]nonan-9-one		150	74.7	1.02	0.7							

Table 2.3 Chiral analytes separated by DP-CF6

No.	Compound	Structure	T/°C	k1	α	Rs	No.	Compound	Structure	T/°C	k1	α	Rs
1	(±)- α -(Trifluoromethyl)benzyl alcohol		50	131.3	1.01	0.6	5	N-trifluoroacetyl aspartic acid methyl ester		70	65.9	1.06	1.1
2	N-trifluoroacetyl leucine methyl ester		60	32.9	1.02	0.8	6	Di-O-trifluoroacetyl diethyl DL-tartrate		60	18.1	1.01	0.5
3	N-trifluoroacetyl isoleucine methyl ester		50	39.7	1.10	3.0	7	Di-O-trifluoroacetyl diisopropyl DL-tartrate		70	23.4	1.01	0.6
4	N-acetyl isoleucine methyl ester		50	35.6	1.02	0.8	8	Di-O-trifluoroacetyl di-t-butyl DL-tartrate		70	37.0	1.02	0.7

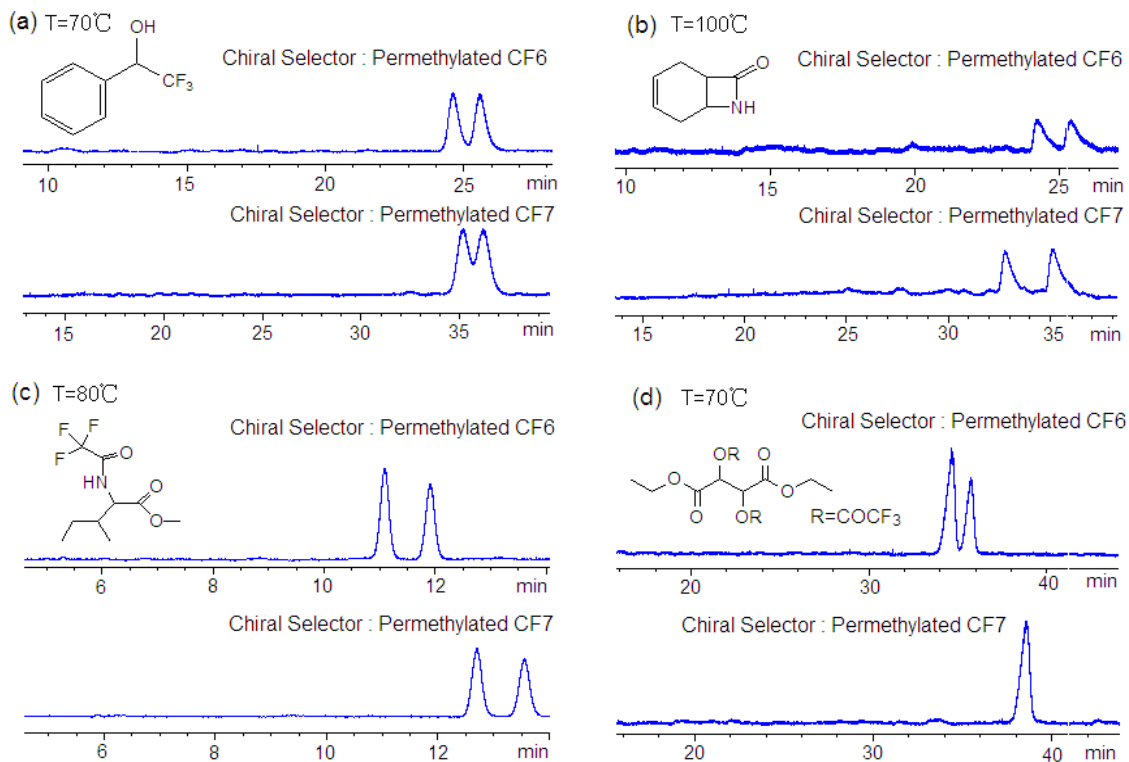


Figure 2.4 Chiral separations obtained by PM-CF6 and PM-CF7. In chromatograms (d), the sample was a mix of D and L enantiomers, the samples in (a), (b) and (c) were racemates. Chromatographic conditions: carrier gas: Helium, flow rate: 1.0 mL/min, split ratio: 100:1, FID.

2.3.3 Influence of Substituents

Eight analytes separated on the DP-CF6 CSP are listed in Table 2.3. All of these analytes also were separated on the PM-CF6 stationary phase. One major difference between the DP-CF6 and PM-CF6 phase is that the DP-derivative has six hydrogen bond donor groups, which appear to have negative effects on chiral recognition in many cases. Most of the separated enantiomers had smaller selectivity factors on the DP-CF6 stationary phase as compared to the PM-CF6 phase. However, DP-CF6 produces a larger selectivity factor for N-trifluoroacetyl aspartic acid methyl ester than does PM-CF6. This may be due to the fact that N-trifluoroacetyl aspartic acid methyl ester has one more hydrogen bond accepting site than the other amino acid derivatives.

The pentyl substituents on the cyclofructans also had an influence on the retention factors of these analytes. Most analytes had smaller retention factors on the DP-CF6 phase than on the PM-CF6 phase. The steric effect of the $-OC_5H_{11}$ groups in DP-CF6 is much larger than that of the $-OMe$ groups of the PM-CF6. This steric effect could weaken dipole-dipole interactions or hydrogen bonding interactions involving the ether oxygens in the $-OC_5H_{11}$ groups. However, α -(trifluoromethyl)benzyl alcohol and N-acetyl isoleucine methyl ester have larger retention factors on the DP-CF6 stationary phase than on the PM-CF6 phase. It appears that their retention is not affected by the steric effect of the pentyl substituents.

2.3.4 Comparison with Synthetic Chiral Crown Ethers

Cyclofructans are, in fact, chiral crown ethers. However, the enantioselectivity of cyclofructans is considerably different when compared to Chiralsil-man-18C6-25, a synthetic chiral crown ether based CSP which has an aromatic moiety in the structure.⁷⁴ The Chiralsil-man-18C6-25 showed enantioselectivity to racemic compounds. However, these racemic analytes had to have both an aromatic group and either a primary amine or hydroxyl group in the structure.⁷⁵ When the $-OH$ groups or $-NH_2$ moieties of the analytes are derivatized to $-OCOCF_3$ or $-NHCOCF_3$ groups, the Chiralsil-man-18C6-25 phase lost enantioselectivity for those analytes. Thus, the hydrogen bonding interactions between the chiral crown ether with the primary amino group or hydroxyl group of the analytes were crucial for the enantioselectivity of the Chiralsil-man-18C6-25 stationary phase. For comparison, 2-phenyl-1-propanol, 2-phenylpropan-1-amine, phenylalanine isopropyl ester and their trifluoroacetylated derivatives were tested on the PM-CF6 CSP. The experimental data on the PM-CF6 phase and the literature data on the Chiralsil-man-18C6-25 phase are listed in Table 2.4. The PM-CF6 phase separated none of the 3 underivatized compounds. However, after trifluoroacetylation of the analytes, the N-trifluoroacetyl phenylalanine isopropyl ester enantiomers were separated on the PM-CF6 phase. This is opposite to the result obtained on the Chiralsil-man-18C6-25 phase. Also an investigation of the retention factors of 2-phenylpropan-1-amine and phenylalanine

isopropyl ester indicated that they significantly increased after trifluoroacetylation. This shows that the trifluoroacetyl group has stronger interactions with the PM-CF6 stationary phase than does the primary amine group, and it facilitates the enantiomeric separation of N-trifluoroacetyl phenylalanine isopropyl ester on the the PM-CF6 phase. Also seen from the data in Tables 1 and 2 are that PM-CF6 and PM-CF7 showed enantioselectivities towards analytes most of which had their hydroxyl groups or amino groups trifluoroacetylated. The crown ether core of PM-CF6 and PM-CF7 may be irrelevant to these enantiomeric separations. Thus, PM-CF6 or PM-CF7 stationary phases have unique enantioselectivities compared to the Chiralsil-man-18C6-25 phase.

Table 2.4 Comparison of some enantiomeric separations on PM-CF6 CSP and Chiralsil-man-18C6-25 phase

No.	Compound	Structure	Experimental data on PM-CF6 CSP				Literature values on Chiralsil-man-18C6-25 phase [18]	
			T/°C	k1	α	Rs	T/°C	α
1	2-Phenyl-1-propanol		100	5.9	1.00	-	140	1.046
2	Trifluoroacetylated 2-phenyl-1-propanol		100	3.2	1.00	-		
3	Phenylalanine isopropyl ester		100	49.1	1.00	-	150	1.068
4	N-trifluoroacetyl phenylalanine isopropyl ester		100	98.4	1.02	0.7		
5	2-phenylpropan-1-amine		100	6.0	1.00	-	140	1.027
6	Trifluoroacetylated 2-phenylpropan-1-amine		100	28.8	1.00	-		

2.3.5 Mechanism

As mentioned previously, the crown ether core of the cyclofructan phases does not appear to be involved in the separation mechanism for most of the enantiomers that were separated in this study. The active interaction sites for these analytes are likely to be located on

the outer surface of the molecule, especially on the hydrophilic side. This is because the hydrophilic side of the chiral selector provides far more possible interaction sites than the hydrophobic side, which consists of aliphatic groups that are limited to dispersive interactions.

There are two types of associative interactions that are likely to contribute to the chiral recognition of the β -lactams and amino acid derivatives, both of which have amide groups. The first type is the dipole-dipole interaction occurring between the amide groups of the analytes and the $-\text{OMe}$ groups of the permethylated cyclofructans. The second is the hydrogen bonding interaction occurring between the hydrogen in the amide groups of the analytes and the $-\text{OMe}$ groups in the permethylated cyclofructans. The trifluoroacetylation of the amine groups appears to be essential for the enantiomeric separation of the amino acid derivatives. The $-\text{COCF}_3$ groups not only make the amino acids more volatile but also create a strong dipole.⁷⁵ When using acetyl derivatization of the amino groups, only PM-CF6 showed a small enantiomeric selective factor and retention factor for N-acetyl isoleucine methyl ester, while the other acetylated racemic analytes could not be separated. This may be due to less pronounced dipole of $-\text{NHCOCH}_3$ as compared to $-\text{NHCOCF}_3$.⁷⁶ However, this could also be explained by the hydrogen bonding interactions occurring between the hydrogen in the amide groups of the analytes and the $-\text{OMe}$ groups in the permethylated cyclofructans. Due to the strong electronegativity of the trifluoromethyl group, the hydrogen in the $-\text{NHCOCF}_3$ group is more acidic than the hydrogen in the $-\text{NHCOCH}_3$ group.^{77, 78} Thus, the N-trifluoroacetylated amino acid methyl esters have stronger hydrogen bonding interactions with the permethylated cyclofructans than their N-acetylated counterparts.

The most plausible interactions facilitating the enantiomeric separation of the di-O-trifluoroacetylated tartrates are dipole-dipole interactions occurring between the ester groups of the analytes and the $-\text{OMe}$ groups in the permethylated cyclofructans. This is because that the di-O-trifluoroacetylated tartrates are no longer hydrogen bond donors after trifluoroacetylation of all the hydroxyl groups and the permethylated cyclofructans are not hydrogen bond donors

either. Thus hydrogen bonding interactions are not likely to occur due to lack of hydrogen bond donor. However, there are four ester groups in each di-O-trifluoroacetyled tartrate molecule. Ester groups have permanent dipole moments.⁷⁸ Thus the dipole-dipole interactions between di-O-trifluoroacetyled tartrate and permethylated cyclofructans are very likely. The mono-trifluoroacetyled tartrates and native tartrates are likely to interact with permethylated cyclofructans via hydrogen bonding interactions since there are one or two hydroxyl groups available. However, it appears that the hydrogen bonding interactions only greatly increase the retention factors but do not improve the chiral recognition of these analytes.

Permethylated cyclofructans also can provide hydrogen bonding interactions with alcohols, particularly with –OH groups that are alpha to –CF₃ groups. Both PM-CF6 and PM-CF7 could separate underivatized α -(trifluoromethyl)benzyl alcohol. When the hydroxyl group of α -(trifluoromethyl)benzyl alcohol was derivatized to –OCOCF₃, both PM-CF6 and PM-CF7 lost enantioselectivity, and the retention factor was greatly reduced (as shown in Tables 1 and 2). Thus, the hydroxyl group of α -(trifluoromethyl)benzyl alcohol provides an important interaction with the PM-CF6 and PM-CF7 phases. However, 1-phenylethanol, which has a methyl group rather than the trifluoromethyl group, could not be separated by either PM-CF6 or PM-CF7, and the retention factor also was significantly reduced. This is because the trifluoromethyl group of α -(trifluoromethyl)benzyl alcohol makes the hydroxyl group more acidic and significantly enhances its hydrogen bonding interaction with PM-CF6 and PM-CF7.⁷⁹ Whether this hydrogen bonding interaction occurs on the outer surface of permethylated cyclofructan or involves the exposed crown ether ring oxygens remains unclear and is the subject of future studies.

2.4 Conclusions

PM-CF6 and PM-CF7 have different enantioselectivities when used as chiral selectors in gas chromatography. The hydrogen bonding and dipole-dipole interactions occurring on the pendant fructose moieties of the cyclofructan molecules play an important role in chiral recognition. Also, due to the lack of inclusion complexation as seen with cyclodextrins, PM-CF6

and PM-CF7 have more limited enantioselectivities when compared to similarly derivatized α -cyclodextrin and β -cyclodextrin.³⁹ However, this manuscript serves only as an initial report on the feasibility of using cyclofructans as CSPs in GLC. Ongoing efforts to find the best cyclofructan derivatives are being conducted with the hopes that these cyclofructan based stationary phase will become very effective and competitive chiral selectors for GLC.

CHAPTER 3
4,6-DI-O-PHENYL-3-O-TRIFLUOROACETYL/PROPIONYL CYCLOFRUCTAN CHIRAL
SELECTORS

4,6-Di-O-pentyl-3-O-trifluoroacetyl cycloinulohexaose (DP-TA-CF6) and 4,6-Di-O-pentyl-3-O-propionyl cycloinulohexaose (DP-PN-CF6) were synthesized and used as chiral stationary phases (CSPs) in gas chromatography (GC). The chiral recognition ability of the two CSPs was investigated. A total of 47 racemic compounds were separated on the two new CSPs, including derivatized amino acids, amino alcohols, amines, alcohols, tartrates and lactones. Interestingly, several analytes were only separated on either the DP-TA-CF6 or the DP-PN-CF6 phase. The chiral recognition mechanism was evaluated through thermodynamic analysis. The result indicated there was no inclusion complex formation involved in the chiral recognition process.

3.1 Introduction

Because of the high efficiency, sensitivity and simplicity, chiral gas chromatography has been widely applied to separate enantiomers that are volatile and thermally stable. Over the last two decades, direct enantiomeric separations of a variety of racemic compounds had been done on gas chromatographic chiral stationary phases.⁸⁰ Three types of chiral stationary phases are mainly used for those enantiomeric separations: 1) chiral amino acid derivatives,^{1,81-88} 2) chiral metal coordination compounds^{89,90} and 3) cyclodextrin derivatives.^{11,13,15-19,38,91-93} Of these, the cyclodextrin-based selectors dominate the field. A few other types of chiral stationary phases were reported, such as chiral crown ethers,⁷⁴ chiral ionic liquids⁹⁴ and mixed binary chiral selectors.^{29,32} Recently, a completely new series of chiral selectors, cyclofructan

derivatives, has attracted attention in high performance liquid chromatography (HPLC),⁹⁵⁻⁹⁸ gas chromatography⁹⁹ and capillary electrophoresis (CE).¹⁰⁰

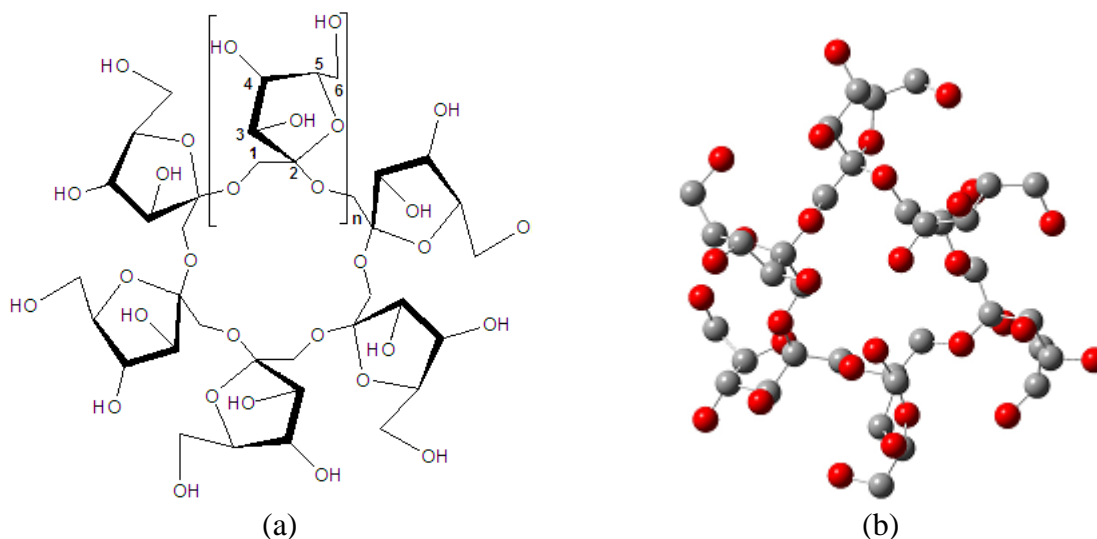


Figure 3.1 Structure of native cyclofructan (a) and 3D view of native CF6 (b). The grey spheres are carbons and the red spheres are oxygens.

Cyclofructans are a family of cyclic oligosaccharides which consist of 6 to 8 β -(2 \rightarrow 1) linked D-fructofuranose units. The linkage forms a crown ether core in the central part of the macrocyclic molecule (as shown in Figure 1). In native cyclofructans, the crown ether core is blocked by intramolecular hydrogen bonds formed between the hydroxyl groups.^{101,102} When various hydroxyl groups are derivatized the crown ether core becomes more accessible to guests.^{95,99} However, derivatized cyclofructans behave significantly different from the other synthetic chiral crown ether CSPs in HPLC^{96,97} and GC.⁹⁹ Also, cyclofructans have very different chiral recognition capabilities than their cyclodextrin isomers.^{99,104,105}

In HPLC and CE, native cyclofructans have very limited enantioselectivity while several derivatized cyclofructans have shown exceptional chiral recognition ability towards a variety of racemic compounds. An aliphatic functionalized cyclofructan CSP provided effective enantiomeric separations for racemic primary amine-containing compounds⁹⁷ while two aromatic

functionalized cyclofructans showed chiral recognition towards a variety of non-primary amine-containing compounds.⁹⁵ In CE, sulfated cyclofructans had good enantioselectivity towards primary, secondary and tertiary amine-containing compounds.¹⁰⁰

In GC, the chiral recognition abilities of permethylated cycloinulohexaose (PM-CF6), permethylated cycloinuloheptaose (PM-CF7) and 4,6-dipentylated cycloinulohexaose (DP-CF6) have been investigated and compared in detail.⁹⁹ Those three CSPs showed limited enantioselectivities and no thermodynamic analyses were performed due to the complexity of studying chiral selectors that are dissolved in achiral matrixes.^{106,107} In this study, DP-TA-CF6 and DP-PN-CF6 were synthesized and used as chiral selectors in GC. Their enantioselectivity was investigated by injecting a variety of racemic compounds and their derivatives. The enantiomeric separation is based on the formation of reversible diastereomeric associates or complex between enantiomers and chiral selectors via intermolecular interactions and the process could be characterized by thermodynamic parameters, ΔG° , ΔH° and ΔS° .¹⁰⁷ Thus thermodynamic analyses were carried out to gain possible insights into the enantiomeric separation mechanism. This was more easily achieved when these chiral selectors were directly coated without dissolving them in any achiral matrix.

3.2 Experimental

3.2.1 Materials

Sodium hydroxide, dimethyl sulfoxide, 1-bromopentane, trifluoroacetyl anhydride and propionic anhydride were purchased from Sigma-Aldrich (Milwaukee, WI, USA). Salt treated fused silica capillary (I.D. 0.25mm) was purchased from Supelco (Bellefonte, PA, USA). The cyclofructans were obtained from AZYP (Arlington, TX, USA). All the analytes were purchased from Sigma-Aldrich.

3.2.2 Stationary phases

3.2.2.1 4, 6-Di-O-pentyl cycloinulohexaose

Cycloinulohexaose (2g, 2mmol) was dissolved in anhydrous DMSO (30mL). The solution was cooled in ice bath, and finely grounded NaOH powder (5g, 125mmol) was added into the solution as small portions. After the NaOH totally dissolved, 1-bromopentane (12mL, 96mmol) was added into the above mixture. The mixture was brought to room temperature and stirred for 48hrs. Subsequently, water (60mL) and CHCl_3 (60mL) was added to the mixture. The organic phase was collected and washed with water (60mL \times 8 times). A white waxy phase was collected. After evaporation of the solvent, a clear viscous liquid was obtained (3g, yield 80%).

3.2.2.2 4, 6-Di-O-pentyl-3-O-trifluoroacetyl cycloinulohexaose (DP-TA-CF6)

4, 6-Di-O-pentyl cycloinulohexaose (0.5g, 0.27mmol) was dissolved in anhydrous THF (20mL). Trifluoroacetyl anhydride (5mL) was added in the solution under argon protection. The mixture was stirred and refluxed for 3hrs while extra trifluoroacetic anhydride (2mL) was added to the mixture every 30min to compensate for the lose of trifluoroacetic anhydride at high temperature. Subsequently, the mixture was poured over ice and the product was extracted by CHCl_3 (80mL). The organic phase was washed with cold aqueous NaHCO_3 solution (5%, 80mL \times 3 times) and ice cold water (80mL \times 3 times), then dried with Na_2SO_4 . After evaporation of the solvent, a clear viscous liquid was obtained (0.47g, yield 72%).

3.2.2.3 4, 6-Di-O-pentyl-3-O-propionyl cycloinulohexaose (DP-PN-CF6)

4, 6-Di-O-pentyl cycloinulohexaose (0.5g, 0.27mmol) was dissolved in anhydrous THF (20mL). Propionic anhydride (10mL) was added to the solution under argon protection. The mixture was stirred and refluxed for 8hrs. The solvent and the excess propionic anhydride were evaporated under vacuum at 80°C. The crude product was dissolved in methyl t-butyl ether (15mL), and washed with a cold NaHCO_3 solution (5%, 10mL \times 2 times) and ice cold water (10mL \times 3 times). The organic phase was dried with Na_2SO_4 . After evaporation of the solvent, a clear viscous liquid was obtained (0.41g, yield 71%).

3.2.3 Columns

20 meter salt treated fused silica capillary columns were coated with DP-TA-CF6 and DP-PN-CF6, via the static coating method. The chiral stationary phase was dissolved in dichloromethane (0.25% w/v). The solution was used to fill 20m salt treated silica capillary which was set in a water bath at 40°C. One end of the column was sealed while the other end was connected to an adjustable vacuum in order to evaporate the solvent at constant speed. After all the solvent was evaporated the column was conditioned while being flushed with helium. The temperature program for conditioning was: 30 to 120°C at 1°C/min, 120°C for 2hrs. Then the column was cooled to 100°C and kept at 100°C overnight. The efficiency was tested by injecting naphthalene at 100°C. The two columns had efficiency over 3500 plates/m.

3.2.4 Sample preparation and GC method

All the hydroxyl and amino groups were trifluoroacetylated unless stated otherwise. The carboxyl groups were methylated. The derivatized analytes were dissolved in dichloromethane at 1mg/mL. An Agilent model 6890N network gas chromatograph system was used for all the enantiomeric separations. Helium was used as the carrier gas with a flow rate of 1mL/min. The injection volume was 1µL. The split ratio was 1:100 at the injector. Detection was achieved with a FID detector. The injector and detector temperatures were 250°C.

3.3 Results and Discussion

3.3.1 Enantiomeric separations

As indicated in Table 3.1, 41 enantiomeric separations were obtained on the DP-TA-CF6 stationary phase while the DP-PN-CF6 phase separated 44 racemates. The separated analytes included derivatized amino acids, amino alcohols, amines, alcohols, tartrates and lactones. The majority of the separated analytes have at least two non-alkyl functional groups closely bonded to the chiral center. Only a few racemic amines which only contained one non-alkyl functional group were separated with the DP-PN-CF6 stationary phase.

Table 3.1 Separations on DP-TA-CF6 and DP-PN-CF6

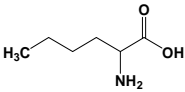
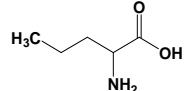
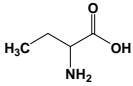
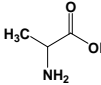
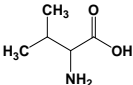
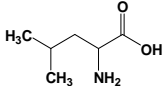
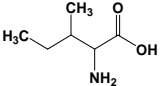
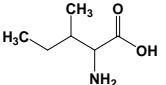
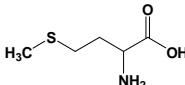
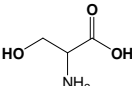
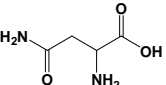
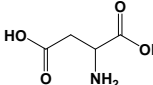
No.	racemic compound ^a	structure	T/°C	k1	α	Rs	CSP
1	Norleucine		70	32.77	1.03	1.5	DP-TA-CF6
			70	38.71	1.03	1.5	DP-PN-CF6
2	Norvaline		60	30.35	1.03	1.5	DP-TA-CF6
			60	36.22	1.03	1.5	DP-PN-CF6
3	2-Aminobutyric acid		50	27.50	1.03	1.5	DP-TA-CF6
			50	31.92	1.03	1.5	DP-PN-CF6
4	Alanine		40	29.70	1.03	1.5	DP-TA-CF6
			40	37.28	1.03	1.5	DP-PN-CF6
5	Valine		50	35.09	1.03	1.5	DP-TA-CF6
			50	35.99	1.03	1.5	DP-PN-CF6
6	Leucine		70	24.43	1.03	1.5	DP-TA-CF6
			70	29.83	1.03	1.5	DP-PN-CF6
7	Allo-isoleucine		100	0.97	1.05	1.5	DP-TA-CF6
			100	1.19	1.06	2.6	DP-PN-CF6
8	Isoleucine		100	4.32	1.06	2.7	DP-TA-CF6
			100	4.57	1.06	2.6	DP-PN-CF6
9	Methionine		80	105.74	1.02	0.8	DP-TA-CF6
			80	158.00	1.01	1.0	DP-PN-CF6
10	Serine		60	46.02	1.01	0.6	DP-TA-CF6
			60	70.69	1.01	0.5	DP-PN-CF6
11	Asparagine		80	43.34	1.01	0.5	DP-TA-CF6
12	Aspartic acid		80	43.68	1.01	0.5	DP-TA-CF6
			80	52.10	1.01	0.5	DP-PN-CF6

Table 3.1-continued

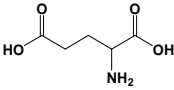
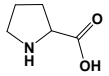
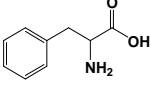
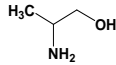
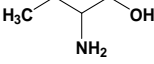
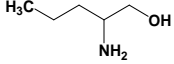
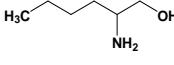
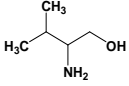
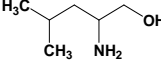
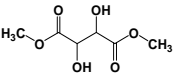
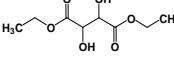
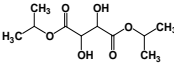
13	Glutamic acid		100	35.38	1.01	0.6	DP-TA-CF6
			100	46.17	1.01	0.8	DP-PN-CF6
14	Proline		70	58.14	1.01	0.8	DP-TA-CF6
15	Phenylalanine		100	73.76	1.01	0.8	DP-PN-CF6
16	2-Amino-1-propanol		45	47.69	1.01	0.6	DP-TA-CF6
			45	73.30	1.02	0.6	DP-PN-CF6
17	2-Amino-1-butanol		50	50.95	1.01	0.6	DP-TA-CF6
			60	49.63	1.01	0.6	DP-PN-CF6
18	2-Amino-1-pentanol		60	44.69	1.02	0.8	DP-TA-CF6
			60	81.10	1.02	0.8	DP-PN-CF6
19	2-Amino-1-hexanol		60	95.72	1.02	0.6	DP-TA-CF6
			60	154.53	1.02	1.1	DP-PN-CF6
20	2-Amino-3-methyl-1-butanol		60	28.24	1.01	0.7	DP-TA-CF6
			60	46.54	1.02	1.0	DP-PN-CF6
21	Leucinol		60	57.02	1.02	1.0	DP-TA-CF6
			60	110.28	1.02	0.8	DP-PN-CF6
22	Dimethyl tartrate		60	29.90	1.01	0.8	DP-TA-CF6
			60	30.21	1.02	1.5	DP-PN-CF6
23	Diethyl tartrate		60	69.54	1.01	0.7	DP-TA-CF6
			60	66.27	1.02	1.0	DP-PN-CF6
24	Diisopropyl tartrate		60	98.27	1.01	0.7	DP-TA-CF6
			60	85.26	1.01	0.6	DP-PN-CF6

Table 3.1-continued

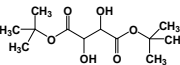
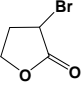
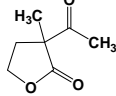
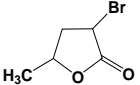
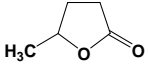
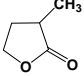
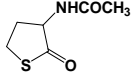
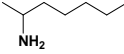
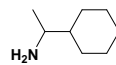
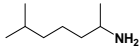
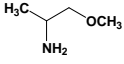
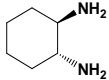
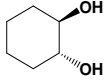
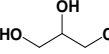
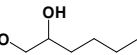
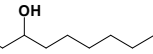
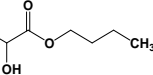
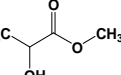
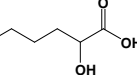
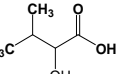
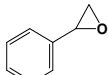
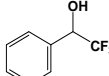
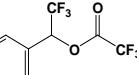
25	Di-tert-butyl tartrate		60	134.44	1.01	0.6	DP-TA-CF6
			60	124.88	1.02	1.3	DP-PN-CF6
26	α -Bromo- γ -butyrolactone		60	58.17	1.01	0.5	DP-TA-CF6
			60	81.15	1.01	0.6	DP-PN-CF6
27	α -Acetyl- α -methyl- γ -butyrolactone		60	41.06	1.01	0.5	DP-TA-CF6
			60	40.22	1.01	0.5	DP-PN-CF6
28	α -Bromo- γ -valerolactone ^b		60	63.77	1.02	1.1	DP-TA-CF6
				96.96	1.01	0.5	DP-TA-CF6
			60	77.22	1.03	1.6	DP-PN-CF6
				126.08	1.00	0.0	DP-PN-CF6
29	γ -Valerolactone		45	28.04	1.01	0.6	DP-TA-CF6
			45	20.46	1.02	0.7	DP-PN-CF6
30	α -Methyl- γ -butyrolactone		45	23.73	1.01	0.6	DP-TA-CF6
			45	17.84	1.01	0.8	DP-PN-CF6
31	N-Acetylhomocysteine thiolactone		125	43.84	1.01	0.6	DP-PN-CF6
32	2-Aminoheptane		60	37.06	1.01	0.7	DP-PN-CF6
33	1-Cyclohexyl-ethylamine		80	34.23	1.01	0.6	DP-PN-CF6
34	1,5-Dimethylhexylamine		80	17.48	1.01	0.6	DP-PN-CF6
35	1-Methoxy-2-propylamine		30	24.50	1.02	0.5	DP-TA-CF6

Table 3.1-continued

36	(±)-trans-1,2-Diaminocyclohexane		115	31.36	1.04	1.3	DP-TA-CF6
			130	26.08	1.03	1.3	DP-PN-CF6
37	(±)-trans-1,2-Cyclohexanediol		40	47.06	1.01	0.5	DP-TA-CF6
			40	38.92	1.01	0.7	DP-PN-CF6
38	3-Chloro-1, 2-propanediol		40	27.48	1.01	0.6	DP-TA-CF6
			40	37.69	1.02	0.6	DP-PN-CF6
39	1, 2-Hexanediol		40	30.15	1.01	0.6	DP-PN-CF6
40	1, 2-Octanediol		60	47.04	1.01	0.6	DP-PN-CF6
41	Butyl lactate		45	24.58	1.01	0.8	DP-TA-CF6
			45	20.24	1.01	0.5	DP-PN-CF6
42	Methyl lactate		30	5.37	1.02	0.8	DP-TA-CF6
			30	4.52	1.02	0.6	DP-PN-CF6
43	2-Hydroxyhexanoic acid		30	63.41	1.01	0.8	DP-TA-CF6
44	2-Hydroxy-3-methylbutyric acid		30	15.39	1.01	0.7	DP-TA-CF6
			30	12.41	1.01	0.6	DP-PN-CF6
45	Styrene oxide		40	40.64	1.02	1.2	DP-TA-CF6
			40	52.98	1.02	1.3	DP-PN-CF6
46	(±)-α-(Trifluoromethyl)benzyl alcohol		70	23.57	1.03	1.7	DP-TA-CF6
			70	61.23	1.01	0.6	DP-PN-CF6
47	O-Trifluoroacetyl (±)-α-(trifluoromethyl)benzyl alcohol		30	12.14	1.01	0.5	DP-TA-CF6
			30	12.44	1.02	0.9	DP-PN-CF6

^aOnly tartrates were mixtures of D and L enantiomers. All the other analytes were racemates. All analyte amino and hydroxyl groups were trifluoroacetylated and carboxyl groups were converted to their methyl esters except (±)-α-(trifluoromethyl)benzyl alcohol. ^bα-Bromo-γ-valerolactone has two pairs of enantiomers.

3.3.2 Enantiomeric separation mechanism

3.3.2.1 Influence of substituents

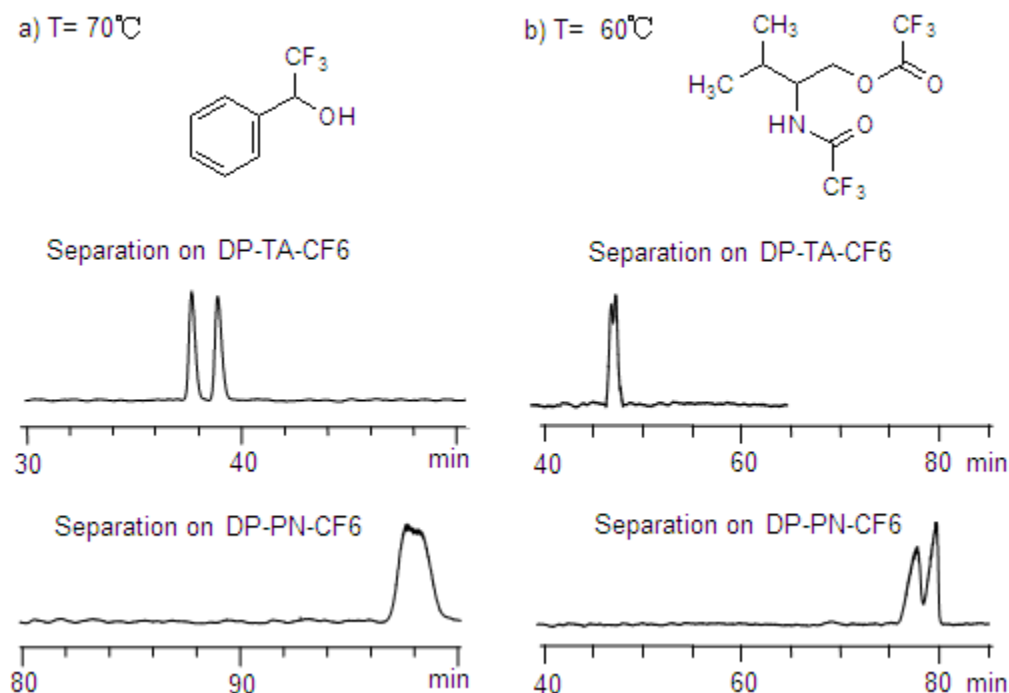


Figure 3.2 Enantiomeric separations of a) $(\pm)\text{-}\alpha\text{-}(\text{trifluoromethyl})\text{benzyl alcohol}$ and b) $N,O\text{-trifluoroacetyl 2-amino-3-methyl-1-butanol}$ on DP-TA-CF6 and DP-PN-CF6 CSPs.

Although all the analytes except $(\pm)\text{-}\alpha\text{-}(\text{trifluoromethyl})\text{benzyl alcohol}$ had been derivatized in this study, the analytes which contained a primary amine group had one hydrogen left on the amide group after derivatization. Thus the derivatized amines, amino acids and amino alcohols still possessed hydrogen bonding capacities.⁸⁵⁻⁸⁸ As shown in Table 1, the DP-PN-CF6 yielded larger retention factors for the analytes that had hydrogen bonding donor groups than did DP-TA-CF6. However, analytes, which possess no hydrogen bonding donor capabilities but only have permanent dipole moments, resulted in larger retention factors on the DP-TA-CF6 stationary phase. Since all the hydroxyl groups in DP-TA-CF6 and DP-PN-CF6 have been derivatized the two CSPs can only act as hydrogen bonding acceptors. The

difference in structures between the two CSPs is that DP-PN-CF6 has propionic groups bonded to the 3-O atoms in the fructofuranose moieties while DP-TA-CF6 has trifluoroacetyl groups bonded to the 3-O atoms. The trifluoromethyl moiety is more electronegative than the ethyl moiety.^{108, 109} Thus, the carbonyl moiety in trifluoroacetyl groups is less electron rich than the carbonyl moiety in propionic groups. Consequently, the DP-PN-CF6 is a better hydrogen bonding acceptor than the DP-TA-CF6 stationary phase. This is in agreement with the empirical finding that analytes containing hydrogen bonding donor groups, such as amino acids and amino alcohols were retained longer on DP-PN-CF6. On the other hand, since the trifluoroacetyl groups have stronger dipole moments than the propionic groups DP-TA-CF6 can provide stronger dipole-dipole interactions with the analytes than can DP-PN-CF6.^{75, 78} Again, this agrees with the experimental findings in which DP-TA-CF6 provided larger retention factor towards the analytes which have permanent dipole moments but no hydrogen bonding donor groups.

It must be noted, however, that the enantioselectivity of the analytes on these two CSPs are independent of their retention factors. Most of the analytes had very similar selective factors on the two CSPs. As shown in Figure 3.2, the two analytes with hydrogen bonding donor capability were retained longer on DP-PN-CF6 phase while one is better separated on DP-TA-CF6 and the other was better separated on DP-PN-CF6. Also, O-trifluoroacetyl butyl lactate and di-O-trifluoroacetyl diethyl tartrate which had no hydrogen bonding donor groups had greater retention on the DP-TA-CF6 phase while O-trifluoroacetyl butyl lactate is better separated on DP-PN-CF6, and di-O-trifluoroacetyl diethyl tartrate was better separated on DP-TA-CF6 (as shown in Table 3.1).

3.3.2.2 Retention behavior of homologous series

Table 3.2 lists the retention data for three homologous series of compounds: amino acids, amino alcohols and tartrates. All of the analyte's carboxylate groups were methylated and all of the amino and hydroxyl groups were trifluoroacetylated. For the amino acid series and the

amino alcohol series, the retention factors of the members with linear alkyl chains increased exponentially with the length of the alkyl chain (as shown in Figure 3.3). The retention time for the analogous analytes having branched alkyl chains is shorter than their linear alkyl chain isomers.

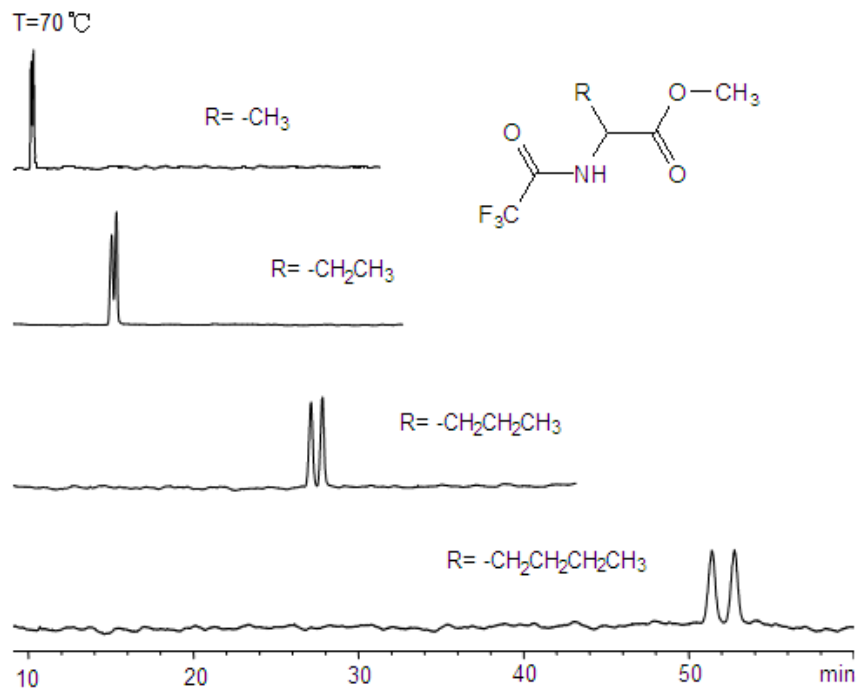


Figure 3.3 Enantiomeric separations of N-trifluoroacetyl amino acid methyl ester containing linear alkyl groups on DP-TA-CF6 stationary phase at 70°C.

It is interesting that allo-isoleucine has the same number of carbons in the branched alkyl chain as leucine and isoleucine, however, its retention factor is much smaller than those of these two isomers. For the tartrate series, the retention factors increased linearly with the carbon number of the alkyl ester groups. However, the enantiomeric selectivity factor did not vary significantly with increasing retention within each homologous series. Only isoleucine and allo-isoleucine had a relatively larger enantioselectivity factor than the rest of the homologous members. For all of the three series, the substituent of the two CSPs has no significant effect on enantioselectivity, but a significant effect on retention.

Table 3.2 Retention and enantioselectivity of three homologous series on DP-TA-CF6 and DP-PN-CF6

Racemic compound*	T/°C	k ₁	α	CSP
Alanine	70	5.39	1.02	DP-TA-CF6
	70	7.22	1.01	DP-PN-CF6
2-Aminobutyric acid	70	8.74	1.02	DP-TA-CF6
	70	10.24	1.02	DP-PN-CF6
Norvaline	70	16.91	1.03	DP-TA-CF6
	70	20.00	1.03	DP-PN-CF6
Norleucine	70	32.77	1.03	DP-TA-CF6
	70	38.71	1.03	DP-PN-CF6
Valine	70	10.89	1.02	DP-TA-CF6
	70	11.45	1.02	DP-PN-CF6
Leucine	70	24.43	1.03	DP-TA-CF6
	70	29.83	1.03	DP-PN-CF6
Allo-isoleucine	70	3.45	1.06	DP-TA-CF6
	70	4.23	1.11	DP-PN-CF6
Isoleucine	70	20.03	1.08	DP-TA-CF6
	70	20.92	1.08	DP-PN-CF6
2-Amino-1-butanol	60	49.63	1.01	DP-PN-CF6
2-Amino-1-pentanol	60	44.69	1.02	DP-TA-CF6
	60	81.10	1.02	DP-PN-CF6
2-Amino-1-hexanol	60	95.72	1.02	DP-TA-CF6
	60	154.53	1.02	DP-PN-CF6
2-Amino-3-methyl-1-butanol	60	28.24	1.01	DP-TA-CF6
	60	46.54	1.02	DP-PN-CF6
Leucinol	60	57.02	1.02	DP-TA-CF6
	60	110.28	1.02	DP-PN-CF6
Dimethyl tartrate	60	29.90	1.01	DP-TA-CF6
	60	30.21	1.02	DP-PN-CF6
Diethyl tartrate	60	69.54	1.01	DP-TA-CF6
	60	66.27	1.02	DP-PN-CF6
Diisopropyl tartrate	60	98.27	1.01	DP-TA-CF6
	60	85.26	1.01	DP-PN-CF6
Di-tert-butyl tartrate	60	134.44	1.01	DP-TA-CF6
	60	124.88	1.02	DP-PN-CF6

* All amino and hydroxyl groups in the analytes were trifluoroacetylated and carboxyl groups were transferred to methyl esters.

3.3.2.3 The role of hydrogen bonding interactions

Although DP-TA-CF6 and DP-PN-CF6 could only act as hydrogen bonding acceptors, hydrogen bonding interactions seem to play an important role in enantiomeric separations on these two CSPs. Generally, analytes with hydrogen bonding donor capabilities were better separated on both CSPs than analytes only having permanent dipole moments. Most of the baseline separations were obtained for the amino acid derivatives. Two types of hydrogen bonding interactions are very likely involved in the chiral recognition process on these two CSPs.

The first type of hydrogen bonding interactions is intramolecular hydrogen bonding within the analyte molecules. To discriminate between enantiomers, the chiral selector should interact with at least one enantiomer via a minimum of three configuration-dependent interaction points. Chiral recognition more easily occurs between chiral selectors and enantiomers with fewer degrees of rotation freedom, as long as they meet the general geometrical requirements of the selectors and selectands. Analytes with intramolecular hydrogen bonds typically have greater structure rigidity. Figure 3.4 shows the enantiomeric separations of three structurally related racemic compounds on the DP-TA-CF6 stationary phase. N-trifluoroacetyl valine methyl ester was baseline separated (Figure 3.4a) while the other two compounds were partially separated (Figure 3.4b and 3.4c). In the N-trifluoroacetyl valine methyl ester molecule, a stable intramolecular hydrogen bond can be formed between the amide hydrogen and the carbonyl oxygen of the ester group.⁸⁵⁻⁸⁸ Thus the conformational rigidity of the molecule increases. This more restricted analyte conformation appears to favor enantioselectivity with these cyclofructan based chiral selectors. Conversely, the ester group in N,O-trifluoroacetyl 2-amino-3-methyl-1-butanol is one additional carbon away from the chiral center making it difficult to form an intramolecular hydrogen bond.⁸⁵ Thus the molecule has more rotational freedom than N-trifluoroacetyl valine methyl ester which may hinder the chiral recognition process. O-trifluoroacetyl 2-hydroxy-3-methylbutyric methyl ester has no intramolecular hydrogen bonding

capabilities. The three functional groups can freely rotate along the axis of the single bond connected to the chiral center. Thus it also has poorer enantioselectivity than N-trifluoroacetyl valine methyl ester on DP-TA-CF6. Similar results were observed with DP-PN-CF6 stationary phase.

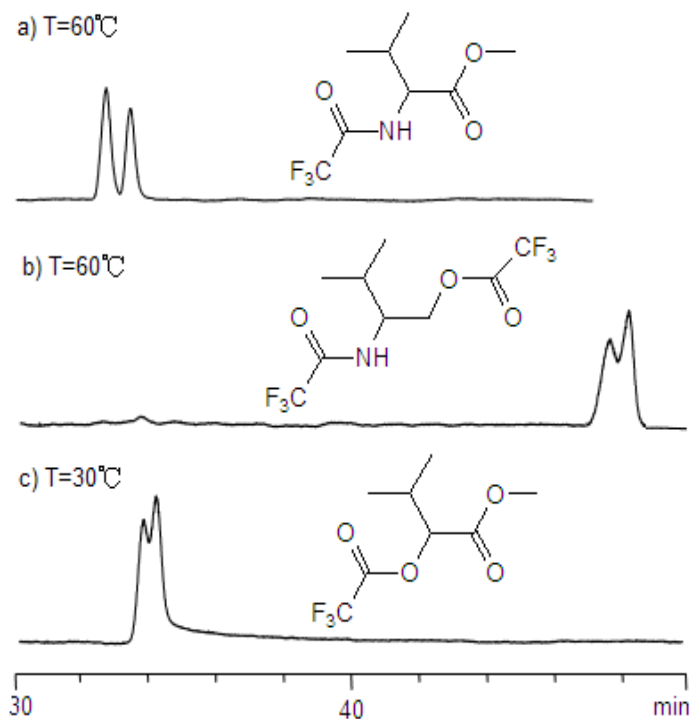


Figure 3.4 Enantiomeric separations of a) N-trifluoroacetyl valine methyl ester, b) N, O-trifluoroacetyl 2-amino-3-methyl-1-butanol and c) O-trifluoroacetyl 2-hydroxy-3-methylbutyric methyl ester on DP-TA-CF6 stationary phase.

Intermolecular hydrogen bonding interactions between the analyte and the stationary phases also are important. For example, trifluoroacetylated (\pm)-trans-1,2-diaminocyclohexane and trifluoroacetylated (\pm)-trans-1,2-cyclohexanediol had significantly different retention and selectivity behaviors on both CSPs. Trifluoroacetylated (\pm)-trans-1,2-diaminocyclohexane had a resolution of 1.3 at 115°C and 130°C on DP-TA-CF6 and DP-PN-CF6, respectively, while trifluoroacetylated (\pm)-trans-1,2-cyclohexanediol had a resolution of 0.5 and 0.7 at 40°C on the

DP-TA-CF6 and DP-PN-CF6 columns, respectively. An important difference between the structures of trifluoroacetylated (\pm)-trans-1,2-diaminocyclohexane and trifluoroacetylated (\pm)-trans-1,2-cyclohexanediol is that the former has two amide hydrogens which could act as intermolecular hydrogen bond donors. This hydrogen bonding interaction apparently facilitates the chiral recognition of trifluoroacetylated (\pm)-trans-1,2-diaminocyclohexane on both CSPs.

3.3.2.4 Effect of derivatization reagents

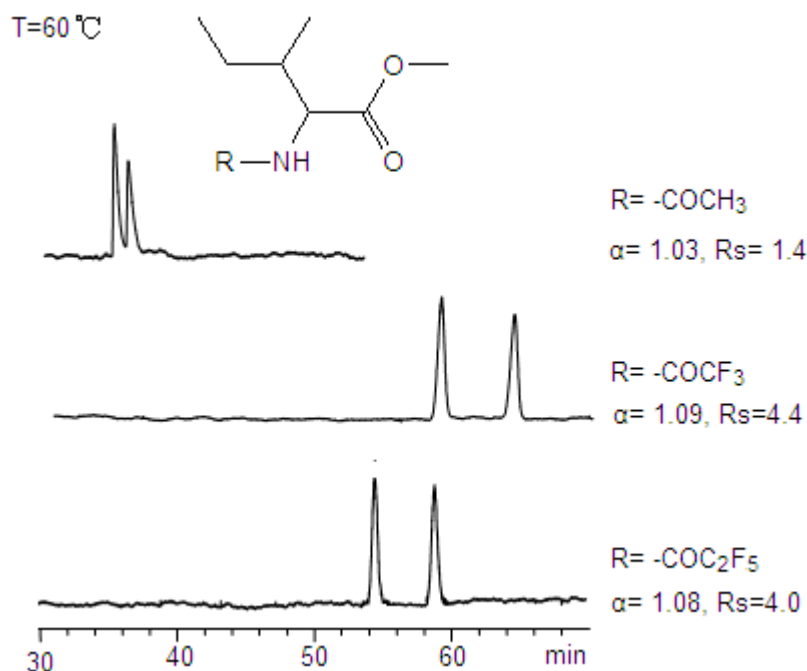


Figure 3.5 Enantiomeric separations three different derivatives of isoleucine methyl ester on DP-TA-CF6 stationary phase.

Achiral derivatization can effect enantiomeric separations by altering the volatility of the analyte and changing the interactions of the analyte with stationary phase. In certain cases, changing the derivatization moiety can enhance enantioselectivity or reverse elution order of enantiomers.^{38, 41} Fig 3.5 shows the enantiomeric separation of three different isoleucine methyl ester derivatives on DP-TA-CF6. The trifluoroacetate and pentafluoropropionate derivatives have similar retention and enantioselectivities while the acetate derivative has shorter retention and a smaller enantioselectivity factor. The decrease in retention and selectivity could be the

result of the amide hydrogen of the acetamide group being less acidic than the corresponding moiety in the trifluoroacetamide or pentafluoropropionic amide groups as well as the less pronounced dipole of the acetamide group as compared to the trifluoroacetamide or pentafluoropropionic amide groups.^{75, 77, 78} Similar results were observed on DP-PN-CF6 phase. Thus, fluoroalkylation reagents are preferred for the analyte derivatization when using these two cyclofructan based CSPs.

Table 3.3 Thermodynamic parameters measured by GC on DP-TA-CF6 CSP

Racemic compound ^a	temp range, °C ^b		$\Delta(\Delta G^\circ)$, J/mol		$\Delta(\Delta H^\circ)$, kJ/mol	$\Delta(\Delta S^\circ)$, J/(mol·K)
	min	max	min	max		
Isoleucine	60	100	-245	-171	-0.9	-1.8
Allo-isoleucine	60	100	-183	-160	-0.3	-0.5
Valine	50	90	-78	-29	-0.5	-1.2
Alanine	40	80	-89	-31	-0.5	-1.3
2-Aminobutyric acid	50	90	-84	-34	-0.5	-1.3
Norvaline	60	100	-87	-35	-0.5	-1.3
Norleucine	60	100	-89	-38	-0.5	-1.3
(±)- α -(Trifluoromethyl)benzyl alcohol	60	100	-121	-42	-0.8	-2.0

^aAmino and hydroxyl groups in the analytes were trifluoroacetylated and carboxyl groups were converted to their methyl esters except (±)- α -(trifluoromethyl)benzyl alcohol. ^bRetention and α values were measured at 10°C interval. Every van't Hoff plot contained five data points.

3.3.2.5 Thermodynamic analysis

Derivatized cyclofructans have more open relaxed structures than native cyclofructans. Also, the crown ether core becomes more accessible to guest molecules.^{95, 99} To further understand and elucidate the chiral recognition mechanism of these cyclofructan based chiral selectors, it is important to investigate whether or not the enantiomers are forming enantioselective inclusion complexes with the crown ether core. Two methods are often used to examine inclusion complex formation. One is an overloading experiment and the other one is

thermodynamic analysis.¹¹⁰ In HPLC, sample loading tests had been done on isopropyl carbamate-CF6 and R-naphthylethyl carbamate-CF6. Both CSPs had significantly higher loading capability than other synthetic crown ethers which usually have 1:1 binding stoichiometry with analytes.^{96,97} This indicated that multiple analyte molecules can interact with a single chiral selector molecule simultaneously in HPLC. Recently, it was reported that a linear free energy relationship method was used to reveal the enantiomeric separation mechanism of R-naphthylethyl carbamate-CF6 in the HPLC normal phase mode. It is known that cyclofructans do not possess a central hydrophobic cavity as do cyclodextrins.¹⁰⁴ In this study, the thermodynamic parameters were measured by gas chromatography and compared with the literature data of derivatized cyclodextrins.¹¹⁰

Table 3.4 Thermodynamic parameters measured by GC on DP-PN-CF6 CSP

Racemic compound ^a	temp range, °C ^b		$\Delta(\Delta G^\circ)$, J/mol		$\Delta(\Delta H^\circ)$, kJ/mol	$\Delta(\Delta S^\circ)$, J/(mol·K)
	min	max	min	max		
Isoleucine	60	100	-239	-168	-0.8	-1.8
Allo-isoleucine	60	100	-327	-259	-0.9	-1.7
Valine	50	90	-82	-33	-0.5	-1.3
Alanine	40	80	-80	-29	-0.5	-1.2
2-Aminobutyric acid	50	90	-85	-33	-0.5	-1.3
Norvaline	60	100	-91	-44	-0.5	-1.2
Norleucine	60	100	-101	-49	-0.5	-1.3
(±)- α -(Trifluoromethyl)benzyl alcohol	50	70	-44	-17	-0.5	-1.4

^aAmino and hydroxyl groups in the analytes were trifluoroacetylated and carboxyl groups were converted to their methyl esters except (±)- α -(trifluoromethyl)benzyl alcohol. ^bRetention and α values were measured at 10°C interval for all the amino acid and at 5°C interval for (±)- α -(trifluoromethyl)benzyl alcohol. Every van't Hoff plot contained five data points.

When a pair of enantiomers is separated by a CSP, the difference in the Gibbs free energy of association, $\Delta(\Delta G^\circ)$, can be approximately estimated from the selectivity factor, α , by

$$-\Delta(\Delta G^\circ) = RT \ln \alpha \quad (1)$$

Where R is the gas constant and T is the temperature in Kelvin. $\Delta(\Delta G^\circ)$ is related to enthalpy $\Delta(\Delta H^\circ)$ and entropy $\Delta(\Delta S^\circ)$ by the following relationship:

$$-\Delta(\Delta G^\circ) = -\Delta(\Delta H^\circ) + T\Delta(\Delta S^\circ) \quad (2)$$

Thus the relationship between α , $\Delta(\Delta H^\circ)$ and $\Delta(\Delta S^\circ)$ can be rewritten as the van't Hoff equation:

$$\ln\alpha = -\Delta(\Delta H^\circ)/RT + \Delta(\Delta S^\circ)/R \quad (3)$$

The $\Delta(\Delta H^\circ)$ and $\Delta(\Delta S^\circ)$ values for a pair of enantiomers on a certain CSP can be obtained by measuring the α values at different temperatures and plotting $\ln \alpha$ versus $1/T$.

Eight pairs of enantiomers best separated on the two CSPs in this study were chosen. The thermodynamic parameters are listed in Table 3.3 and 3.4. All of the van't Hoff plots were linear with regression coefficients higher than 0.99. The $-\Delta(\Delta H^\circ)$ and $-\Delta(\Delta S^\circ)$ values were equal to or lower than 0.9 kJ/mol and 2.0 J/mol·K, respectively, on both CSPs. In 1992, Armstrong and co-workers studied the enantioselective retention mechanisms on two cyclodextrin-based CSPs (DP-TFA- β -CD and DP-TFA- γ -CD).¹¹⁰ They postulated two different enantioselective retention mechanisms. One involved enantioselective inclusion complex formation. The analytes separated via this mechanism showed high values for $-\Delta(\Delta H^\circ)$ and $-\Delta(\Delta S^\circ)$ (equal to or higher than 7.5 kJ/mol and 18.0 J/mol·K, respectively, on DP-TFA- β -CD, and 6.9 kJ/mol and 13.4 J/mol·K, respectively, on DP-TFA- γ -CD,) and low loading capabilities. The other mechanism was a much looser, probably external association of multiple analytes per cyclodextrins. The analytes separated through the second mechanism had relatively lower $-\Delta(\Delta H^\circ)$ and $-\Delta(\Delta S^\circ)$ values (equal to or lower than 6.9 kJ/mol and 14.2 J/mol·K, respectively, on DP-TFA- β -CD, and 3.8 kJ/mol and 10.0 J/mol·K, respectively, on DP-TFA- γ -CD,).¹¹⁰

When compared with the literature data, the $\Delta(\Delta H^\circ)$ and $\Delta(\Delta S^\circ)$ values obtained on the two cyclofructan-based CSPs are closer to the $\Delta(\Delta H^\circ)$ and $\Delta(\Delta S^\circ)$ values of the analytes separated through external, multiple, associations with cyclodextrins. This indicates that there is

likely no cavity complex formation involved for the enantioselective recognition and separation of these analytes.

3.4 Conclusion

Both DP-TA-CF6 and DP-PN-CF6 CSPs showed enantioselectivity towards a variety of racemic compounds. The enantiomers separated include derivatized amino acids, amino alcohols, amines, alcohols, tartrates and lactones. Generally, analytes with hydrogen bonding donor groups were better separated on both CSPs than the analytes only having permanent dipole moments. Both DP-TA-CF6 and DP-PN-CF6 CSPs provided best enantioselectivity towards amino acids with alkyl side chains. The thermodynamic parameters indicated that no inclusion complex formation occurs during the chiral recognition process. Weak, external associations likely contribute most to the enantioselective retention mechanism.

PART TWO: IONIC LIQUID BASED GAS CHROMATOGRAPHIC STATIONARY PHASES

CHAPTER 4

OVERVIEW OF IONIC LIQUIDS IN GC SEPARATIONS

Room temperature ionic liquids are a class of low melting point salts consisting of only ions. The weak interactions between cations and anions are the essential factor that governs the formation of room temperature ionic liquids. Generally, room temperature ionic liquids are composed of at least one organic ion either cation or anion whose charge is highly delocalized. The first room temperature ionic liquid was reported in 1914 by Walden et al.¹¹¹ However, room temperature ionic liquids did not attract much attention until the first air and water stable imidazolium based room temperature ionic liquid was reported by Wilkes et al. in 1992.¹¹² Since then, many room temperature ionic liquids with new structures have been synthesized and widely applied in separation science,¹¹³ organic synthesis¹¹⁴ and electrochemistry.¹¹⁵ The common cations and anions of room temperature ionic liquids are shown in Figure 4.1. When two cationic moieties are connected by linear alkyl chains^{116,117} or polyethylene glycol chains (PEG),¹¹⁸ dications are produced. The two cationic moieties can have the same structure^{116,118} or different structures.¹¹⁷ Linear tricationic and tetracationic ionic liquids can be synthesized by connecting three or four cationic moieties with alkyl chains.^{119,120} Trigonal tricationic ionic liquids are synthesized by connecting cationic moieties to benzene-based or tertiary amine-based core.^{121,122} The structures of the cations with multiple charges are listed in Figure 4.2.

Room temperature ionic liquids are potential stationary phases for gas-liquid chromatography (GLC) since they have negligible volatility, wide stable liquid ranges, variable viscosities, high thermal stabilities and capabilities of undergoing solvation interactions with a variety of molecules.¹²³⁻¹²⁵ Monocationic, dicationic and tricationic room temperature ionic liquids have been used directly as stationary phases^{116,118,122,124,125} or as stationary phase matrix

¹²⁶ in GLC. Tetracationic ionic liquids are more often used as ion pairing reagent in mass spectrometry than as stationary phase in GC since they usually have higher melting points compared to the monocationic, dicationic and tricationic ionic liquids.¹²⁰

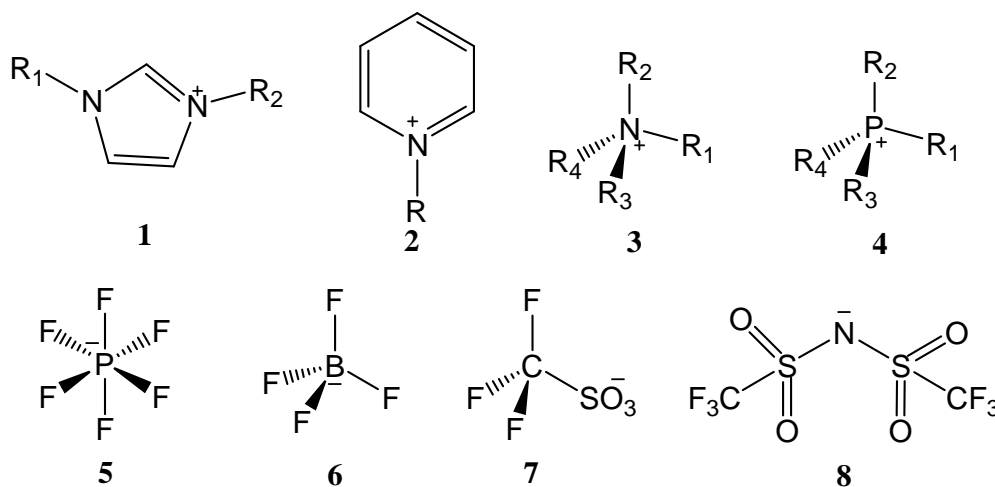


Figure 4.1 Common cations and anions of room temperature ionic liquids. Cations: **1.** imidazolium ion, **2.** N-alkylpyridinium ion, **3.** tetraalkylammonium ion, **4.** tetraalkylphosphonium ion. R groups are alkyl groups and can be the same or different. Anions: **5.** hexafluorophosphate, [PF₆], **6.** tetrafluoroborate [BF₄], **7.** trifluoromethylsulfonate [TfO], **8.** bis(trifluoromethanesulfonyl)imide [NTf₂].

The chromatographic properties of these ionic liquid stationary phases are often characterized by their solvation parameters, thermal stability and selectivity towards analytes with particular properties.^{116,118,122,124,125} Their solvation parameter models can be used to determine the multiple solvation interactions between probe molecules and stationary phases.¹²⁷ The most important interactions between ionic liquids and solutes are dipole-type interactions, hydrogen bond interactions and dispersion interactions.^{113,122} Both the cation and anion can affect the solvation parameters of the ionic liquids. The anions usually have a greater effect on the hydrogen bond basicity of the ionic liquids.¹²⁴

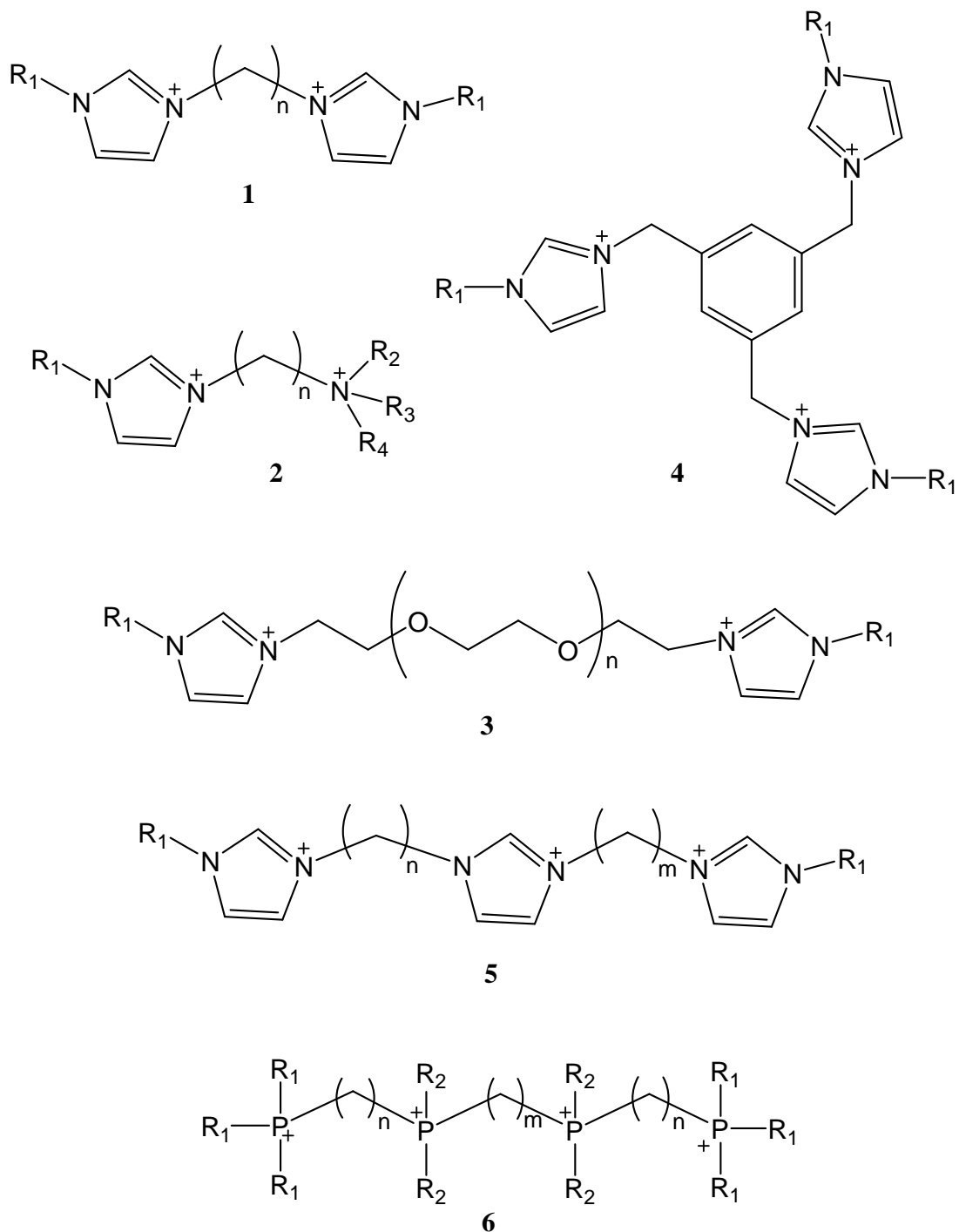


Figure 4.2 Structures of cations with multiple charges. 1. symmetric dication, 2. unsymmetric dication, 3. symmetric dication with PEG linkage, 4. trigonal trication, 5. linear trication, 6. linear tetracation

Most of the 1-butyl-3-methylimidazolium based ionic liquids are not thermally stable above 200°C. However, ionic liquids consisting of bulkier imidazolium cations and with trifluoromethanesulfonate anions possess higher boiling temperature (~250°C).¹²⁵ The thermal stability of the geminal dicationic ionic liquids with alkyl linkage chain is greater than those of the monocationic ionic liquids.¹¹⁶ The pyrrolidinium-based dicationic ionic liquid containing a C9 alkyl linkage chain between the two pyrrolidinium moieties and a NTf₂ anion is thermally stable over 400°C. When ionic liquids with vinyl substituents are cross linked via a free radical reaction, the cross-linked ionic liquids have higher thermal stability than the ionic liquids containing monomers.¹²⁸ The trigonal tricationic ionic liquids with NTf₂ anions show exceptional thermal stability. They are stable at temperature above 300°C and some of them are stable above 400°C.¹²²

Ionic liquids show a dual nature selectivity compared to traditional polysiloxane and carbowax stationary phases.^{118,122,124} They can separate nonpolar analytes as would a nonpolar stationary phase and also separate polar analytes as would a polar stationary phase.

In this part of the dissertation, the chromatographic properties of a series of trigonal tricationic ionic liquids are discussed. A trigonal tricationic and two dicationic ionic liquid stationary phases are used for quantification of water in solvents and solvents in water.

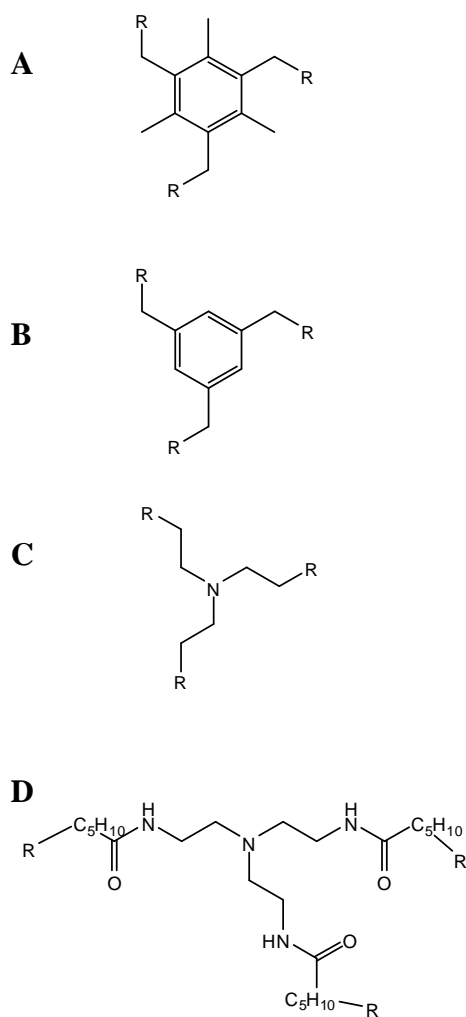
CHAPTER 5

TRIGONAL TRICATIONIC IONIC LIQUID STATIONARY PHASES

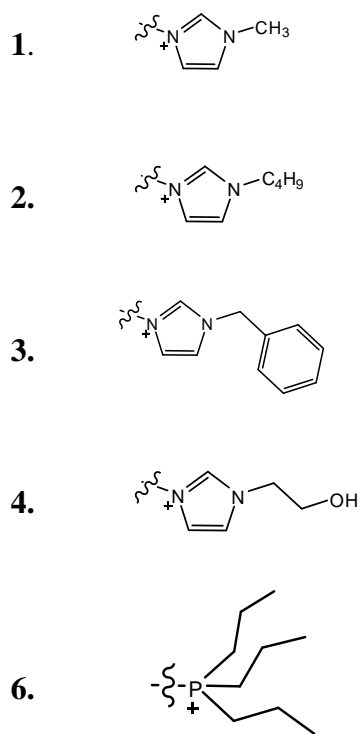
Trigonal tricationic ionic liquids (ILs) are a new class of ILs that appear to be unique when used as gas chromatographic stationary phases. They consist of four core structures; 1. **A** = mesitylene core, 2. **B** = benzene core, 3. **C** = triethylamine core, and 4. **D** = tri(2-hexanamido)ethylamine core; to which three identical imidazolium or phosphonium cationic moieties were attached. These were coated on fused silica capillaries and their gas chromatographic properties were evaluated. They were characterized using a linear solvation parameter model and a number of test mixtures. Based on the literature, it is known that both monocationic and dicationic ionic liquids possess almost identical polarities, solvation characteristics, and chromatographic selectivities. However some of the trigonal tricationic ILs were quite different. The different solvation parameters and higher apparent polarities appear to generate from the more rigid trigonal geometry of these ILs as well as their ability to retain the positive charges in relatively close proximity to one another in some cases. Their unique selectivities, retention behaviors and separation efficiencies were demonstrated using the Grob mixture, a flavor and fragrance test mixture, alcohols/alkanes test, and FAME isomer separations. Two ionic liquids **C1** (methylimidazolium substitution) and **C4** (2-hydroxyethylimidazolium substitution) had higher apparent polarities than any known ionic liquid (mono, di and tricationic ILs) or commercial stationary phases. The tri(2-hexanamido)ethylamine core IL series proved to be very interesting in that it not only showed the highest separation efficiency for all test mixtures, but it also is the first IL stationary phase (containing Ntf_2^- anions) that eliminates peak tailing for alcohols and other H-bonding analytes. The thermal stabilities

were investigated using 3 methods: thermogravimetric analysis (TGA) method, temperature programmed gas chromatographic method (TPGC) and isothermal gas chromatographic method. The **D** core series had a high working temperature range, exceptional selectivities and higher separation efficiencies than comparable polarity commercial columns. It appears that this specific type of multifunctional ILs may have the most promising future as a new generation of gas chromatographic stationary phases.

Core structures:



Ligand (R) structures:



Accompanying anion:

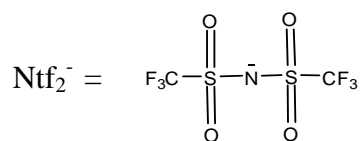


Figure 5.1 Structures of trigonal tricationic ionic liquids used in this analysis

5.1 Introduction

New types of stationary phases are explored constantly in order to come up with entities that have better physico-chemical properties in order to provide better stabilities, selectivities, resolutions and separation efficiencies for qualitative and quantitative determination of increasingly complex analyte systems. Ionic liquids have attracted much attention recently as stationary phases in gas-liquid chromatography (GLC) due to the unique properties these compounds seem to possess. These characteristics include negligible vapor pressure at room temperature, a wide liquid phase temperature range, good thermal stability, non-flammability, resistance to decomposition, ability to undergo multiple solvation interactions, ionic conductivity ($>10^{-4}$ S/cm), and large electrochemical windows ($>2V$). These properties are highly desirable for many applications in areas of chemistry, physics, and engineering. Some of these applications include replacement for volatile organic solvents in organic synthesis,¹²⁹⁻¹³⁷ solvents for high temperature reactions,¹³⁸ solvents for enzyme catalyzed reactions,¹³⁹⁻¹⁴² electrochemical applications in photovoltaic cells and fuel cells,¹⁴³⁻¹⁴⁷ high temperature lubricants,^{148, 149} liquid – liquid extractions,¹⁵⁰⁻¹⁵³ and mass spectrometric applications.^{126, 154-156} The thermal stability, ability to form multiple solvation interactions, and low volatility makes them ideal candidates for use in gas chromatography as stationary phases. In the recent past, ultra stable stationary phases based on ionic liquids were the focus of many important publications.^{116, 123-125, 128, 157-163} Based on the literature it is evident that multifunctional ionic liquids can show greater thermal stability than most common monocationic ionic liquids in GC applications but have almost identical solvent properties.¹¹⁶

However, when multiple cationic moieties are present the ionic liquid tends to be a solid at room temperature. For the best performance as a gas chromatographic stationary phase, it is necessary that the ionic liquid be a room temperature ionic liquid (RTIL). These are defined as ionic liquids that are liquids at ambient temperatures.¹³² Literature indicates that the highest probability for a multi-functional ionic liquid to be a room temperature ionic liquid is by

incorporating the bis(trifluoromethanesulphonyl)imide (NTf_2^-) anion.^{116, 116, 117, 121, 164, 165} This anion not only gives low melting ionic liquids but also shows high thermal stability.^{117, 121, 165} These two characteristics make the NTf_2^- anion ideal for ILs in GC applications. However, there is a distinct disadvantage of using this anion. That is, NTf_2^- produces peak tailing for alcohols and sometimes for other H-bonding analytes. Many different types of cation combinations have been tested in order to come up with a solution for this peak tailing and so far these attempts have failed. In this work we introduce another class of ionic liquids that not only solves this problem but also provides unique properties and selectivities not found in previously reported ILs. These are trigonal tricationic ionic liquids and they are comprised of three positively charged moieties linked to a central core.

Since trigonal tricationic ILs are a new class of ionic liquids, it is necessary to characterize them based on their solvation properties and relative polarity compared to the general monocationic, dicationic ionic liquids and other common organic solvents. Many methods have been developed over the years for the characterization of ionic liquid solvation properties.¹⁶⁶ Some of the earliest developments include an empirical solvent polarity scale derived from either by a solvent dependent reaction rate constant or by the shift in maxima of an absorption or emission band of a solvatochromic dye or a fluorescent probe dissolved in a particular solvent.^{165, 167-169} However, these methods have failed to provide a comprehensive picture of the polarity of ionic liquids due to the fact that these are single parameter polarity scales and therefore specific solvent-solute interactions are not taken into account. Ionic liquids can undergo multiple solvation interactions simultaneously such as ionic, dispersive, dipole-dipole, dipole-induced dipole, H-bond donating, H-bond accepting, π - π interactions and π -nonbonding interactions. Furthermore, ionic liquids may have complex extended three-dimensional liquid structures and possibly a supramolecular structure depicted by hydrogen bonding.¹⁶⁷ Hence, single parameter polarity does not correlate with the actual chemical environment of the ionic liquid. The next major development in this field comes with the inverse

GLC application of Rohrschneider-McReynolds process.¹²³ In this method, specific solute-solvent interactions are evaluated by utilizing 5 probe molecules which are assumed to undergo only specific types of interactions.^{123,166,170,171} However, due to the use of only one probe molecule per interaction, statistically the reliability of the values obtained is low.

The method used for the evaluation trigonal tricationic ILs is the Abraham solvation parameter model and it is the most comprehensive method available today.^{127,172-177} This is based on a linear free energy relationship. The principle is similar to Rohrschneider-McReynolds method in that different types of solvent-solute interactions are evaluated separately. However, instead of one probe molecule, several probe molecules are used to characterize one interaction parameter increasing the reliability of the parameter coefficients obtained. The linear solvation energy relationship is given by equation 1:

$$\log k = c + eE + sS + aA + bB + lL \quad (1)$$

Here, the higher case letters *E*, *S*, *A*, *B* and *L* are solute descriptors. *E* represents excess molar refraction of the solute at 20°C, *S* is solute dipolarity and polarizability, *A* is Hydrogen bond acidity, *B* is Hydrogen bond basicity and *L* is gas-hexadecane partition coefficient at 25 °C. Solute descriptor values are evaluated and published in the literature for a number of solutes.⁶¹ The lower case letters are assigned to characterize different types of interactions between the solutes and the solvent. In this case the solvent is the ionic liquid acting as the stationary phase. The value of these coefficients depicts the strength of the interaction. Here *e* is π and non-bonding electron interactions, *s* is the ability of the phase to interact with dipolar/polarizable solutes, *a* is H-bond donating (H-bond basicity) interactions, *b* is H-bond accepting (H-bond acidity) interactions, *l* coefficient is composed of dispersion forces (positive contribution) and cavity term (negative contribution) and *c* is the system constant. For all the solutes the retention factor *k* can be calculated chromatographically. These values can then be subjected to multiple linear regression analysis (MLRA) to find the five coefficients and system constant.

Table 5.1 Solute descriptor values for all the probe molecules used in this analysis

Probe molecule	E	S	A	B	L
1,2-Dichlorobenzene	0.872	0.78	0	0.04	4.518
Phenol	0.805	0.89	0.6	0.31	3.766
Octylaldehyde	0.16	0.65	0	0.45	4.36
Valeraldehyde	0.163	0.65	0	0.45	2.851
o-Xylene	0.663	0.56	0	0.16	3.939
p-Xylene	0.613	0.52	0	0.16	3.839
m-Xylene	0.623	0.52	0	0.16	3.839
Cyclohexanol	0.46	0.54	0.32	0.57	3.758
Nitrobenzene	0.871	1.11	0	0.28	4.511
N,N-Dimethylformamide	0.367	1.31	0	0.74	3.173
2-Pentanone	0.143	0.68	0	0.51	2.755
1-Nitropropane	0.242	0.95	0	0.31	2.894
Toluene	0.601	0.52	0	0.14	3.325
Benzaldehyde	0.82	1	0	0.39	4.008
Pyridine	0.794	0.87	0	0.62	3.003
Aniline	0.955	0.96	0.26	0.53	3.993
Butanol	0.224	0.42	0.37	0.48	2.601
Acetic acid	0.265	0.65	0.61	0.44	1.75
1-Octanol	0.199	0.42	0.37	0.48	4.619
Acetophenone	0.818	1.01	0	0.49	4.501
2-Chloroaniline	1.033	0.92	0.25	0.31	4.674
Pyrrrole	0.613	0.73	0.41	0.29	2.865
Benzonitrile	0.742	1.11	0	0.33	4.039
Propionitrile	0.162	0.9	0.02	0.36	2.082
1-Chlorohexane	0.201	0.4	0	0.1	3.777
p-Cresol	0.82	0.87	0.57	0.31	4.312
Ethylphenyl ether	0.681	0.7	0	0.32	4.242
Naphthalene	1.34	0.92	0	0.2	6.161
2-propanol	0.212	0.36	0.3	0.14	2.786
Cyclohexanone	0.403	0.86	0	0.56	3.792

5.2 Experimental

5.2.1 Materials

Figure 5.1 gives the structures of all the trigonal tricationic ionic liquids synthesized. The reagents 1-methylimidazole, 1-butylimidazole, 1-benzylimidazole, 1-(2-hydroxyethyl)imidazole, tripropylphosphine, 2,4,6-tris(bromomethyl)mesitylene, 1,3,5-tris(bromomethyl)benzene, tris(2-

chloroethyl)amine hydrochloride, tris(2-aminoethyl)amine, 6-bromohexanoyl chloride and all the probe molecules in Table 5.1 were purchased from Sigma Aldrich. Detailed synthesis procedure is given else where.¹²¹ Grob test mixture, flavor and fragrance mixture and alcohols and alkanes mixture were also purchased from Sigma Aldrich. The GC capillaries (250 μm internal diameter) were purchased from Supelco. The FAME isomer mixture and the commercial columns Equity-1701, SUPELCOWAX, and SP-2331 were graciously donated by Supelco.

5.2.2 Methods

For the determination of solvation parameter the ionic liquids were coated using static coating technique on salt treated fused silica capillary (5m x .25mm). In this method, the IL was dissolved in dichloromethane to obtain 0.25% (w/v) coating solution and this was injected from one end of the capillary. The capillary tube was kept inside a water bath at 40 °C. After that, one end of the capillary was sealed while the solvent was evaporated from the other end under high vacuum conditions. Finally the coated columns were flushed with helium gas and conditioned overnight from 30 °C to 120 °C at 3 °C/min. Efficiencies of the 12 IL columns were determined by using naphthalene at 100 °C and were higher than 2000 plates m^{-1} . For the determination of solvation parameters, 30 probe molecules were used. The solute descriptors for the 30 probe molecules are listed in Table 5.1. For the determination of each parameter, more than 4 probe molecules having significant range of solute descriptor values were used in order to meet the statistical requirement to obtain meaningful results for the parameters.¹⁷⁷ The solvation parameters were determined using inverse GC method at 2 different temperatures, 70 °C and 100 °C. Probe molecules were injected and retention times were measured in triplicate. Methane was used to measure the column hold-up time. For the trigonal tricationic IL columns the three retention factors calculated for each probe molecule were identical within the experimental error. The log of average retention factor from triplicate measurement ($\log k$) and solute descriptors (E, S, A, B, L) were then subjected to a multi parameter linear least squares fit on Analyse-it for Microsoft Excel software to determine the coefficients. Helium carrier gas

flow rate was set at 1 mL min⁻¹ for all the analysis with split ratio 100:1. Inlet and detector temperatures were kept at 250 °C. The values obtained for the solvation coefficients using inverse GC approach are listed in Table 5.4. The value *n* represents the maximum number of probe molecules that could be used for MLRA. The value is less than 30 because some compounds co-eluted with the solvent peak especially at the higher temperature. Also, some of the data points had to be removed in order to obtain higher correlation coefficients ($R^2 \geq 0.98$). It was noted that highly peak tailing analytes such as acetic acid and N,N-dimethylformamide were common among the analytes that were removed from the data set.

Separations of Grob test mixture, flavor and fragrance mixture, alcohols and alkanes mixture, and FAME isomers were carried out in Agilent Technologies 6890N Network GC System equipped with Agilent Technologies 5975 inert Mass Selective Detector. Column dimensions: 30 m x .25 mm x 0.20 µm. Separation conditions for Grob test mixture: 40 – 190 °C at 6 °C/min. Flavor and fragrance mixture: 40 °C for 3 min, 10 °C/min to 150 °C. Alcohols and alkanes mixture: 30 °C for 3 min, 10 °C/min to 160 °C. FAME isomers: 165 °C isothermal.

Thermal stability of ionic liquids was evaluated using three methods. The first method involves thermogravimetric analysis (TGA) of the pure ionic liquid at 10 °C/min heating rate. The decomposition temperature of 5% weight loss of the sample is reported in Table 5.2. The second approach is a temperature programmed GC (TPGC) method where the ionic liquid is coated in a 5 m x .25mm capillary and a temperature ramp of 3 °C/min was applied from 100 °C until decomposition is observed (see Figure 5.2). Third method is carried out for **D** core ionic liquids only. In this method, the ionic liquid is coated on a NaCl treated fused silica capillary of 5m x .25mm x .15 µm film thickness. and the retention factor of naphthalene was determined at 100 °C isothermally. It was then subjected to conditioning at higher temperatures for 12 hours (see Table 5.3) and the naphthalene retention factor was determined again at 100 °C after each conditioning step. This method yields the most relevant thermal decomposition temperature of the IL stationary phases.

5.3 Results and Discussion

Four types of central cores were investigated in this study (see Figure 5.1) and in the order of increasing flexibility they are; **A** mesitylene core, **B** benzene core, **C** triethylamine core, and **D** tri(2-hexanamido)ethylamine core. These core structures also vary in their ability to form hydrogen bonds with the NTf₂⁻ anion and other solutes. The **A** and **B** cores do not have any intrinsic H-bonding capabilities. In the case of **C** core, the central nitrogen can be H-bond basic and in **D** core, the central nitrogen and amide oxygen both can be H-bond basic and the amide hydrogen can be H-bond acidic. It is important to note that to the best of our knowledge this is the first time an amide group is introduced in to the cationic fragment of an ionic liquid. Detailed information of synthesis and impurities present in these ionic liquids were discussed elsewhere.⁶⁷ In summary, the purities of these ILs were checked using NMR methods, Mass spectroscopy and elemental analysis. The only detectable contamination found was H₂O which can be removed by drying in vacuum oven at 80 °C under P₂O₆.

5.3.1 Physical properties of trigonal tricationic ionic liquids

The physical properties of this series of multifunctional ILs are summarized in Table 5.2. Ionic liquid **A3** and **C1** were solids at room temperature with melting points 62 and 37 °C respectively. The remaining 10 ionic liquids were room temperature ILs with melting points below 20 °C. The RTILs were viscous liquids that did not show any air or moisture sensitivity that leads to decomposition at laboratory atmosphere. Densities of these tricationic ILs lie in the range observed for common monocationic and dicationic ILs¹¹⁷ and are between 1.41 g/cm³ and 1.64 g/cm³. Refractive indices range from 1.451 to 1.588. However viscosities of trigonal tricationic ILs are at least one or two orders of magnitude higher than those observed for typical monocationic ILs and dicationic ILs. In fact these are the highest viscosities reported for any ionic liquids. Ionic liquids **D3** and **D5** have the highest viscosities which range between 40,000-45,000 cSt and 35,000-40,000 cSt respectively. High viscosities are preferable for ILs that are to be used as stationary phases in GC.^{124,125} Furthermore when the benzyl imidazolium moiety

is present the viscosities are markedly higher than other imidazolium cationic moieties. This trend was observed for symmetrical and unsymmetrical dicationic ILs as well.¹¹⁷ This may be attributed to the added π - π stacking of the aromatic ring. Thermal stabilities of the trigonal tricationic ILs were measured using three methods (see Experimental Section) and a detailed discussion follows.

Table 5.2 Physical properties of the trigonal tricationic ILs used as stationary phases.¹¹⁸

IL	M.W.	Melting Point (°C)	Density ^a (g/cm ³)	Refractive index	Viscosity ^b (cSt)	Thermal Stability ^c (°C)
A3	1474.3	60-62	1.59	-	-	365
B1	1203.9	-38.6*	1.56	1.467	1280	414
B2	1330.2	-24.6*	1.53	1.467	2320	401
B3	1432.2	-87.4*	1.55	1.588	20,000-25,000	361
C1	1184.9	36-37	1.56	-	-	393
C2	1311.2	-47.5*	1.41	1.451	1580	363
C3	1413.2	-6.7*	1.51	1.493	25,000-30,000	381
C4	1276.0	-38.5*	1.64	1.460	7980	392
D1	1524.4	-16.4*	1.59	1.465	7760	351
D2	1650.6	-54.1*	1.49	1.466	10,200	335
D3	1752.7	-16.6*	1.54	1.495	40,000-45,000	337
D5	1758.8	-31.4*	1.48	1.466	35,000-40,000	388
BMIM-Cl ^d	174.7	65	1.10	-	-	145 ^e
BMIM-TfO ^d	322.3	27	1.30	1.438	69.8	175 ^e
BMIM-NTf ₂ ^d	419.4	-4	1.43	1.427	36.4	185 ^e

* Phase transition temperature determined by using differential scanning calorimetry (DSC).
^a Measured using pycnometer. ^b Kinematic viscosity determined using capillary viscometer at 30 °C. ^c Temperature of 5% thermal degradation determined by thermogravimetric analysis (TGA). ^d Values taken from the reference 40, 53, 70, and 71. ^e Thermal stability determined by GC method.

5.3.2 Thermal stability

The thermal stability of ionic liquids is important as it defines the upper limit of the temperature range where the column can be used as a separation medium. Three methods

were used to evaluate thermal stability: First two methods, TGA method and temperature programmed GC method were used to obtain a general idea of the thermal stability. Using the TGA method, the temperatures of 5% thermal degradation of the trigonal tricationic IL samples are reported as the decomposition temperature in Table 5.2. All ionic liquids were thermally stable to at least 335 °C in the TGA method. In the TPGC method, the baseline rise at the beginning of the decomposition event can be due to two reasons (see Figure 5.2).

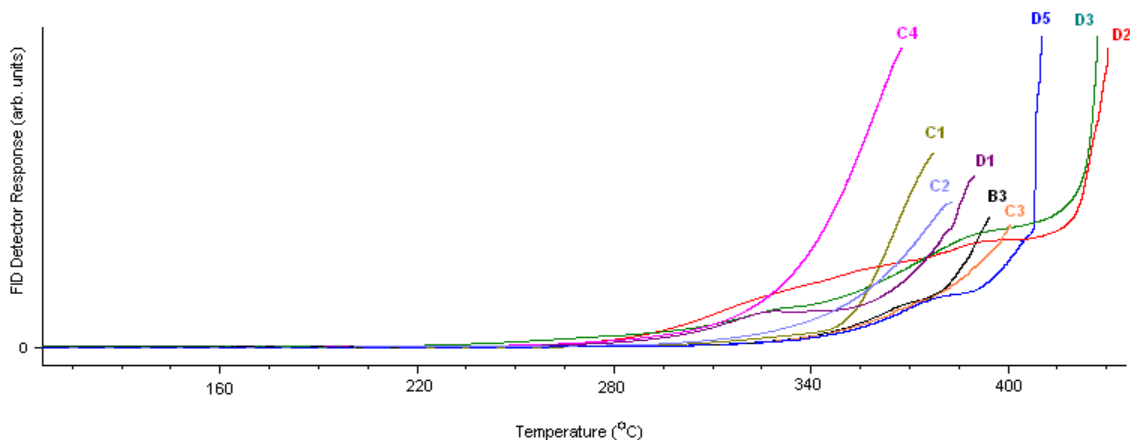


Figure 5.2 Temperature profile for column bleeding in gas chromatography due to thermal decomposition or volatilization of trigonal tricationic ionic liquids **B3**, **C1**, **C2**, **C3**, **C4**, **D1**, **D2**, **D3**, and **D3**.

It can be due to the volatilization of the ionic liquid or it can be due to the actual decomposition. Either way, this region cannot be used for chromatographic separations due to the increasing baseline from column bleed. At the end of Table 5.2, the thermal stability of some common monocationic ionic liquids (determined by the TP GC method) is listed for comparison purposes.¹²⁵ It is important to note that the thermal stability values reported in Table 5.2 for monocationic ionic liquids can be directly compared to the values obtained for trigonal tricationic ionic liquids by the TPGC method in Figure 5.2 as both experiments employed identical procedures. It is evident that the tricationic ionic liquids are much more thermally stable than the common monocationic ionic liquids. All 3 monocationic ILs start to decompose or volatilize

before 185 °C while for the trigonal tricationic ILs, no appreciable bleed is observed before 280 °C. There is at least a 90 degree advantage of workable temperature range for tricationic ILs over the common monocationic IL stationary phases in gas chromatography. Within the tricationic series since all the ionic liquids have the same anion, the thermal stability variations are solely due to variations in the cationic fragment. IL **C4** with hydroxyethylimidazolium cationic moiety and nitrogen core seems to decompose at somewhat lower temperature whereas IL **D5** with propylphosphonium cationic moiety and amide linkage shows the highest onset temperature of decomposition. In fact it appears that for **D5** the base line does not start to rise appreciably until the temperature exceeds 315 °C. The above mentioned two methods were used to present general thermal stability comparison between the trigonal tricationic ILs and other ionic liquid based stationary phases since these are the most common methods used in the literature. The third method, an isothermal GC method, is probably the most relevant method for the determination of actual upper limit of temperature for the use of ionic liquids as stationary phases. The retention factor of naphthalene after each thermal treatment is listed in Table 5.3. For all the **D** core ILs listed, symmetrical sharp peaks were obtained up to 290 °C conditioning. At 300 °C thermal treatment the columns show reasonable retention for naphthalene. However the peaks show some tailing. After 310 °C, there was no retention which indicates column bleed of the ionic liquid stationary phase. These results confirm that the **D** core IL series is thermally stable up to 300 °C as a GC stationary phase. In previous work it was shown that the phosphonium cationic moiety is more resistant to thermal degradation than most other N-based cations such as imidazolium and ammonium.⁶⁴ This implies that from this set of tricationic ionic liquids, **D5** has the largest workable temperature range as a stationary phase in gas chromatography. It exists as a liquid for a range of 331 °C from – 31.4 °C to at least 300 °C. This in itself is quite impressive compared to the monocationic ionic liquids which generally have a liquid temperature range of about 200 °C or less. It is important to note that the commercial stationary phase SP-2331 which has similar polarity to **D5** ionic liquid has an upper

temperature limit of 275 °C. Therefore, IL **D5** has at least 25 °C advantage over the comparable commercial stationary phase which in gas chromatographic terms leads to better separation efficiencies for heavy and highly polar compounds.

Table 5.3 Variation of retention factors (k_{naph}) with thermal treatment of D core trigonal tricationic IL columns.^a

Thermal treatment ^b (°C)	k_{naph} in D1	k_{naph} in D3	k_{naph} in D5
100	3.20	8.11	7.21
130	3.11	6.93	7.02
150	3.02	6.50	6.75
200	2.91	6.20	6.51
230	2.86	4.60	6.40
250	2.82	4.28	6.33
270	2.46	3.20	6.19
290	2.12	2.31	6.00
300	3.04 ^c	2.34 ^c	6.74 ^c
310	^d	^d	^d

^a Measure isothermally for naphthalene, column temperature 100 °C, He flow rate 1 ml/min. ^b Thermally treated for 12 hours under He 1 ml/min. ^c Peak tailing was observed. ^d No retention was observed for naphthalene.

5.3.3 Ionic liquid solvation parameters

The solvation parameters obtained for the trigonal tricationic ionic liquids are listed in Table 5.4. In Table 5.5 these values are compared with the same parameters found for common monocationic and dicationic ionic liquids.^{124, 128} By comparison, nearly all interaction parameters obtained for monocationic and dicationic ILs are similar to each other whereas those obtained for some of the new tricationic ILs are quite unique. These unique parameters give rise to different behaviors in terms of retention, selectivity and separation efficiency.

Three of the five interaction parameter coefficients i.e., s = dipole–type interactions, a = H–bond donating interactions, and l = dispersion and cavity formation interactions have the

greatest magnitude. This implies that solute retention is mainly due to these three types of interactions. Similar observations were made for monocationic and dicationic IL stationary phases.^{116, 124, 125} Ionic liquid **C4** (with hydroxyethylimidazole charge carrying moieties and a “N” core) had the lowest *s* and *a* terms ever reported for any ionic liquid stationary phases carrying NTf₂⁻ anion. Hence the **C4** IL column exhibited the lowest retention for all the test mixtures investigated (Grob test, flavor and fragrance mixture, alcohols and alkanes, see Figures 5.4, 5.5 and 5.7.) The *e* term which corresponds to π- and nonbonding electron interactions is essentially negligible in this series of trigonal tricationic ionic liquids.

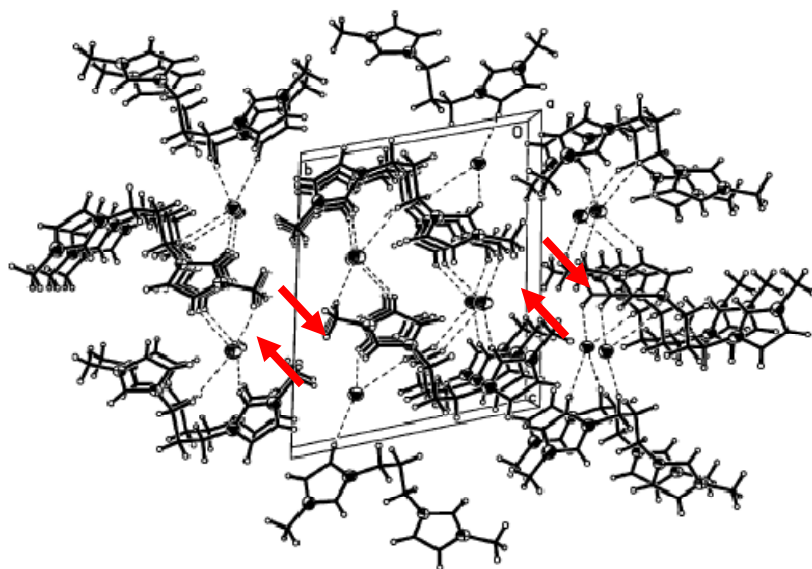


Figure 5.3 X-ray crystallographic data of $C_3(mim)_2 2Br^-$ showing stacks along short *a* – axis and H-bonding.

It was observed that the *s*, *a*, *b*, and *l* coefficients decrease with increasing temperature. The most substantial decrease in magnitude is observed for the *s* and *a* values (dipole–type interactions and H–bond basicity). This is mainly due to the fact that these interactions result from directional bonds and therefore depend largely on the orientation of the solute molecules and the interacting stationary phase molecules. As the temperature increases, translational and rotational energy of the molecules increase. This disrupts the intermolecular interactions

between the solute and stationary phase and leads to lower retention and coefficients.¹⁷⁷ When benzylimidazole is the ionic liquid's charge carrying moiety, the H-bond acidity term (b) is increased compared to the other cationic moieties (with the exception of the **D** core ionic liquids in which the methylimidazole cationic moiety shows a higher b value). This is observed in symmetrical dicationic ionic liquids as well.¹²⁸ This may be due to the increased H-bond acidity of the bridging methylene hydrogens of the benzyl group. This contention is supported by previously published results (illustrated in Figure 5.3 which is a packing diagram of a symmetrical dicationic ionic liquid, $C_3(\text{methylimidazolium})_2 2Br^-$). This crystal structure shows H-bonding between the acidic hydrogens and the bromide anion.¹²⁸ The hydrogens that are marked with a red arrow are from the methyl group substituted at the 3 position of the imidazole ring. If the methyl group is substituted by a benzyl group, these would be the bridging methylene hydrogens. In that case due to the presence of the benzene ring in the adjacent carbon these hydrogens would be even more acidic giving rise to a larger b term.

The **D** core series of tricationic ILs has the highest a values (i.e., hydrogen bond basicities). This is due to the three amide groups present in each ionic liquid. Both amide nitrogen and carbonyl oxygen can participate in H-bonding. The central core nitrogen may be sterically hindered for effective hydrogen bonding.

The e term is probably the least significant coefficient for most of the tricationic ILs investigated. It implies that the interaction between solute and IL stationary phase through π - π and non-bonding electrons is minimal compared to other types of interactions. One would expect the benzylimidazole cationic moiety to introduce some π - bonding interactions but that is not what is observed. The only statistically significant e terms are observed for the **C4** ionic liquid, with the hydroxyethylimidazole charge carrying moiety; and for the **D1** ionic liquid with methylimidazole charge carrying moiety. It is expected that **C**-core series has the lowest e term, as there are no core π - bonding electrons and only one relatively inaccessible non-bonding electron pair on the central nitrogen. However, **C4** with hydroxyethylimidazole as the cationic

moiety shows the highest π - π and n - π interactions among the trigonal tricationic IL series. Furthermore this ionic liquid has a very low H-bond acidity (b coefficient). This implies that the hydroxyl group interacts with solutes through the non-bonding electrons of oxygen and not as much through H-bonding. Dispersion forces are one of the prominent type of interaction that contributes to analyte retention in these IL stationary phases. However, interaction of tricationic ILs through dispersion forces (l coefficient) seems to be similar since there is not much variation in the l value from one trigonal tricationic ionic liquid to another. The magnitude of l ranges from 0.43 to 0.67 and this falls within the range observed for symmetrical dicationic and monocationic ionic liquids.^{116, 124, 125}

5.3.4 *Grob test mixture*

This is a single test mixture that is used to evaluate a capillary column chromatographically.^{178, 179} This mixture can be used to evaluate separation efficiency, acid/base characteristics, adsorptive activity and relative polarity of the column. The mixture contains 12 components and each peak gives information about the column. 1. n-decane and 2. n-undecane represents 100% recovery marker. Symmetrical sharp peaks are expected for properly produced and installed columns. 3. 1-nonanal is used to identify adsorption unique to aldehydes independent of H-bonding. 4. 1-octanol and 6. 2,3-butanediol peak shapes indicate presence of H-bonding sites. Reduced peak heights and unsymmetrical peak shapes for 6. 2-ethylhexanoic acid and 7. 2,6-dimethylphenol indicate H-bonding or basic sites. 8. methyl decanoate, 9. methyl undecanoate and 10. methyl dodecanoate are a homologous series of fatty acid methyl esters and is used to determine the separation efficiency of the column. 11. 2,6-dimethylaniline and 12. dicyclohexylamine peak shapes give information of the acidic nature of the column.

According to Figure 5.4, in trigonal tricationic ionic liquids with **B** and **C** core structures (see Figure 5.1), n-decane and n-undecane elute with or near the methylene chloride solvent peak and could not be separated with the given temperature program. Also, 2,3-butanediol, 2-

ethylhexanoic acid, and dicyclohexylamine were either retained on the column or eluted with high peak tailing so that they were indistinguishable from the baseline. All of these 3 compounds are polar, have H-bonding capabilities and lack any aromatic substituents. Furthermore, 1-nonanal and 1-octanol show peak tailing and reduced peak heights. These results imply that the **B** and **C** core structures can produce IL stationary phases that are highly polar with H-bond accepting capabilities. The **C4** IL shows the least retention for Grob test mixture compounds which is in accordance with the previously discussed solvation parameter coefficient results. The homologous series of fatty acid methyl esters were well separated with both **B** and **C** core IL stationary phases and showed good separation efficiencies. The acid 2,6-dimethylphenol and the base 2,6-dimethylaniline were the latest eluting detectable peaks. Despite the presence of H-bonding sites, these did not show much peak tailing. The elution orders on the **B1** and **C4** ILs were similar to highly polar commercial stationary phase SP-2331, whereas the elution order on the **C1** IL stationary phase was more comparable with the polar SUPELCOWAX column.

All 12 test compounds were eluted from stationary phases with **D** core ionic liquids. In **D3** and **D5** the alkanes are better separated from the solvent peak compared to the **B** and **C** core ILs. All **D**-type columns separated the homologous series of fatty acid methyl esters with exceptionally good separation efficiencies. In both **D1** and **D3**, the two bases elute after the acids which indicate that **D1** and **D3** are more acidic stationary phases than **D6**. This also is in agreement with the solvation parameter coefficients obtained. The H-bond acidity term (*b*) for **D5** is significantly smaller than that of **D1** and **D3**. In **D5**, the two acids elute last indicating a more basic, less acidic stationary phase. The **D** core IL stationary phases show elution orders similar to the highly polar SP-2331 column. This leads to the conclusion that the **D** series ionic liquids are highly polar and the polarity is comparable to that of SP-2331 (100% cyanopropyl polysiloxane) stationary phase.

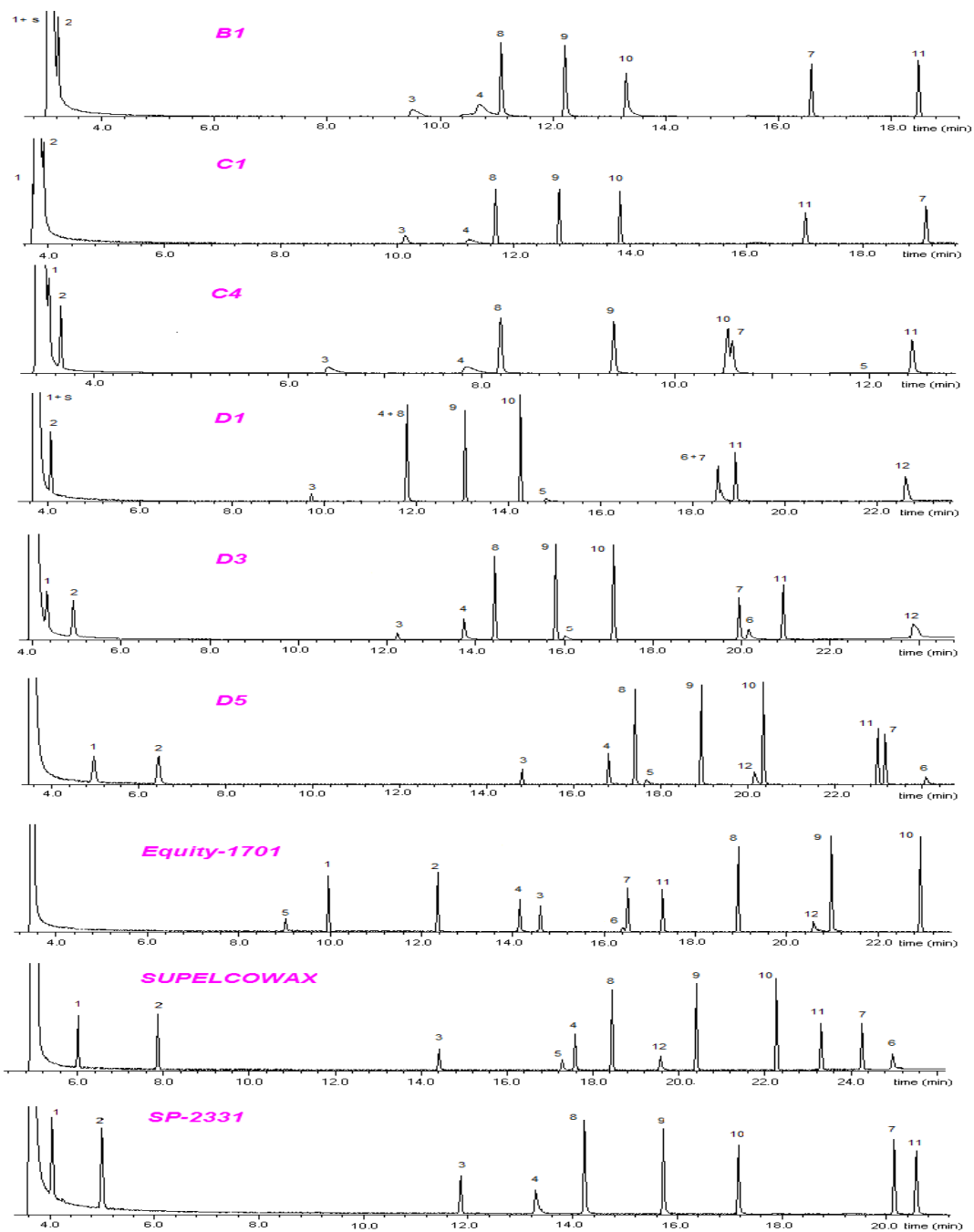


Figure 5.4 Separation of Grob test mixture in trigonal tricationic IL columns and commercial columns with varying degrees of polarity; intermediate polar (Equity-1701), polar (SUPELCOWAX), and highly polar (SP-2331). 1 n-decan, 2 n-undecane, 3 1-nonanal, 4 1-octanol, 5 2,3-butanediol, 6 2-ethylhexanoic acid, 7 2,6-dimethylphenol, 8 methyl decanoate, 9 methyl undecanoate, 10 methyl dodecanoate, 11 2,6-dimethylaniline, 12 dicyclohexylamine, s dichloromethane,. GC separation conditions: 40 °C to 190 °C at 6 °C min⁻¹; 1 mL min⁻¹ He; MS Detector. All chromatograms were obtained using 30 m x .25 mm x 0.20 µm d_i columns.

Table 5.4 Interaction parameters obtained for trigonal tricationic IL stationary phases

Temperature (°C)	<i>c</i>	<i>e</i>	<i>s</i>	<i>a</i>	<i>b</i>	<i>l</i>	<i>n</i>	<i>R</i> ²
A3 (BzIM)Mst								
70 (std. err.)	-3.34 (.10)	0.07 (.08)	2.02 (.09)	1.86 (.08)	0.72 (.11)	0.47 (.02)	29	0.99
100 (std. err.)	-3.37 (.09)	0.10 (.07)	1.87 (.08)	1.61 (.07)	0.58 (.10)	0.39 (.02)	29	0.99
B1 (MIM)Ph								
70 (std. err.)	-2.94 (.12)	0.14 (.10)	1.67 (.11)	1.68 (.10)	0.05 (.14)	0.50 (.03)	29	0.98
100 (std. err.)	-3.00 (.11)	0.18 (.08)	1.51 (.09)	1.42 (.08)	0.02 (.12)	0.42 (.03)	29	0.99
B2 (BuIM)Ph								
70 (std. err.)	-3.18 (.08)	0.07 (.07)	1.72 (.08)	1.80 (.07)	0.23 (.10)	0.56 (.02)	29	0.99
100 (std. err.)	-3.26 (.08)	0.09 (.07)	1.56 (.08)	1.57 (.07)	0.15 (.10)	0.48 (.02)	29	0.99
B3 (BzIM)Ph								
70 (std. err.)	-3.49 (.10)	0.04 (.07)	2.11 (.08)	2.09 (.08)	0.46 (.10)	0.51 (.03)	28	0.99
100 (std. err.)	-3.55 (.09)	0.06 (.07)	1.97 (.07)	1.78 (.07)	0.39 (.10)	0.43 (.02)	28	0.99
C1 (MIM)N								
70 (std. err.)	-3.53 (.11)	0.05 (.08)	1.55 (.10)	1.81 (.08)	0.35 (.11)	0.53 (.03)	28	0.99
100 (std. err.)	-3.70 (.12)	0.04 (.08)	1.58 (.08)	1.51 (.08)	0.31 (.11)	0.45 (.03)	25	0.98
C2 (BuIM)N								
70 (std. err.)	-2.92 (.09)	0.05 (.07)	1.57 (.08)	1.55 (.07)	0.14 (.10)	0.55 (.02)	27	0.99
100 (std. err.)	-2.98 (.09)	0.06 (.07)	1.43 (.08)	1.29 (.06)	0.16 (.10)	0.46 (.02)	27	0.99
C3 (BzIM)N								
70 (std. err.)	-3.23 (.09)	-0.03 (.07)	1.85 (.08)	1.62 (.07)	0.37 (.10)	0.54 (.02)	28	0.99
100 (std. err.)	-3.29 (.08)	-0.02 (.06)	1.10 (.07)	1.37 (.07)	0.30 (.09)	0.46 (.02)	28	0.99
C4 (HyIM)N								
70 (std. err.)	-3.18 (.10)	0.22 (.09)	0.66 (.10)	0.95 (.09)	0.09 (.12)	0.67 (.03)	29	0.99
100 (std. err.)	-3.05 (.09)	0.22 (.06)	0.45 (.07)	0.70 (.06)	0.03 (.08)	0.57 (.02)	25	0.99
D1 (MIM)NAmid								
70 (std. err.)	-3.42 (.12)	0.23 (.09)	2.15 (.11)	2.82 (.11)	0.31 (.14)	0.43 (.03)	28	0.99
100 (std. err.)	-3.58 (.12)	0.16 (.09)	2.10 (.10)	2.50 (.10)	0.17 (.14)	0.37 (.03)	26	0.99
D2 (BuIM)NAmid								
70 (std. err.)	-2.89 (.13)	0.11 (.11)	1.59 (.12)	2.23 (.10)	0.05 (.15)	0.52 (.03)	28	0.99
100 (std. err.)	-2.94 (.11)	0.10 (.09)	1.45 (.10)	1.84 (.09)	0.01 (.13)	0.45 (.03)	28	0.98
D3 (BzIM)NAmid								
70 (std. err.)	-3.10 (.12)	0.07 (.10)	1.85 (.11)	2.29 (.10)	0.15 (.14)	0.50 (.03)	29	0.99
100 (std. err.)	-3.16 (.10)	0.08 (.08)	1.69 (.09)	1.93 (.08)	0.10 (.11)	0.42 (.02)	29	0.99
D5 (PrP)NAmid								
70 (std. err.)	-3.30 (.10)	0.13 (.08)	1.91 (.09)	2.72 (.08)	0.03 (.11)	0.52 (.03)	29	0.99
100 (std. err.)	-3.34 (.10)	0.14 (.08)	1.72 (.09)	2.17 (.08)	0.07 (.11)	0.44 (.02)	29	0.99

Table 5.5 Comparison of the interaction parameters of monocationic and dicationic RTILs with trigonal tricationic ionic liquids.

Temperature ($^{\circ}\text{C}$)	<i>c</i>	<i>e</i>	<i>s</i>	<i>a</i>	<i>b</i>	<i>l</i>	<i>n</i>	R^2
BMIM-NTf₂^a								
70 (std. err.)	-3.03(.09)	0(.08)	1.67(.09)	1.75(.09)	0.38(.11)	0.56(.02)	35	0.99
100 (std. err.)	-3.13(.12)	0(.09)	1.60(.10)	1.55(.10)	0.24(.12)	0.49(.03)	32	0.98
C₉(mim)₂-NTf₂^b								
70 (std. err.)	-2.95(.14)	0.11(.07)	1.76(.08)	1.75(.07)	0.20(.10)	0.51(.02)	33	0.99
100 (std. err.)	-3.06(.08)	0.11(.06)	1.64(.07)	1.50(.06)	0.15(.09)	0.43(.02)	32	0.99
D1 (MIM)NAmid								
70 (std. err.)	-3.42 (.12)	0.23 (.09)	2.15 (.11)	2.82 (.11)	0.31 (.14)	0.43 (.03)	28	0.99
100 (std. err.)	-3.58 (.12)	0.16 (.09)	2.10 (.10)	2.50 (.10)	0.17 (.14)	0.37 (.03)	26	0.99

^a values taken from reference 40. ^b values taken from reference 43.

The **B** and **C** core ionic liquid stationary phases produce tailing peaks for the alcohols. This is a common phenomenon observed for ionic liquid stationary phases with the NTf₂⁻ (bis(trifluoromethane)sulfonimide) counter anion. Both monocationic and dicationic ionic liquids have shown peak tailing for alcohols and this has been one drawback of these types of ionic liquids as stationary phases. To overcome this problem NTf₂⁻ anion has been replaced by the triflate (TfO⁻) anion.¹¹⁸ However, with multifunctional ionic liquids the NTf₂⁻ anion is used more frequently in order to obtain lower melting point ILs.

One of the unique and probably the more important property of the trigonal tricationic ionic liquid stationary phases is that the **D** core ILs have reduced and in the some cases almost eliminated the peak tailing of alcohols even though the NTf₂⁻ anion is present. As discussed previously, the polarity of the **D5** IL stationary phase is comparable to the highly polar SP-2331 commercial phase. However, as shown in Figure 5.5, peak asymmetry for alcohols is less for the **D5** stationary phase than for the commercial SP-2331 phase at higher temperatures. Also nonane (5) and dichloromethane (s) were barely separated with SP-2331 phase whereas these compounds are much better separated with the **D5** IL stationary phase.

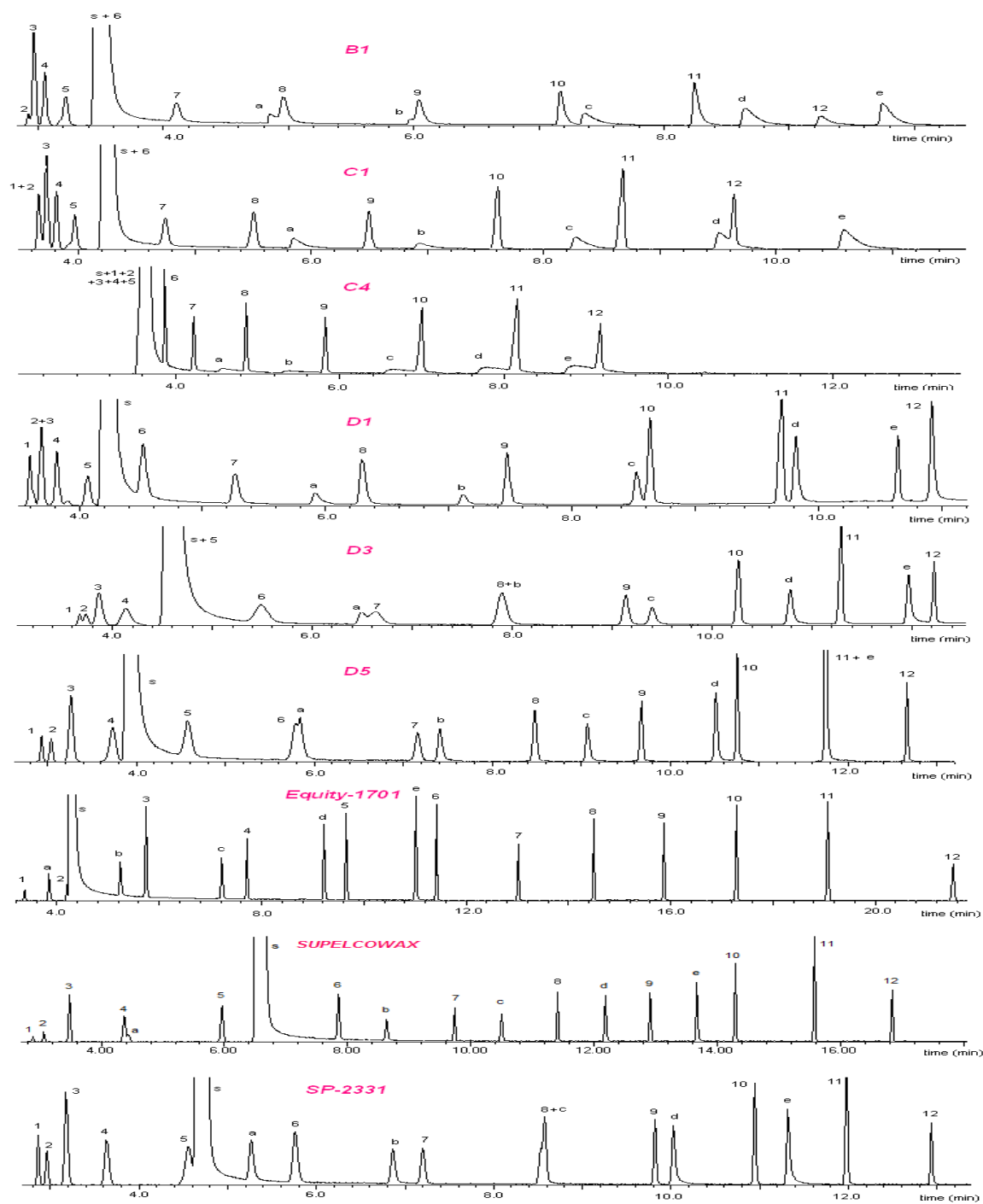


Figure 5.5 Separation of homologous alkane and alcohol mixture: 1 pentane, 2 hexane, 3 heptane, 4 octane, 5 nonane 6, decane, 7 undecane, 8 dodecane, 9 tridecane, 10 tetradecane, 11 pentadecane, 12 hexadecane, **a** ethanol, **b** 1-propanol, **c** 1-butanol, **d** 1-pentanol, **e** 1-hexanol, **s** dichloromethane,. GC separation conditions: 30 °C for 3 min, 10 °C min⁻¹ to 160 °C; 1 mL min⁻¹ He; MS detector. All chromatograms were obtained using 30 m x .25 mm x 0.20 μm d_f columns.

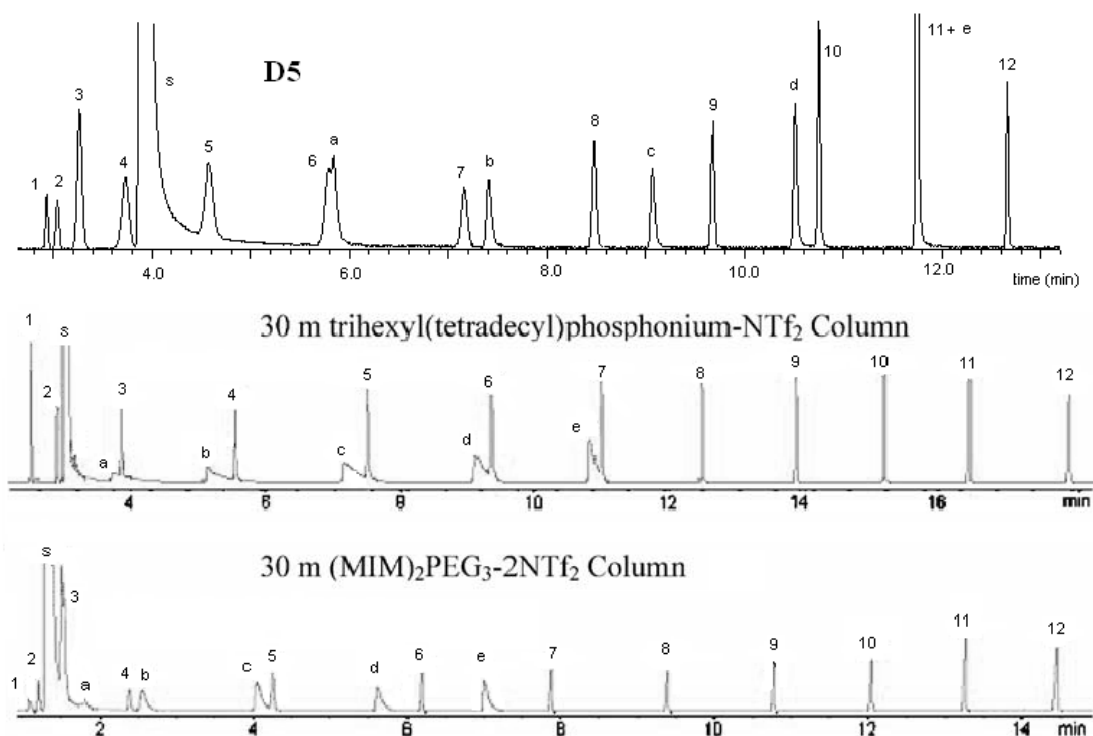


Figure 5.6 Comparison of separation of homologous alkane and alcohol mixture using trigonal tricationic IL **D5**, monocationic ionic liquid trihexyl(tetradecyl)phosphonium-NTf₂ and dicationic ionic liquid (MIM)₂PEG₃-NTf₂ columns under identical conditions.: 1 pentane, 2 hexane, 3 heptane, 4 octane, 5 nonane, 6 decane, 7 undecane, 8 dodecane, 9 tridecane, 10 tetradecane, 11 pentadecane, 12 hexadecane, **a** ethanol, **b** 1-propanol, **c** 1-butanol, **d** 1-pentanol, **e** 1-hexanol, **s** dichloromethane. GC separation conditions: 30 °C for 3 min, 10 °C min⁻¹ to 160 °C; 1 mL min⁻¹ He; MS detector for **D6**. FID for monocationic and dicationic columns. All chromatograms were obtained using 30 m x .25 mm x 0.20 μm d_f columns.

Similarly dodecane (8) and 1-butanol (c) co-elute in SP-2331 while these two are completely separated with the **D5** IL column. Columns **D1** and **D5** seem to be complementary to one another in that one column always separates peaks that co-elute on the other (see Figure 5.5). For example hexane (2) and heptane (3) co-elute on **D1** and are baseline separated on **D6**. Decane (6) and ethanol (a) peaks overlap on **D5** and separate on **D1**. Pentadecane (11) and 1-hexanol (e) co-elute in **D5** but are well separated on **D1**. Furthermore, the **D**-core ILs shows the greatest retention for alkenes among the trigonal tricationic ILs evaluated. The

retention times of alkanes in **D1**, **D3** and **D5** columns are directly proportional to the solvation parameter coefficient of interaction through dispersion forces (coefficient J). Within the **D** series, **D1** has the lowest J term, followed by **D3**, and **D6**. Accordingly, **D1** has the lowest retention for alkanes within the **D** series followed by **D3** and **D5** which shows the highest retention. The dual nature of ionic liquids is evident from these separations as both the alkane series and alcohol series are easily separated. Finally it was observed that the retention of alkanes by the tricationic ionic liquids is generally lower than their retention on monocationic and dicationic ionic liquids.^{125, 128} Therefore other than the high separation efficiency and low peak tailing for alcohols, the **D** series of ILs have the distinction of being stationary phases that produce good separations for variety of analytes, but with less retention times than conventional columns. This might render trigonal tricationic ILs as desirable stationary phases in two dimensional GC analysis.

5.3.6 Flavor and fragrance mixture

The flavor and fragrance mixture contains structurally related esters (including two homologous series) and has 24 compounds. The separation of this series provides another indication of the selectivity and separation efficiency of the trigonal tricationic ionic liquids compared to commercial columns. According to the Grob test mixture and the alcohol/alkane test results, the commercial column SP-2331 has comparable polarity to the trigonal tricationic ionic liquids, especially the **D** core series. The flavor and fragrance mixture is used to determine the separation efficiencies of columns with comparable polarities (see Figure 5.7). Column **C1** separated 21 compounds and co-eluted 3. The furfuryl homologous series elutes separately from the other esters. Only the last compound of the series furfuryl octanoate overlapped with benzyl butyrate. Again the **C4** column showed the least retention for the mixture and all the compound were eluted before 14 minutes. Five compounds were not baseline separated with the **C4** column. However, with the **D** series columns the compounds are much better separated.

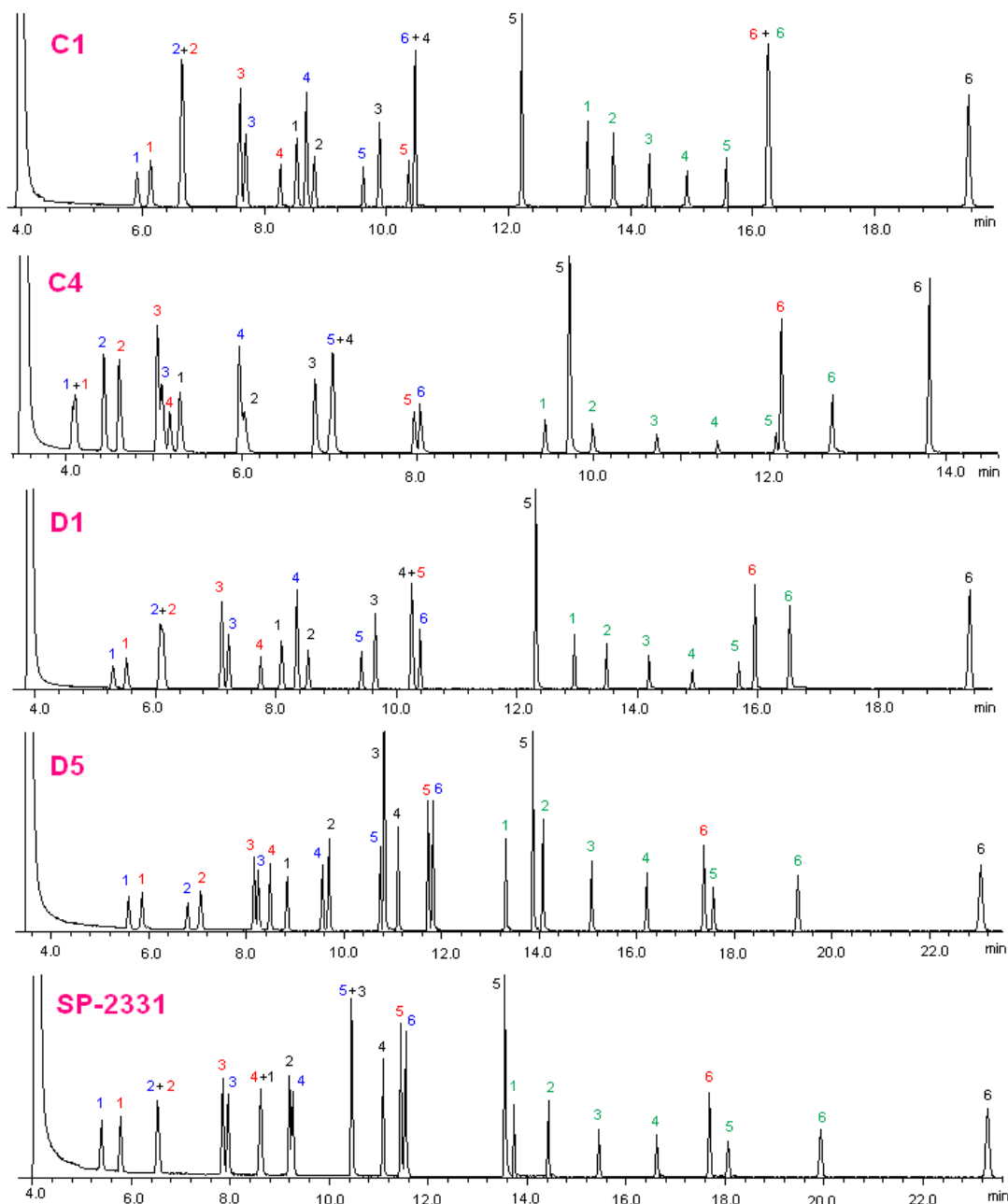


Figure 5.7 Separation of flavor and fragrance mixture. 1 ethyl propionate, 2 ethyl butyrate, 3 ethyl valerate, 4 ethyl hexanoate, 5 ethyl heptanoate, 6 ethyl octanoate, 1 methyl butyrate, 2 isopropyl butyrate, 3 propyl butyrate, 4 allyl butyrate, 5 hexyl butyrate, 6 benzyl butyrate, 1 methyl tiglate, 2 isopropyl tiglate, 3 propyl tiglate, 4 allyl tiglate, 5 hexyl tiglate, 6 benzyl triglate, 1 furfuryl propionate, 2 furfuryl butyrate, 3 furfuryl pentanoate, 4 furfuryl hexanoate, 5 furfuryl heptanoate, 6 furfuryl octanoate, 40 °C for 3 min, 10 °C min⁻¹ to 150 °C; 1 mL min⁻¹ He; MS detector. All chromatograms were obtained using 30 m x .25 mm x 0.20 μm d_f columns.

Especially with the **D5** column, the retention and selectivity were comparable to a commercial (SP-2331) column, but the separation was much better. In **D5** column, all the 24 compounds are nearly base line separated whereas in the commercial column three esters co-elute and two are only partially separated (isopropyl tiglate and ethyl hexanoate). This confirms the fact that **D5** is a highly efficient and selective stationary phase for gas chromatography.

5.3.7 FAME isomer separation

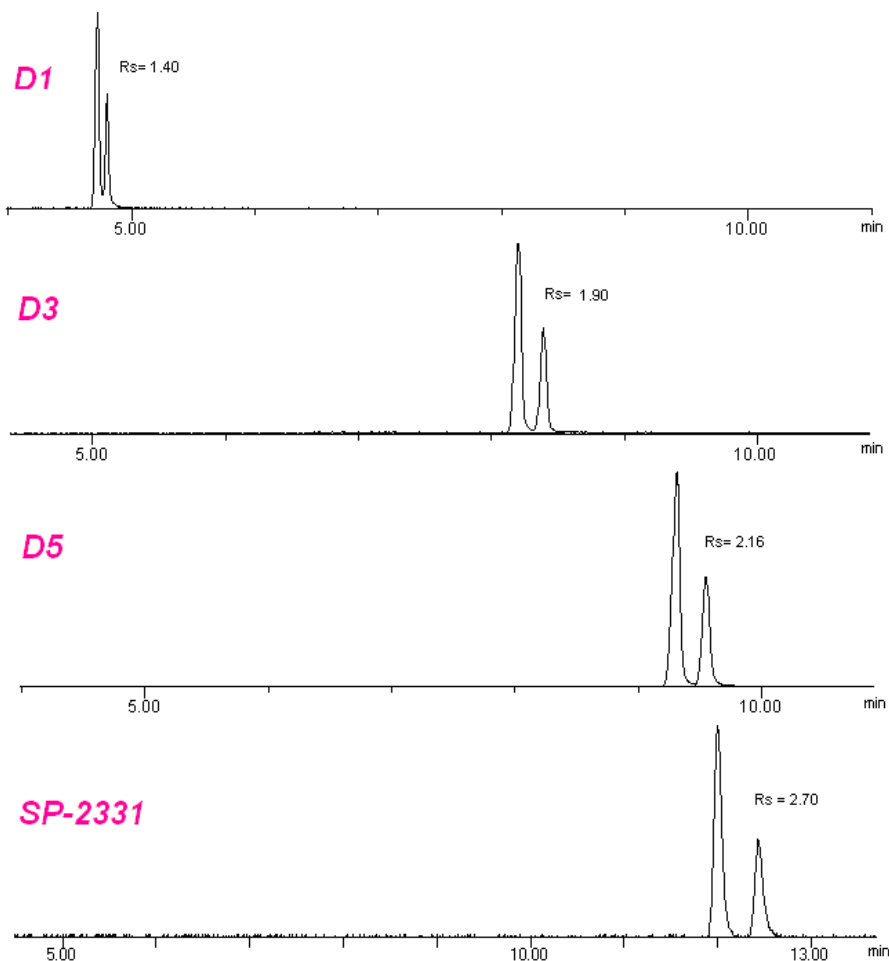


Figure 5.8 Separation of a mixture of methyl oleate (5 mg mL^{-1}) and methyl elaidate (10 mg mL^{-1}). Column dimensions: $30\text{m} \times .25 \text{ mm} \times .20 \mu\text{m}$ d_i columns. GC separation conditions: isothermal at $165 \text{ }^{\circ}\text{C}$; 1 mL min^{-1} He; MS detector.

Determination of fatty acid content in edible oils has been an area of high interest due to its importance in dietary, nutritional and therapeutic fields. Generally these isomeric

unsaturated carboxylic acids are converted to their methyl esters and the fatty acid methyl esters (FAME) are separated using highly polar stationary phases.^{180, 182, 183} In this test, a mixture of methyl oleate (9*cis* 18:1) and methyl elaidate (9*trans* 18:1) were separated using the highly polar trigonal tricationic IL stationary phases **D1**, **D3**, **D5** and the commercial SP-2331 stationary phase (see Figure 5.8). The *trans*- isomer is twice the concentration (10 mg ml⁻¹) of the *cis*- isomer (5 mg ml⁻¹) for ease of identification. In the **D** core trigonal tricationic ionic liquid columns and the commercial SP-2331 column, the *trans* FAME elutes before the *cis* analogue. It is characteristic for cyanopropyl based stationary phases to elute the *trans*- isomer first. With polyethylene glycol-based stationary phases, the *cis*- isomer elutes first. This indicates that the **D** core ionic liquids when used as stationary phases are more similar to the highly polar cyanopropyl stationary phase, but with greater thermal stability. Under similar separation conditions, **D5** shows the best separation for the *cis* and *trans* isomers by the **D** core series of ILs, followed by **D3** and **D1** respectively.

5.4 Conclusions

Use of multifunctional ionic liquids as stationary phases for GC can be limited as the most common counter anion for many ionic liquids (i.e., bis(trifluoromethanesulfonyl)imide) results in peak tailing for alcohols and other H-bond forming analytes. Specific **D**-core trigonal tricationic ILs were shown to overcome this problem. According to the solvation parameter study, all monocationic, dicationic and long chain linear tricationic ionic liquids have almost identical apparent polarities and interaction parameters. However, those were quite different for the some trigonal tricationic ILs, namely the **C4**, and **D**-core series, and resulted in unique selectivities and retention behaviors. This uniqueness appears to be the result of two main factors. First is the rigid trigonal geometry which forces the three positive charges to reside in close proximity for ILs with short linkage chains. The second is the contribution from the Amide group. The prominent interaction types of trigonal tricationic ILs were dipole–type interactions, H–bonding interactions and dispersive interactions. Alcohol/alkane mixture and Grob test

mixtures indicated that these ionic liquids are far more polar than either the monocationic or dicationic ionic liquids reported thus far. Nitrogen core ionic liquids **C1** and **C4** were the most polar stationary phases and displayed very low retention for alkanes. Grob test, FAME isomer separation, and elution order of C18:1 *cis-trans* FAME isomers indicated that **D** core ionic liquids, especially **D5** have polarities comparable to SP-2331, a 100% cyanopropylpolysiloxane commercial stationary phase. Ionic liquid **D5** stands out as it shows minimum peak tailing for alcohols and other H-bonding analytes. According to the flavor and fragrance test, **D1** and **D5** are complementary to each other and show higher selectivity and superior separation efficiencies than the commercial SP-2331 stationary phase which has roughly comparable polarity. Furthermore, **D5** is more thermally stable than the SP-2331. It was observed that benzylimidazolium cationic moiety introduces much higher viscosities to the ionic liquid systems. IL **D3** has the highest viscosity among ionic liquids ever to be reported. All these trigonal tricationic ILs were highly thermally stable and were liquids in a wide temperature range. These values far exceed those observed for traditional monocationic ionic liquids. According to these results, trigonal tricationic ionic liquid **D5** is very promising as a highly polar stationary phase that has high thermal stability and yields symmetrical peaks for H-bonding analytes.

CHAPTER 6
RAPID, EFFICIENT QUANTIFICATION OF WATER IN SOLVENTS AND SOLVENTS IN
WATER USING AN IONIC LIQUID-BASED GC COLUMN

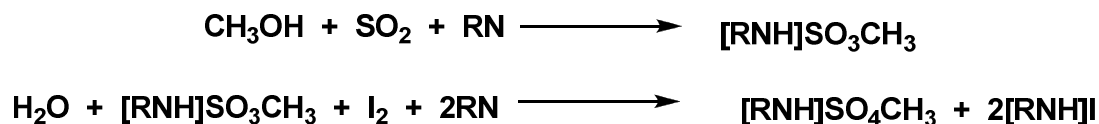
Developing versatile, rapid and accurate analytical techniques for the detection and quantification of water in a variety of materials remains an important and ubiquitous analytical problem. Water is one of the most prevalent impurities in many industrial and consumer products and processes. In other cases water is an essential component, the concentration of which must be known accurately and controlled. Here, we report an effective and sensitive ionic liquid (IL)-based capillary gas chromatographic (GC) method with a thermal conductivity detector (TCD) for the determination of water content in liquid samples. The open tubular capillary columns, coated with specific ILs developed in this study, increased the sensitivity and significantly increased the ruggedness of this technique. The absolute water content in 50 different solvent samples was determined by using either acetone or acetonitrile as an internal standard (IS). The lower limit of detection (LOD) of this method is ~2 ng water. Samples containing higher levels of water are also readily analyzed without pretreatment. Conversely organic solvents can be measured in water by the same approach using either a TCD or a flame ionization detector (FID). A comparison between IL based columns and commercial columns revealed the enhanced performance of the IL based columns. Standardization was performed with National Institute of Standards and Technology (NIST) reference materials and the accuracy was compared with another independent method (Karl-Fischer titration). The developed method is highly sensitive, fast, and is not affected by interferences and side reactions common with existing Karl Fischer titration (KFT) methods.

6.1 Introduction

The determination of water content in solvents and consumer products, including foods, pharmaceuticals, and industrial materials is of great importance. Indeed analytical testing for the presence and concentration of water is one of the most frequent, important and ubiquitous measurements made in modern industrial society. Thus a versatile, simple and efficient analytical technique for the accurate quantification of water is imperative. Due to the essentially universal presence of water, accurate, facile and sensitive techniques are needed. Though various techniques such as gravimetry,¹⁸⁴ Karl Fisher titration (KFT),^{185, 186} gas chromatography,¹⁸⁷⁻¹⁹⁴ near IR spectrophotometry,^{187, 195-197} solvatochromic sensing,¹⁹⁸ fluorine nuclear magnetic resonance spectroscopy (F-NMR),¹⁹⁹ isotope ratio mass spectrometry (IRMS)²⁰⁰ and others have been reported in the literature, only few methods are widely accepted and used.

Currently, the most commonly used method for water analysis is the KFT, which was first reported in 1935.¹⁸⁵ In this titrametric method, I₂ is reduced to HI in the presence of water.¹⁹² There are four components in the Karl Fischer reagent consisting of: iodine, sulfur dioxide, a suitable base (RN); [originally pyridine was used, but now imidazole is more common] and a suitable solvent (methanol, ethanol, diethylene glycol monomethyl ether, etc).²⁰¹

The accepted mechanism of this two step reaction is:²⁰¹



The end point is determined potentiometrically. Two types of KFT methods are used. They are the coulometric titration and the volumetric titration. The former is used to detect trace amounts of water, ranging from 10 µg to 99 µg (1 ppm – 5%), and it requires ~ 5 g or more of sample.²⁰² On the other hand, volumetric titration is used to detect higher water quantities; > 1 mg (10 ppm – 100%) and the amount of sample required varies from 0.1 mg to 500 mg.²⁰³

Therefore, prior knowledge of the approximate amount of water present in the sample is required in choosing the correct KF method of analysis.

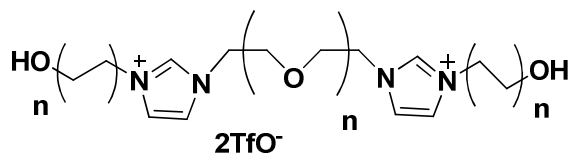
Although this is a well established method, interference of side reactions,¹⁹² reagent instability,²⁰⁴ sample insolubility²⁰⁵ and pH issues¹⁸⁷ prevent it from being accepted as a universal method. Variations on the basic KFT methodologies have been developed in an attempt to overcome these problems.^{186, 192, 205} However, many issues still remain, not the least of which is that the reagents degrade with time and there is residual water in all KFT reagents. Another applied method for water detection is based on gas chromatography. Early attempts using gas chromatography were mainly based on packed (molecular sieve) columns, involving both direct detection by thermal conductivity detector (TCD)^{190-192, 194, 206} and indirect detection (i.e. reacting water with calcium carbide to convert to acetylene) with a flame ionization detection (FID)¹⁸⁸. Peak asymmetry,¹⁸⁷ poor sensitivity, poor efficiency, strong adsorption of water and many solvents by the stationary phase,¹⁹⁰ overlapping of the water peak by other larger peaks, and the inability to detect higher amounts of water¹⁸⁷ limited its application in many cases. Attempts to eliminate peak asymmetry,^{187, 207} using wide-diameter open tubular columns¹⁸⁹ and capillary columns¹⁹³ showed some improvement. Also most conventional capillary column GC stationary phases are degraded by water.

A truly useful, broadly effective capillary GC method for water should meet several criteria including the following. 1) Water should not alter or degrade the stationary phase, thereby altering retention times and peak shapes. 2) There must be a considerable difference in the retention of water and most/all organic solvents especially when the solvent peak is very large relative to the water peak. 3) The water peaks should show good efficiency and symmetry. 4) The water and solvent chromatogram should have sufficient separation space for an appropriate, baseline separated internal standard.

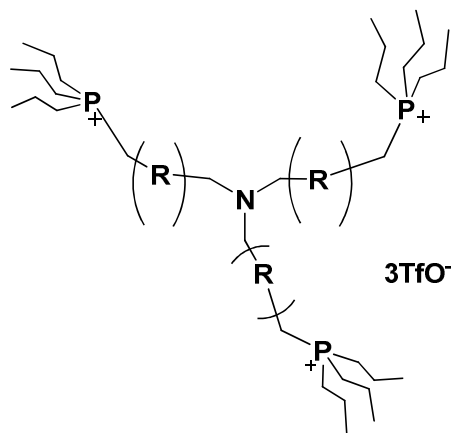
In this study, we examine an ionic liquid (IL) based capillary gas chromatographic method with TCD for the direct determination of water content in liquid samples. The unique

nature of ILs including; high thermal stabilities,¹¹⁸ variable polarities^{113, 208} and exceptional stability to water and oxygen make them excellent choices as stationary phases for this methodology.

1) HMIM-PEG TfO⁻



2) TPT TfO⁻



3) DMIM-PEG TfO⁻

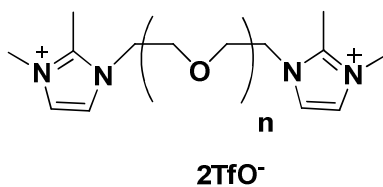


Figure 6.1 Ionic liquid GC stationary phases used in this study

As will be shown, open tubular capillary columns, coated with specific IL stationary phases (developed for water analysis) can tremendously enhance the sensitivity, applicability and reliability of this technique. Furthermore analysis times can be decreased to 6 min or even less

than 3 min in many cases, and samples with virtually any concentration of water can be analyzed. The efficacy of this approach is demonstrated with 50 different solvent samples.

6.2 Experimental

6.2.1 Apparatus

The analysis was performed using an Agilent Technologies 6890N gas chromatograph (Agilent technologies Inc., Wilmington, DE), equipped with a 7683B series autoinjector, TCD and Chemstation plus software (Rev. B.01.03). An Agilent technologies 10 μ l syringe (5181-1267), was used with the autosampler, while a Hamilton 10 μ l syringe was used for all manual injections. The other experimental parameters are given in Tables 1 & 2. The fused silica capillary columns were coated with IL stationary phases synthesized as previously reported.^{118, 121} The columns were 30 m long, 0.25 mm internal diameter (I.D.) and 0.2 μ m film thickness. KF analysis was performed using Aquastar V1B volumetric titrator (EM Science, a division of EM industries, Inc., Cherry Hill, NJ).

6.2.2 Materials

The water reference material: 8509, moisture in methanol (MeOH, 97 ± 13 ppm water) was obtained from National Institute of Standards and Technology (NIST, Gaithersburg, MD). The 4Å molecular sieves, hydranal water standard 1.0, tetrahydrofuran (THF) and both the internal standards (IS), acetone and acetonitrile, were purchased from Sigma-Aldrich (St. Louis, MO). Aquastar combititrant 2 and Aquastar methanol were purchased from EMD chemicals (Gibbstown, NJ). The high purity water was obtained by filtering the deionized water with Millipore, synergy 186. The testing solvents were from, Sigma-Aldrich, Mallinckrodt, EMD, Fisher, Omni solvent, and Acros organics.

6.2.3 Sample preparation

The accurate quantification of water was achieved using one of two internal standards (ISs), either acetone or acetonitrile. Two different ISs were available in case one co-eluted with the analyte solvent under the conditions of the experiment. Internal standards were dried to

<10mg/kg by storing over 30% w/v 3Å molecular sieves for seven days prior to use. A typical sample preparation involved drying a 2ml autosampler vial overnight at 130°C followed by the addition of approx. 1ml of solvent. The mass of the solvent was recorded using an analytical balance. 6.0mg of internal standard was added prior to analysis.

6.2.4 Methods

For initial screening, the columns were conditioned at 120°C for 2 hours and high purity water was injected, 0.1 µl, using 100:1 split ratio at the desired temperature. The sample of interest is injected in the splitless mode (0.2 µl to 5 µl), in order to examine the separation between water and the bulk solvent. This preliminary experiment helped in determining which IS should be used.

Water quantitation was achieved by integration of the internal standard peak and the water peak. The concentration of internal standard in mg/kg was multiplied by the ratio of water peak to internal standard peak and the result was divided by the response factor. The resulting number represents the concentration of water in the sample in mg/kg. Each solvent was prepared in triplicate and each individual sample was injected in triplicate for a total of n=9 individual integrations for each solvent analyzed.

6.2.5 Detection limit and quantitation limit

The detection limit (LOD) and the quantitation limit (LOQ) were calculated according to the guidelines of the US Food and Drug Administration (FDA),^{209, 210} using the following equations:

$$\text{LOD} = \frac{3.3 \sigma}{S}$$

LOD =

$$\text{LOQ} = \frac{10 \sigma}{S}$$

Where,

σ = the standard deviation of the response

S = the slope of the calibration plot

The σ is normally obtained from the standard deviation of the blank sample.²¹⁰ Since it is impossible to obtain a sample without water, the 1st point of the calibration plot, where there is no added water is used as the blank sample and its standard deviation was used as σ . The slope was obtained from the regression analysis of the plot; peak area ratio of water and I.S. vs amount of water.

6.3 Results and Discussion

Figure 6.1 shows the structures of the three ILs that were used as stationary phases in this study. Generally, IL stationary phases containing trifluoromethylsulfonate (TfO⁻) anions resulted in more symmetric water peak shapes than those of that contained PF₆⁻, BF₄⁻ or bis[(trifluoromethyl)sulfonyl]imide (NTf₂⁻), with the same cation (data not shown). In addition to the IL-based GC columns, a commercially available polyethylene glycol (PEG) column also was evaluated for comparison purposes.

Figure 6.2 shows the GC separations of small amounts of water impurities from two of the organic solvents that were analyzed. Note that the water peak can be eluted either before or after the large organic solvent peak depending on the relative elution order of the two on the ionic liquid-based stationary phases (Figs. 6.2A-C). In most cases the "separation window" between the water and solvent peaks is sufficiently large (Figure 6.2A) that a thermal gradient can be used to further narrow the peak width of water and reduce analysis times (Figure 6.2B). A comparison of the separation of water from methylene chloride on an IL column versus a commercial PEG type column (see Experimental) is shown in Figure 6.3. Note that the ionic liquid based column (Figure 6.3A) produced better peak shapes and selectivity even though the separation conditions were optimized for the PEG column and not the IL one. In all cases (for all solvent samples) the IL-based separations were substantially better in terms of selectivity and efficiency.

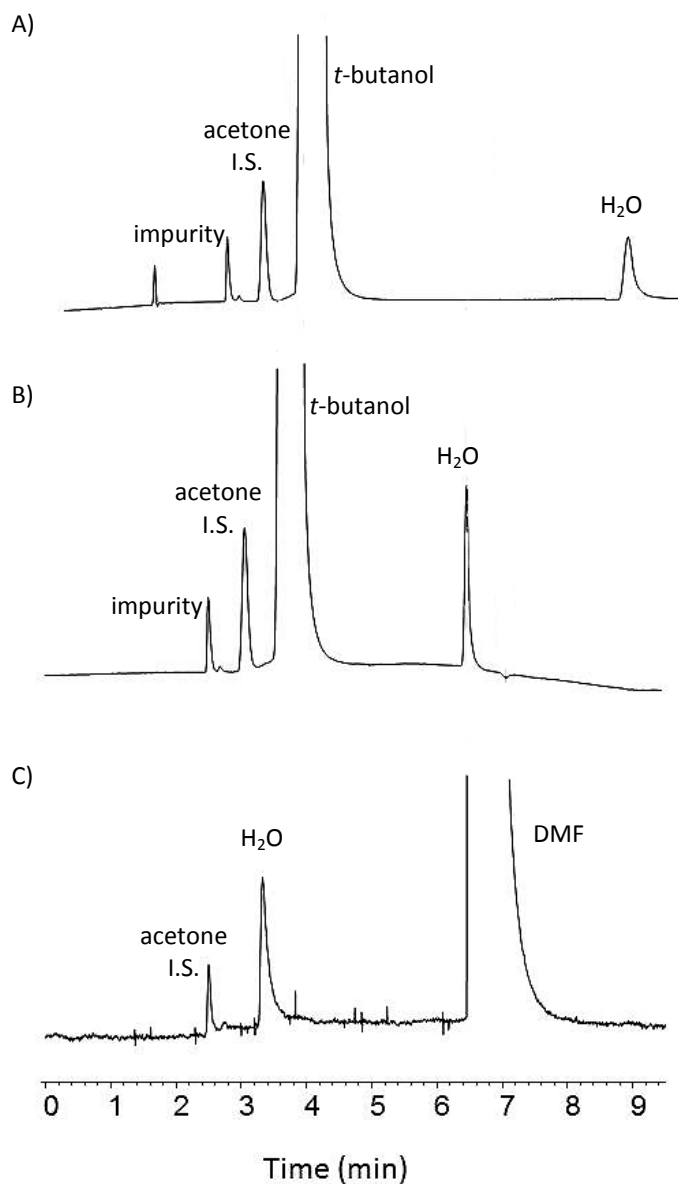


Figure 6.2 Chromatograms illustrating the relative retention orders of water and different organic solvents. Chromatograms A and C are isothermal separations. Chromatogram B is for the same sample as in A, however a temperature gradient was used to decrease the analysis time and further “sharpen” the water peak. This enhanced the sensitivity and precision of the method. Chromatogram A: 1 μ L injection, 50°C, analysis time: 9 min, Internal Standard: acetone (0.4%) Chromatogram B: 1 μ L injection; 50°C (hold 2min), ramp 10dpm to 80°C; analysis time: 6min, Internal Standard: acetone (0.4%). Chromatogram C: 0.2 μ L injection; 110°C, analysis time: 8min, Internal Standard: acetone (0.2%).

Table 6.1 compares the amount of water measured in ten solvents and a NIST methanol standard using four different capillary GC methods and the Karl Fischer titration (KFT). The samples were chosen so that the KFT analysis could be done without the use of special reagents (e.g., as are needed to quantify water in aldehydes and ketones).¹⁸⁶ Also most of these samples could be analyzed on the commercial PEG column. As can be seen from the data, the ionic liquid based columns usually produced the most precise and accurate results (as indicated from the RSDs and NIST standard respectively, Table 6.1). It should be noted that no more than one microlitre of sample was used for any of the capillary GC determinations. Conversely the KF titrations utilized between 5 and 15 grams of sample depending on the water content of the solvents (larger samples were required for samples containing the least water (Table 6.1).

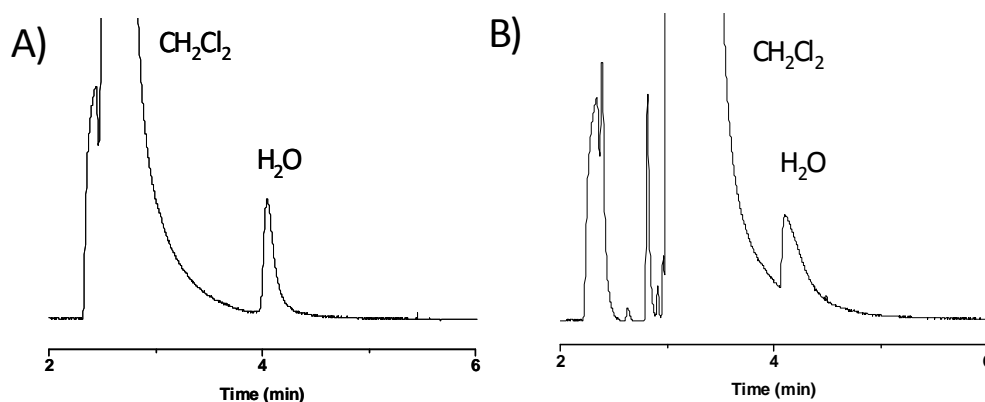


Figure 6.3 Example of improved resolution and peak symmetry using an ionic liquid based stationary phase (A) versus a commercial PEG column (B). Injection $1\mu\text{L}$, Temp 80°C

The limits of detection (LOD) and limits of quantitation for the IL columns were better than those found for the commercial PEG column even when analyzing samples and using conditions that are necessary for favorable separations on the PEG column (Table 6.1). The detection limit of coulometric KFT is $10\mu\text{g}$, and it requires at least 5 g of sample. The IL based

GC method required only 0.2 μl of sample to obtain a much lower detection limit (~ 2.0 ng or $\sim 5,000$ x greater sensitivity).

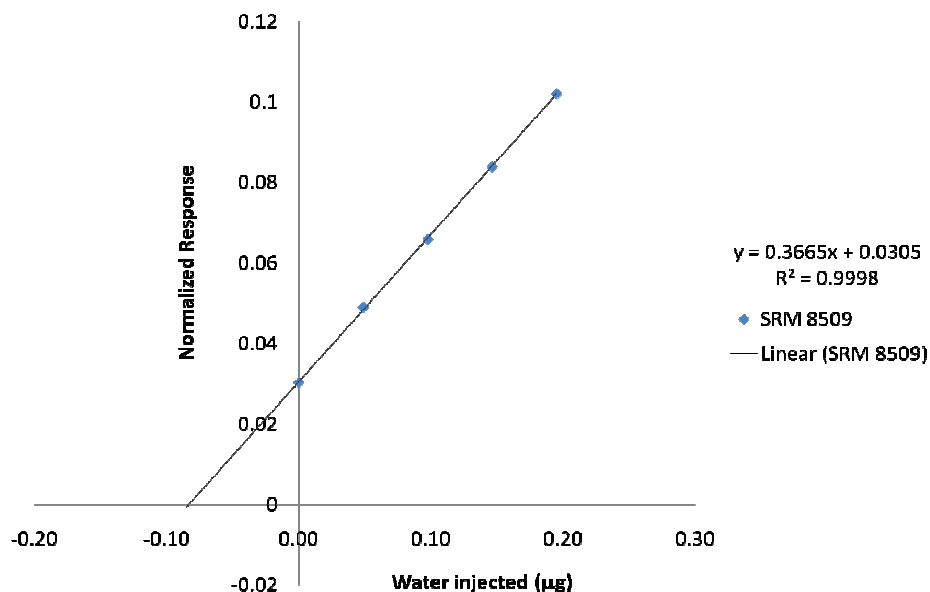


Figure 6.4 Plot of normalized response versus amount of spiked water injected onto column. 50-200nL volumes of water were spiked into 1ml of SRM 8509 using 0.5 μL calibrated Hamilton syringe.

Table 6.2 lists the water content of 50 different solvents as determined with the three IL columns evaluated in this study. Figure 6.4 indicates the number of these solvents that could be successfully analyzed on each column. To be considered a successful separation, the water (analyte) peak had to be separated from both the solvent and at least one of the internal standards (i.e., acetone or acetonitrile). All three IL columns could be used to quantify water in 38 out of the 50 solvents (Figure 6.4). The HMIM-PEG-TFO overall was the most successful as it could be used to quantify water in 47 of the solvent samples, including two samples that were not amenable to separation on the other tested columns.

Table 6.1 Comparison of the ionic liquid GC results with the best results from the Karl Fischer Titration (KFT) and the use of a commercial PEG GC column.

Sample	HMIM-PEG		TPT		DMIM-PEG		Commercial		KF ^a	
	H ₂ O/ppm	RSD ^b	H ₂ O/ppm	RSD ^b	H ₂ O/ppm	RSD ^b	H ₂ O/ppm	RSD ^b	H ₂ O/ppm	RSD ^b
THF ^c	110	6.0	108	6.8	117	8.1	77	12.0	179	6.2
DMF ^d	594	4.0	606	4.9	614	6.2	X ^g	X ^g	678	4.3
<i>t</i> -Butyl alcohol	2130	1.9	2010	6.2	1950	4.0	1868	8.3	2006	6.4
DMSO ^e	773	2.9	800	4.4	820	6.0	740	11.3	796	4.6
Ethanol	890	2.0	880	3.8	880	2.0	670	11.2	809	4.0
Ethyl acetate	370	2.8	365	3.9	371	1.0	327	6.7	509	6.6
Methanol	209	7.1	198	4.6	203	6.0	173	21.0	241	6.0
DCM ^f	48	8.2	52	6.3	47	7.3	78	6.5	117	3.3
1-Propanol	308	4.0	X ^g	X ^g	285	3.2	X ^g	X ^g	365	7.1
2-Propanol	180	3.9	171	2.4	162	3.0	179	14.0	232	4.0
NIST MeOH Std.	104	4.0	99	3.8	114	6.8	47	8.0	158	8.6

^aFive grams of sample were used for all KFT except for those with the lowest water concentrations. Ten grams of sample were used for the methanol and tetrahydrofuran and fifteen grams for methylene chloride. Twelve grams of sample were used for the NIST methanol standard. ^bMinimum of three determinations were done. ^cTetrahydrofuran = THF. ^dDimethylformamide = DMF. ^eDimethyl sulfoxide = DMSO. ^fDichloromethane = DCM. ^gNo adequate value could be obtained with this column because of excess overlap between solvent and internal standard or between the solvent and the water peaks.

Table 6.2 Detection of water in 50 solvents. The symbol “x” indicates that the water peak was not dequately separated from the solvent peak. All other experimental conditions are given in experimental section.

Sample	HMIM-PEG		TPT		DiMIM-PEG	
	Water (ppm)	RSD%	Water (ppm)	RSD%	Water (ppm)	RSD%
Acetic acid	420	1.0	410	6.9	440	6.0
Acetone	2380	3.8	2380	6.1	2520	0.3
Acetonitrile	103	3.0	98	6.9	103	2.7
Anisole	X	X	990	2.6	990	3.5
Benzene	18	2.4	17	8.4	21	9.5
1-Butanol	1190	3.6	1150	6.8	X	X
2-Butanol	3530	2.6	X	X	3380	2.3
2-Butanone	730	3.7	760	1.2	710	6.8
<i>t</i> -Butyl alcohol	2130	1.9	2010	6.2	1950	4.0
Carbon tetrachloride	36	3.7	38	4.4	36	6.7
Chlorobenzene	38	9.6	42	8.9	39	3.1
1-Chlorobutane	27	6.5	23	6.0	28	3.7
Chloroform	155	2.3	153	6.1	162	6.3
2-Chloropropane	120	4.0	113	6.3	125	4.2
Cyclohexane	18	9.7	21	7	20	3.5
Cyclohexanone	8630	0.9	8450	6.4	8710	1.0

Table 6.2-continued

1,2-Dichlorobenzene	X	X	12	6.0	X	X
1,2-Dichloroethane	160	6.9	150	13.7	140	2.4
1,3-Dichloropropane	114	4.9	X	X	102	1.5
Diethyl ether	400	7.6	420	1.6	390	6.4
Di(ethylene glycol) ethyl ether	950	4.3	970	9.5	930	2.1
1,2-Dimethoxy-ethane (glyme, DME)	7500	1.5	7600	1.4	7300	0.6
Dimethyl- formamide (DMF)	594	4.0	606	4.9	614	6.2
Dimethyl sulfoxide (DMSO)	773	2.9	800	4.4	820	6.0
Dioxane	3800	4.0	3700	3.5	3900	2.3
Ethanol	890	2.0	880	3.8	880	2.2
Ethyl acetate	370	2.8	365	3.9	370	1.4
Ethylene glycol	170000	3.5	169000	6.3	179000	3.2
Heptane	18	6.3	17	8.7	16	8.7
Hexane	14	6.3	17	9.5	16	9.0
Methanol	209	7.1	198	4.6	203	6.0
Methyl <i>t</i> -butyl ether (MTBE)	1900	1.1	1800	6.1	1900	6.6
Methylene chloride	48	8.2	52	6.3	47	7.3
<i>N</i> -methyl-2-pyrrolidinone (NMP)	18700	6.7	18500	4.8	19000	2.1

Table 6.2-continued

Nitroethane	770	3.2	X	X	X	X
Octane	13	8.0	17	10.0	14	6.1
1-Octanol	190	4.6	210	7.0	190	6.6
Pentane	16	3.4	18	9.6	15	4.8
Petroleum ether (ligroine)	16	3.9	19	6.1	17	4.6
1-Propanol	308	4.0	X	X	285	3.2
2-Propanol	180	3.9	171	2.4	162	3.0
Pyridine	X	X	910	4.6	X	X
Tetrahydrofuran (THF)	110	6.0	108	6.8	117	8.1
Toluene	31	4.2	29	6.0	32	4.6
Triethyl amine	56	0.3	57	0.2	57	6.7
<i>o</i> -Xylene	74	7.7	X	X	76	4.9
<i>m</i> -Xylene	22	7.9	X	X	24	0.6
<i>p</i> -Xylene	23	9.2	X	X	26	0.2
Nitromethane	920	6.0	X	X	X	X
Nitrobenzene	119	2.5	109	8.5	117	3.9

The TPT TfO⁻ column was used to quantify water in 42 solvents, including pyridine and 1,2-dichlorobenzene which were not possible using the other two columns that were investigated. The DMIM-PEG TfO₂⁻ column often gave the best, separation window between the water peak and solvent peaks, compared to the other columns. Hence all the separations that are possible on this column can be done at even higher temperatures than those used in this report (Tables 6.1 and 6.2) or using temperature gradients (Figure 6.2B) if desired. In most cases this means that many analyses times can be less than 3 min (results not shown).

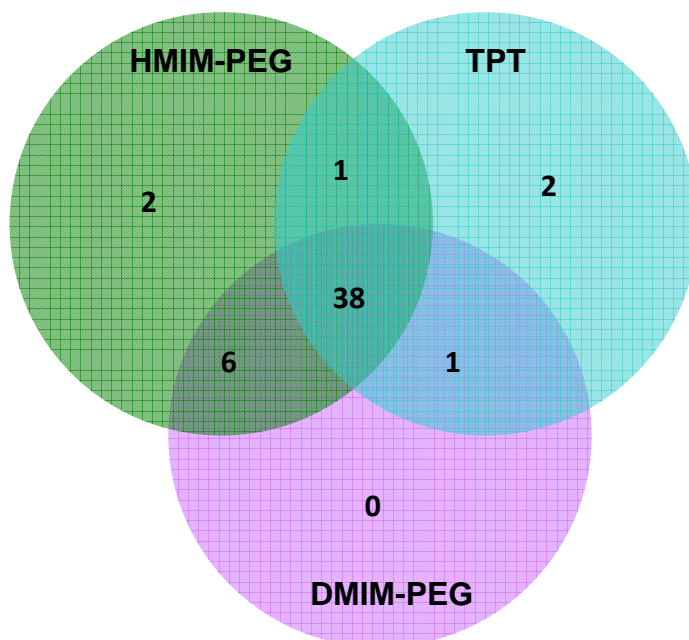


Figure 6.5 Illustration showing the number of successful water separations on each of the three IL based columns. Note that 38 out of the 50 solvents could be analyzed on all three IL columns. However 2 each could only be done on the HMIM-PEG and TPT columns. The HMIM-PEG was the most broadly useful stationary phase as it produced adequate separations of water from 47 out of the 50 tested solvents.

Since capillary columns containing ionic liquid (IL) stationary phases are effective in the measurement of small amounts of water in organic solvents, it would not be surprising if they also can be used to determine trace organic solvents in water. Such a determination is shown in Figure 6.6. Note that in Fig 6.5a, TCD is used in order to show the elution of the water peak

relative to trace organic solvents. In Figure 5b even lower concentrations of the organic contaminants are seen when using flame ionization detection (FID). Of course water cannot be seen with this detector. It should be noted that the injection of water samples is not recommended on ordinary commercial columns that are not based on ionic liquids. Virtually all traditional commercial columns show appreciable degradation and continuously changing chromatograms when analyzing water samples. Analyzing water for organic solvents tends to be much more damaging for these columns than analyzing organic solvents for trace amounts of water. For example three successive commercial PEG columns had to be used for this study while the separations and conditions of all IL columns used remained unchanged throughout the study (>1,600 injections).

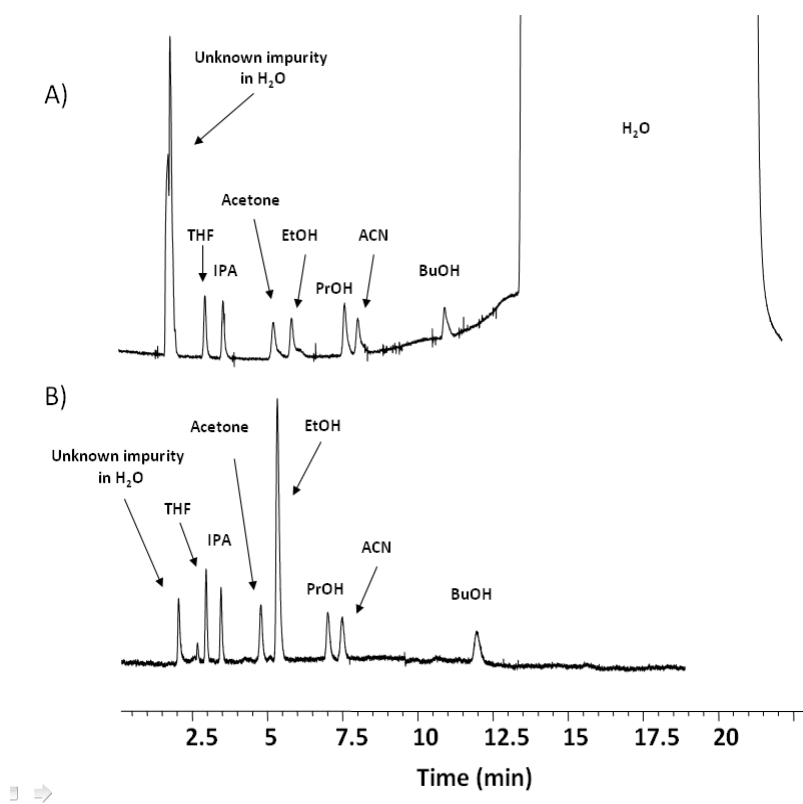


Figure 6.6 Example of the separation of organic solvents in water using ionic liquid based stationary phase. Chromatogram A: DMIM-PEG; 40°C; 0.2ml injection; thermal conductivity detector (all solvents: 100mg/kg)Chromatogram B: DMIM-PEG; 40°C; 0.2ml injection; flame ionization detector (all solvents: 5mg/kg)

6.4 Conclusions

A rapid, facile IL-based GC method has been developed for the quantification of water in extremely diverse solvent samples. Limits of detection using this technique are superior when compared to KFT. Furthermore, the IL-GC methodology requires less sample and is free from other complications associated with KFT. The IL GC method can be used regardless of the chemical nature of the solvent and produces no additional waste products. When compared to other GC methods using commercially available PEG columns, the IL based columns possessed superior selectivity for water in all solvents tested. Further, they show no degradation or chromatographic changes with time. Typical analysis times ranged from <3 min to 7 min. The extension of this approach to gases and solid samples is under investigation and will be reported subsequently.

CHAPTER 7
DEGRADATION STUDY ON CARNOSIC ACID, CARNOSOL, ROSMARINIC ACID AND
ROSEMARY EXTRACT

A study on the degradation of rosmarinic acid, carnosol, carnosic acid and the mixture of the three was conducted in ethanol solution under different temperatures and light exposure conditions. In general, degradation increased with a temperature increase. Some unique degradation products formed only under light exposure conditions. The degradation products have been identified by HPLC-MS-MS, UV and NMR. Also, degradation behavior of rosemary extract in fish oil was investigated. A much slower degradation was observed for carnosic acid in the mixture of rosemary extract and fish oil than that of the carnosic acid in the ethanol solution. Also, it appears that in the mixture of the two antioxidants, carnosic acid tends to stabilize/protect carnosol to some extent.

7.1 Introduction

With the increase of awareness of the health benefits of certain foods and the advent of nutraceutical products, attention has been focused on natural antioxidants as potential replacements for artificial antioxidants.^{211, 211-222} Rosemary is one of the most effective natural antioxidants.²²³⁻²²⁹ Its extracts have been added to lipids or lipid containing foods, such as fish oils^{230, 231}, plant seed oils^{219, 232-235} and meats²³⁶⁻²⁴², to prevent oxidation and prolong their storage time. The antioxidative activity of rosemary is mainly due to its phenolic diterpene constituents.²⁴³⁻²⁴⁶ Carnosic acid (Figure 7.1-1) and carnosol (Figure 7.1-2) are the two most active phenolic diterpenes in rosemary extract.^{243, 247} Other phenolic diterpenes, such as rosmarinic acid (Figure 7.1-3), rosmanol (Figure 7.1-4) and epirosmanol (Figure 7.1-5), also contribute to the antioxidative properties of rosemary extract, albeit to a lesser degree.²⁴⁸ Besides acting as antioxidants in food, rosemary extract has also displayed medicinal properties.²⁴⁹⁻²⁵³

Quantification of the phenolic diterpenes in rosemary extract is therefore of great interest. Two methods are often used to determine the phenolic diterpene contents in rosemary extracts. One is using Folin-Ciocalteu assay to measure the total phenolic diterpenes.^{254,255} In this method the substance being tested is used to titrate the Folin-Ciocalteu reagent and the total content of phenolic compounds is determined by the amount of the substance needed to inhibit the oxidation of the reagent. However, the Folin-Ciocalteu reagent also is able to react with other reducing components that are not phenolic compounds. Thus the total content of phenolic compounds measured by this method is sometimes inaccurate. Furthermore, the composition of specific phenolic diterpenes in the rosemary extracts cannot be known through this method. The other approach is a chromatographic method which separates the phenolic diterpenes. HPLC is the most frequently utilized chromatographic method for quantitative analysis of rosemary extract.²⁵⁶⁻²⁶⁰ However, the reported HPLC methods either require long analysis times, during which the unstable phenolic diterpenes may degrade, or could not provide baseline separation of the phenolic diterpenes in rosemary extract, which caused difficulty in integrating the peak areas of each individual component. A few supercritical fluid chromatography (SFC) methods were also reported for the separation of antioxidative compounds in rosemary extracts.²⁶¹ However, SFC is more often used as preparative method for isolating the functional ingredients in rosemary extract but not for quantification.²⁶²⁻²⁶⁴ In the reported capillary electrophoresis (CE) analyses of rosemary extract, the electropherograms often display a noisy baseline which makes it difficult for accurate quantification.²⁶⁵⁻²⁶⁸

In this study, a Cyclobond 2000 I RSP column is successfully used in the reversed phase mode as an alternative to conventional C18 columns. Carnosic acid, carnosol, rosmarinic acid and the degradation products are separated within 15 min. The same method also is applicable in the separation of all components in rosemary extracts. Flat baseline, sharp peaks and short analysis time were achieved in this study and meet the criteria for accurate quantification. Using this HPLC method, the degradation study of carnosol, carnosic acid and rosmarinic acid standards as well as rosemary extract dissolved in fish oil was carried out. The effect of different storage conditions on degradation was investigated.

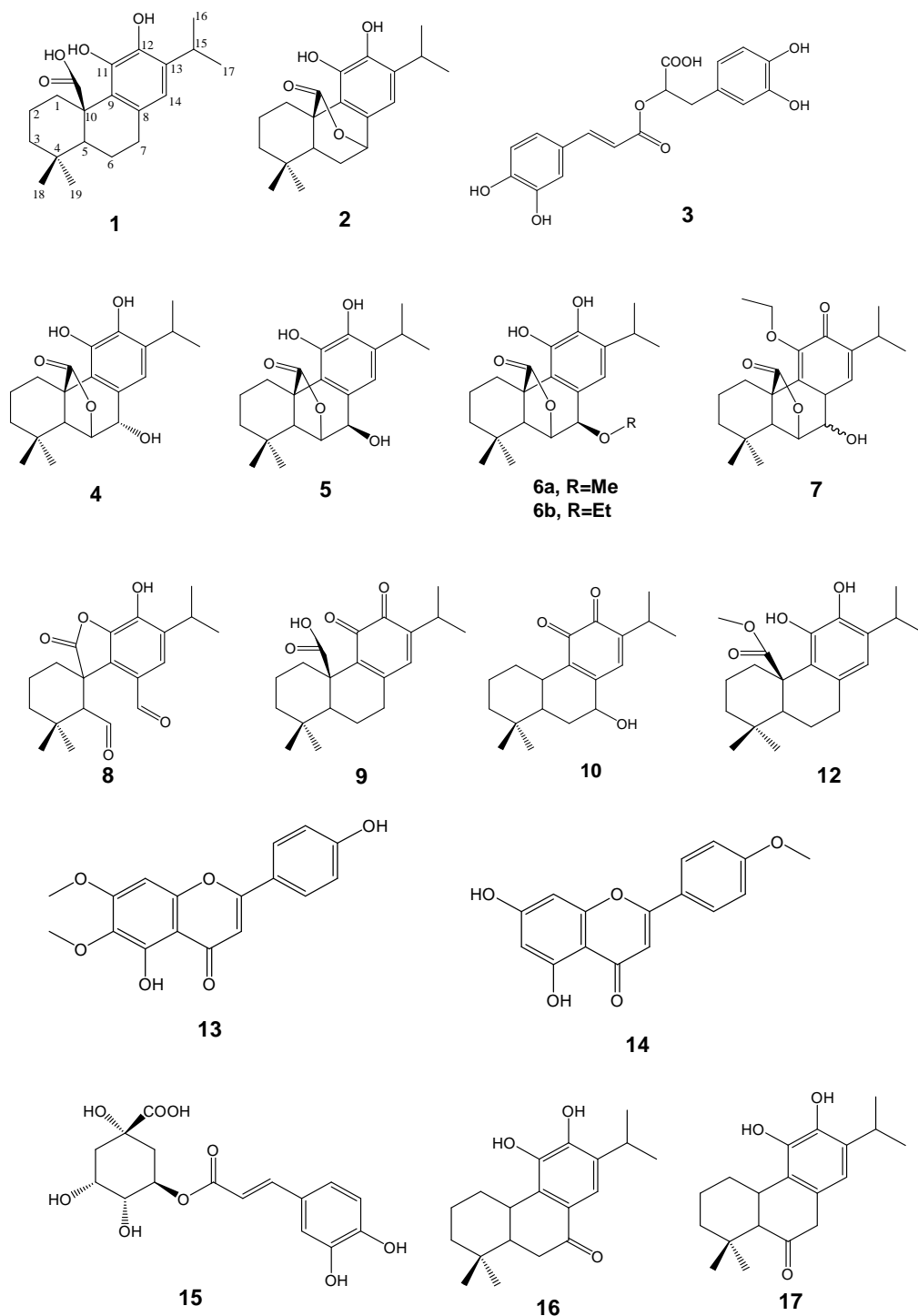


Figure 7.1 Structures of antioxidants. **1.** carnosic acid, **2.** carnosol, **3.** rosmarinic acid, **4.** rosmanol, **5.** epirosmanol, **6a.** epirosmanol methyl ether, **6b.** epirosmanol ethyl ether **7.** 11-ethoxy-rosmanol semiquinone, **8.** rosmadiol, **9.** carnosic acid quinone **10.** 5,6,7,10-tetrahydro-7-hydroxy-rosmariquinone, **11.** light induced degradation product of carnosic acid (structure unknown), **12.** methyl carnosate, **13.** cirsimaritin, **14.** acacetin, **15.** chlorogenic acid, **16** and **17** are structures of carnosic acid degradation product in literature²⁷¹.

7.2 Experimental

7.2.1 Material

Carnosol, carnosic acid and rosmarinic acid were purchased from ChromaDex (Irvine, CA), which are primary standards for analysis (purity \geq 96%). Formic acid and phosphoric acid were purchased from Sigma-Aldrich (Bellefonte, PA, USA). HPLC grade methanol, ethanol, and acetonitrile (ACN) were obtained from EMD (Gibbstown, NJ). Water was purified by a Milli-Q Water Purification System (Millipore, Billerica, MA). Rosemary powders and fish oil containing rosemary extract were provided by Alcon Laboratories (Fort Worth, TX).

7.2.2 HPLC methods

In the HPLC method, Agilent 1200 series autosampler, pump, diode array detector (DAD) and a Cyclobond I 2000 RSP column (25cm \times 4.6mm) were used.^{269, 270} For the degradation study of the carnosol, carnosic acid and rosmarinic acid standards, a gradient of binary solvents was used for elution. Solvent A consisted of 70% H₂O, 30% ACN and 0.1% formic acid. Solvent B consisted of 40% H₂O, 60% ACN and 0.1% formic acid. At a flow rate of 1mL/min, the eluent consisted of 100% A for the initial 4min, then from 4min to 17min the composition was changed to 100% solvent B. From 17min to 20min, the eluent composition was changed to 100% solvent A. For the analysis of rosemary extracts and the degradation study of the rosemary extract in fish oil, the procedure was modified to remove all the lipids remaining in the column after all the phenolic compounds eluted by using 100% ACN as solvent C. Within the first 17min, the procedure remained the same as described above. From 17min to 20min, the eluent composition was change to 100% solvent C and maintained there from 20min to 22min. From 22min to 25min, the eluent composition was changed to 100% solvent A.

7.2.3 HPLC-MS-MS method

In the HPLC-MS-MS method, Thermo Finnigan Surveyor autosampler, MS pump, PDA detector and Thermo LXQ linear ion trap mass spectrometer were used. The HPLC programs were the same as described above. The electrospray (ESI) mass spectra data were recorded

on a negative ionization mode for m/z range of 100 to 1000. Capillary voltage and spray voltage were set at -7V and 4.7kV, respectively. The normalized collision energy was 35 while helium was used as the collision gas.

7.2.4 Calibration Curve

The stock solution was prepared by weighing the respective vials containing carnosol, carnosic acid or rosmarinic acid, dissolving the contents, approximately 10 mg, and transferring them to a 10 mL volumetric flask, drying the vial and then weighing back the empty vial. Thus the transferred contents were accurately determined. The concentration of carnosol, carnosic acid and rosmarinic acid in the stock solution was approximate 1000mg/L for each of them. Standard solutions of carnosol, carnosic acid and rosmarinic acid were made up in the following approximate concentration ranges: 200, 400, 600, 800 and 1000 mg/L. The solvent system consisted of 150 mg/L butylated hydroxytoluene (BHT) in methanol. The addition of the antioxidant BHT was purely precautionary to ensure the stability of carnosol, carnosic acid and rosmarinic acid during the calibration study. All standards were stored at -10°C. The linearity for the calibrations curves for carnosol, carnosic acid and rosmarinic acid had $R^2 \geq 0.999$, therefore ruling out any significant oxidation. The DAD detector was set at four different wavelengths, 230, 254, 280 and 330nm. At 280nm, the chromatograms had the flattest baseline. Thus, the peak areas measured at 280nm were used to calculate the concentrations of the analytes later in the study.

7.2.5 Sample preparation and storage conditions

Individual standards of carnosol, carnosic acid and rosmarinic acid as well as a mixture of the three were prepared in a similar way as described for the stock solution in the calibration study except the solvent used was ethanol. The initial concentrations for carnosol, carnosic acid and rosmarinic acid were 800-900mg/L in the individual standards and the mixture. These four standards were subjected to the following six conditions: 1) -10°C in dark, 2) 4°C in dark, 3) room temperature with light exposure, 4) room temperature in dark, 5) 40°C with light exposure,

6) 40°C in dark. The influence of temperature and light on degradation was observed for 14 days.

The rosemary extract dissolved in fish oil was stored under five conditions: 1) 4°C in dark; 2) room temperature in dark; 3) room temperature with light exposure; 4) 40°C in dark and 5) 40°C with light exposure. This was monitored for 50 days. Prior to HPLC analysis, ~100mg of the fish oil sample was added to a 15mL screw-cap centrifuge tube and dissolved in 5mL of methanol.

The injection volume for each HPLC analysis was 5µL.

7.2.6 Extraction

About 250mg of rosemary powder was weighed onto weighing paper on an analytical balance and then transferred to a 15mL screw-top centrifuge tube. 2mL of methanol was added to the centrifuge tube. The samples were allowed to incubate for 30 min at room temperature and sonicate in an ultrasonication bath for 90 min. The samples were then refrigerated at 4°C overnight. Prior to LC analysis, samples were centrifuged for 5min at 3000 rpm. 100µL of the supernatant was diluted 10 times in an amber vial and then analyzed by HPLC.

7.3 Results and Discussion

7.3.1 Degradation study of carnosic acid, carnosol, rosmarinic acid and their mixture in ethanol solution

The study on the stability of antioxidants is important for determining proper storage conditions and increasing their shelf life. The antioxidative activity of rosemary extract and its constituents has been widely discussed.^{224-226,229,242,243,272,273} However, the stability of rosemary extract or its phenolic components were only mentioned in a few instances.²⁷⁴⁻²⁷⁷ Schwarz and Ternes isolated carnosic acid and carnosol from rosemary extract and investigated their degradation behavior in methanol for 9 days.²⁷⁴ The same authors also reported the stability of the phenolic diterpenes from rosemary extract in lard under thermal stress of 170°C.²⁷⁵ Irmak et al. observed the stability of rosemary extract stored at 4°C in the dark and at room temperature

with light exposure for 14 weeks.²⁷⁶ However, the effect of light and temperature on the degradation process could not be distinguished.

In the present study, the degradation behavior of rosmarinic acid, carnosol, carnosic acid and the mixture of the three antioxidants in ethanol solution was investigated under a series of different storage temperatures with or without light exposure within 14 days.

7.3.1.1 Degradation profiles

Rosmarinic acid, either by itself in the ethanol solution or presented in the ethanol solution of the mixture, did not degrade appreciably under any of the conditions during the 14 days study. Figure 7.2A and 2B showed the degradation profiles of rosmarinic acid by itself and in the mixture under different conditions.

Carnosol, by itself in the ethanol solution, degraded most rapidly out of the three antioxidants. This was particularly notable at 40°C with light exposure where carnosol completely disappeared by the fifth day (as shown in Figure 7.2C). The relative rates of degradation of carnosol in ethanol solution were as follows: 4°C < room temperature in dark < room temperature with light exposure < 40°C in dark < 40°C with light exposure. Carnosol stored at -10°C in the dark exhibited appreciable stability. Thus, storage temperature was a major factor affecting the degradation of carnosol by itself in solution, whereas the exposure to light could accelerate the degradation further. In contrast to this, significantly slower apparent degradation rates were observed for carnosol in the solution of the mixture (as shown in Figure 7.2D). This could be due the protection of other antioxidants present in the mixture solution towards carnosol or the compensation from conversion of carnosic acid to carnosol.

Carnosic acid, by itself in ethanol solution and in the solution of the mixture, was fairly stable at -10°C and 4°C (as shown in Figure 7.2E and F). At higher temperatures and under light exposure conditions it degraded, but not as rapidly as did carnosol by itself in ethanol solution. Carnosic acid exhibited similar degradation behavior in the mixture solution as when by itself in solution.

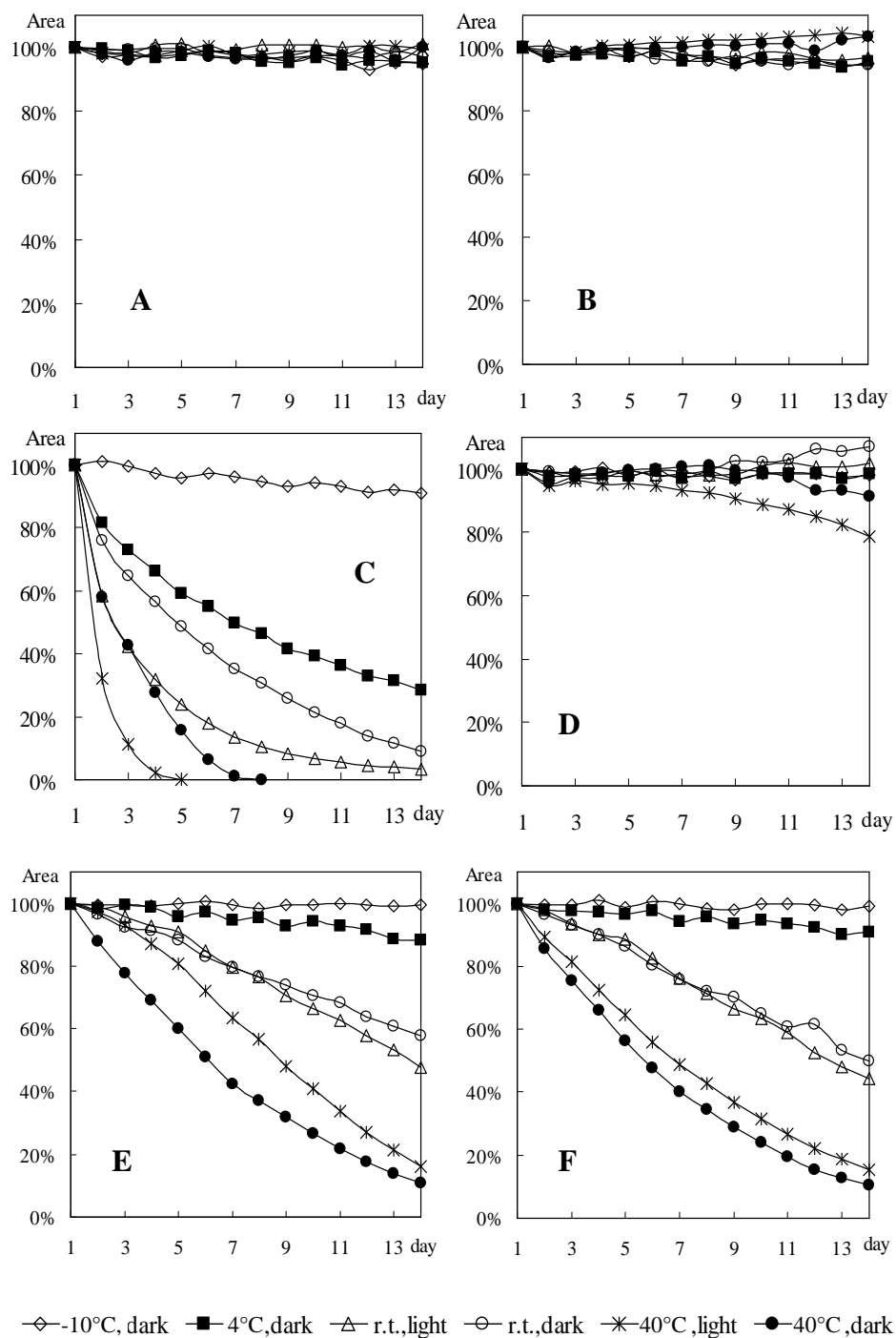


Figure 7.2 Degradation profiles of the ethanolic solutions of A) rosmarinic acid by itself, B) rosmarinic acid in the mixture, C) carnosolic acid by itself, D) carnosolic acid in the mixture, E) carnosolic acid by itself and F) carnosolic acid in mixture under different storage conditions. See experimental section for details.

However, it was noticed that the degradation rate of the carnosic acid stored in dark was higher than that of the carnosic acid exposed to light at the same temperature, especially when stored at 40°C. This was opposite to the results observed for carnosol.

7.3.1.2 Identification of degradation products and pathways

1) Degradation of carnosol

Rosmanol, epirosmanol and epirosmanol ethyl ether

Three major degradation products of carnosol were formed in the ethanol solutions and were labeled as compounds **4**, **5** and **6** (structures shown in Figure 7.3). In negative mode of electrospray ionization (ESI), $[M-H]^-$ m/z values 345, 345 and 373 were observed for the compounds **4**, **5** and **6**, respectively. When collision-induced dissociation (CID) energy was applied, compounds **4** and **5** had the same fragmentation pattern which gave two fragments at m/z 301 and 283, while compound **6** had two fragments at m/z 329 and 283. The λ_{max} values for compound **4**, **5** and **6** were 289, 288 and 289nm, respectively. These data were in good agreement with the literature values of rosmanol, epirosmanol and epirosmanol ethyl ether (Figure 7.1-**6b**).^{278, 279} In the mass spectra, decarboxylation ($[M-H-COO]^-$) of rosmanol, epirosmanol, and epirosmanol ethyl ether resulted in m/z values at 301, 301 and 329, respectively. The m/z value at 283 was caused by the further loss of a H_2O or an ethanol molecule.

It was observed that epirosmanol ethyl ether was not formed when carnosol was dissolved in an aprotic solvent, such as acetonitrile. However, when other protic solvents, such as methanol or isopropanol, were used, the corresponding ether form of epirosmanol was formed. Also, it was noticed that the formation of these three degradation products was affected by temperature. As shown in Figure 7.3F, rosmanol had the largest peak area among the three compounds when stored at -10°C. However, the peak area of rosmanol became relatively smaller than that of the epirosmanol ethyl ether when temperature increased. Apparently, high temperature is more favorable to the formation of epirosmanol ethyl ether.

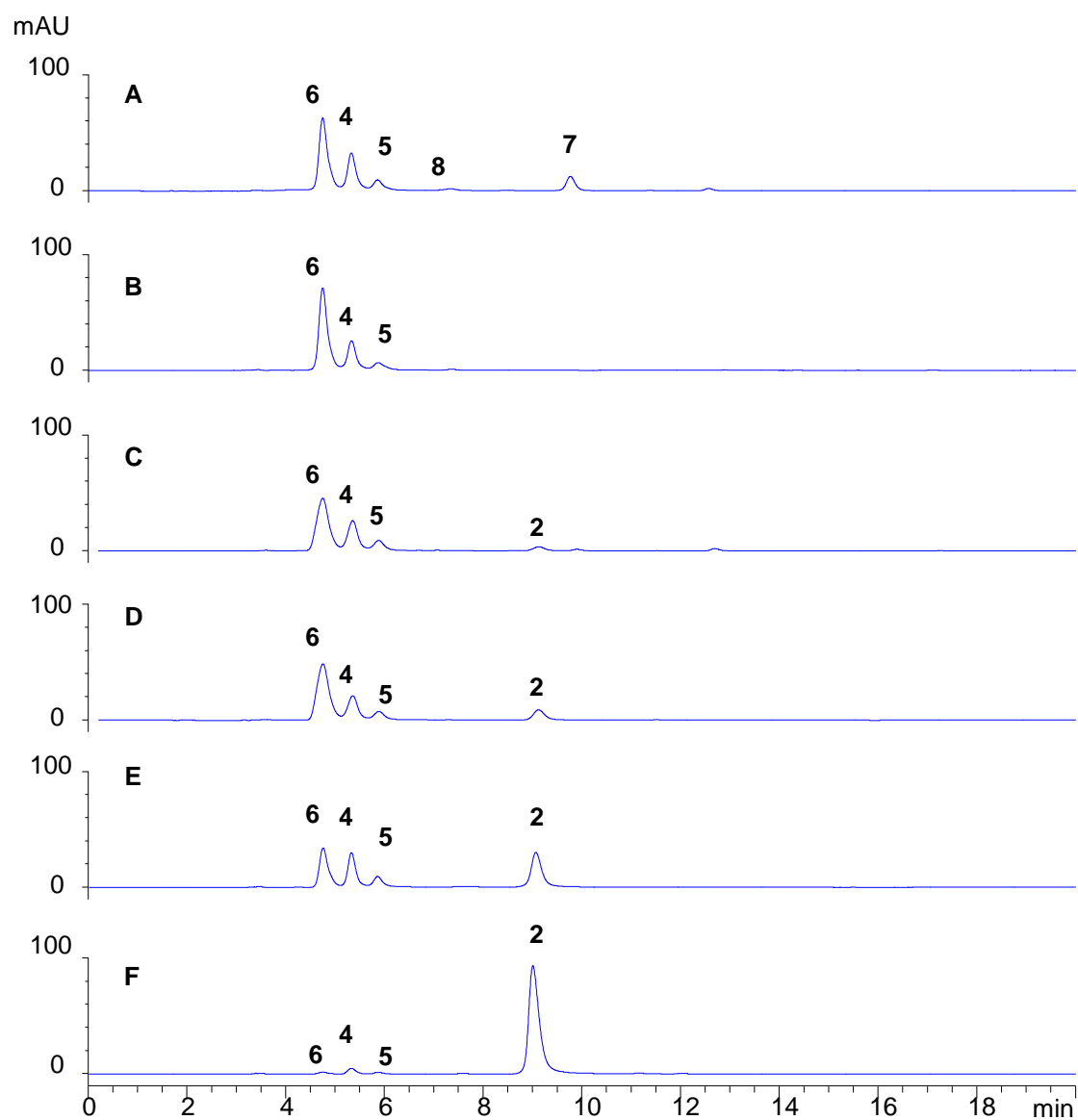


Figure 7.3 HPLC chromatograms of carnosol ethanol solutions stored under different conditions after 14 days. (A) 40°C with light exposure, (B) 40°C in dark, (C) room temperature with light exposure, (D) room temperature in dark, (E) 4°C in dark, (F) -10°C in dark. The peak are labeled as **2**. carnosol, **4**. rosmanol, **5**. epirosmanol, **6**. epirosmanol ethyl ether, **7**. 11-ethoxy- rosmanol semiquinone and **8**. rosmadial.

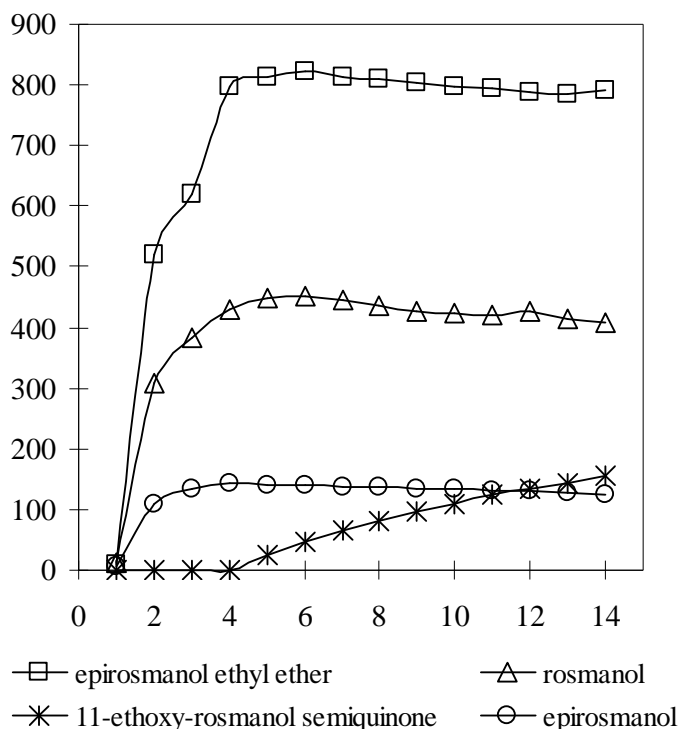


Figure 7.4 The peak areas of the degradation products of carnosol vs. time

11-Ethoxy- rosmanol semiquinone

Degradation product **7** in Figure 7. 3A only appeared in the carnosol solution stored at 40°C with light exposure after carnosol completely degraded. As seen in Figure 7.4, its peak area increased with a slow decrease of the peak areas of epirosmanol ethyl ether, rosmanol and epirosmanol. Thus, this degradation product did not come directly from carnosol but rather via other carnosol degradation products. It was slightly ionized in ESI negative ion mode and the $[M-H]^-$ m/z value was 373. When CID energy was applied, no fragments were observed. Even though the molecular m/z value of compound **7** was the same as epirosmanol ethyl ether, the difference in the ability to ionize indicated a significant difference in their structure. It is very likely that no phenol group or carboxylic group existed in the structure of compound **7**. In the UV spectrum of compound **7**, a maximum absorption peak at 261nm with a shoulder at 296nm and a second maximum absorption peak at 322nm with a shoulder at 335 nm also showed the

difference in the structures of compound **7** and epirosmanol ethyl ether. It was reported that rosmanol and epirosmanol can be further oxidized to rosmanol o-quinone, which can be converted to galdosol via a semiquinone intermediate when subject to heat.²⁸⁰ This semiquinone intermediate appeared to react with ethanol and form an ethyl ether instead of converting to galdosol. The structure as shown in Figure 7.1-7 was proposed for compound **7**. The calculated UV maximum absorption wavelength for this structure was in agreement with the observed values.²⁸¹

Rosmadial

The peak that eluted at 7.34 min in chromatogram Figure 7. 3A and was labeled as peak **8** had a molecular [M-H]⁻ m/z at 343 and two product ions m/z at 315 and 299. The UV λ_{max} value was 286nm. These data were in agreement with the literature values of rosmadial (Figure 7.1-8).^{278, 279} The m/z at 315 suggested a loss of CO and the m/z at 299 may be caused by the cleavage of CO₂ from the molecular ion.

2) Degradation of carnosic acid

Carnosic acid quinone

When carnosic acid was kept at -10°C in dark for 14 days, carnosic acid quinone (Figure 7.1-9) was the only degradation product obtained. Carnosic acid was completely converted to this compound after being stored at -10°C in dark for 30 days. The degradation product was collected for NMR analysis: ¹H NMR (DMSO-d₆) δ 0.76(s, 3H), 0.88(s, 3H), 1.03(dd, 6H), 1.06(d, 1H), 1.09(d, 1H), 1.16(td, 1H), 1.31(dd, 1H), 1.39(tt, 2H), 1.74(m, 1H), 2.01(m, 1H), 2.14(m, 1H), 2.74(m, 1H), 2.80(dt, 1H), 3.14(d, 1H), 6.66(s, 1H), 12.31(broad, 1H). These data were in agreement with the literature data for carnosic acid quinone.²⁸² The chemical shift of the two phenol groups in carnosic acid at 7.74 disappeared while the shift of carboxylic group at 12.31 was retained. Also, the mass spectra showed molecular [M-H]⁻ m/z at 329 and fragment m/z at 285 which was the result of a cleavage of a carboxylic group from the molecular ion.

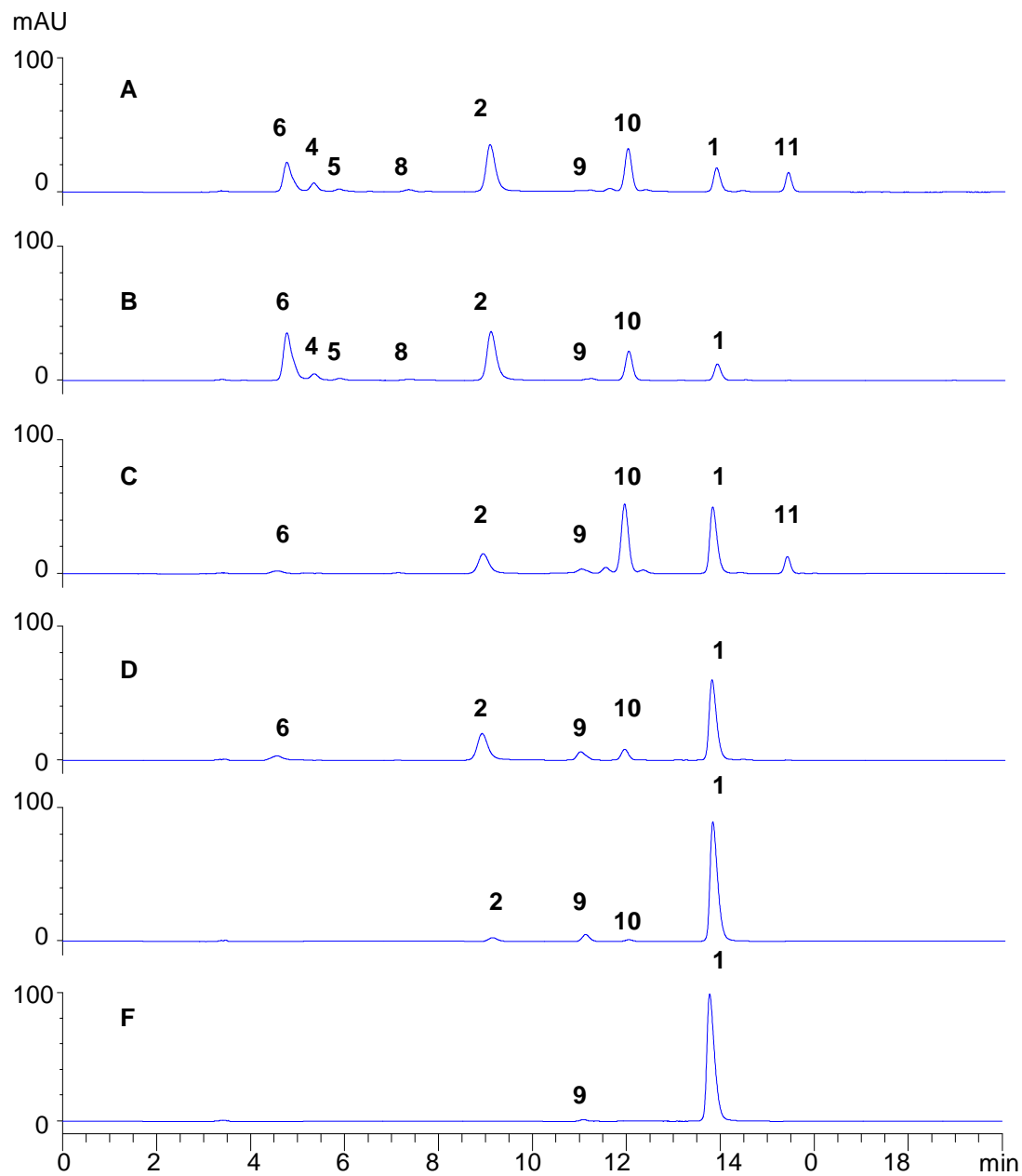


Figure 7.5 HPLC chromatograms of carnosic acid ethanol solutions stored under different conditions after 14 days. A) 40°C with light exposure, B) 40°C in dark, C) room temperature with light exposure, D) room temperature in dark, E) 4°C in dark, F) -10°C in dark. **1.** carnosic acid, **2.** carnosol, **4.** rosmanol, **5.** epirosmanol, **6.** epirosmanol ethyl ether, **8.** rosmadial, **9.** carnosic acid quinone **10.** 5,6,7,10-tetrahydro-7-hydroxy-rosmariquinone, **11.** the light induced degradation product.

The compound had a UV maximum absorption at 428nm which indicated the presence of an o-benzoquinone structure.²⁸³

The peak area of carnosic acid quinone increased slightly when the storage temperature increased from -10°C to room temperature but decreased afterwards. Carnosic acid quinone was postulated to be an intermediate in the oxidation pathway of carnosic acid to carnosol, rosmanol etc.^{215, 280, 284, 285} It was confirmed by Masuda et al. that carnosic acid quinone can convert to carnosol, rosmanol and 7-methylrosmanol when subject to 60°C for 2 hours.^{215, 280, 284, 285} Also, the low temperature needed for the conversion of carnosic acid to carnosic acid quinone indicated a low energy barrier for this conversion. Therefore, carnosic acid quinone was very likely to be the intermediate in the degradation pathway of carnosic acid, and its small peak area in Figure 7. 5 at high temperatures may be due to the conversion of carnosic acid quinone to other degradation products.

Carnosol and its degradation products

At 4°C, a degradation product was eluted at 8.98 min (labeled as peak **2** in Figure 7.5). It was confirmed to be carnosol. As seen in Figure 7.5 the peak area of carnosol increased with increased temperature, whereas exposure to light did not have an affect on its peak area. After carnosol was formed in the solution, degradation products **4**, **5** and **6** appeared in the solutions stored above 4°C. These three degradation products were confirmed to be rosmanol, epirosmanol and epirosmanol ethyl ether, respectively. This result supported that epirosmanol ethyl ether, rosmanol and epirosmanol were converted from carnosol and not directly from carnosic acid. This agrees with the oxidation pathway of carnosic acid postulated by Wenkert et al.,²¹⁵ and Schwarz and Ternes.²⁷⁴

The peak **8** eluted at 7.34 min in Figure 7. 4A and 4B had a molecular [M-H]⁻ at m/z 343 and two product ions at m/z 315 and 299. The UV λ_{max} value of 286nm was observed. These data clearly identified that this compound is rosmadial.

5,6,7,10-Tetrahydro-7-hydroxy-rosmariquinone

Another major degradation product was eluted at 11.50 min and was labeled as peak **10** in Figure 7.5A-D. The formation of this degradation product was promoted by exposure to light (as seen in Figure 7.5C and D) Also, the formation of compound **10** was favored at higher temperatures since it had larger peak area at 40°C than at room temperature under the same light exposure conditions.

Compound **10** was difficult to ionize in either negative or positive mode of ESI. Therefore, the sample was concentrated by 10 times prior to LC-MS-MS analysis. A parent ion $[M-H]^-$ with m/z 301 was observed. The mass spectrum gave fragments at m/z 283, 273 and 258, which suggested a loss of H_2O , CO and an isopropyl group from the molecular ion, respectively. In the literature, two structures with m/z values of 301 were reported and are shown in Figure 7.1-16 and 17.²⁷¹ However, the difficulty in ionization of compound **10** in ESI negative mode indicated the absence of phenol or carboxylic acid group in the structure. The UV spectrum showed strong absorption at 279 and 409nm. Thus, an o-benzoquinone structure was very likely to exist.²⁸³ A structure for compound **10** was proposed as shown in Figure 7.1-10 and it was named as 5,6,7,10-tetrahydro-7-hydroxy-rosmariquinone. The common name of rosmariquinone for this base structure was proposed previously.²⁸⁶

Degradation product generated by light exposure

As shown in Figure 7.5A and C, a compound was eluted after the carnosic acid and was labeled as peak **11**. This compound only appeared in the solutions exposed to light and had strong UV absorption at 260 nm. Unfortunately, it could not be ionized in either negative or positive ion mode of ESI even at high concentrations, and was labile when isolated from the solution. Insufficient amounts of this compound were collected from HPLC fractions for NMR analysis. Thus, no further information was obtained on the structure of this light induced degradation product.

Minor degradation products

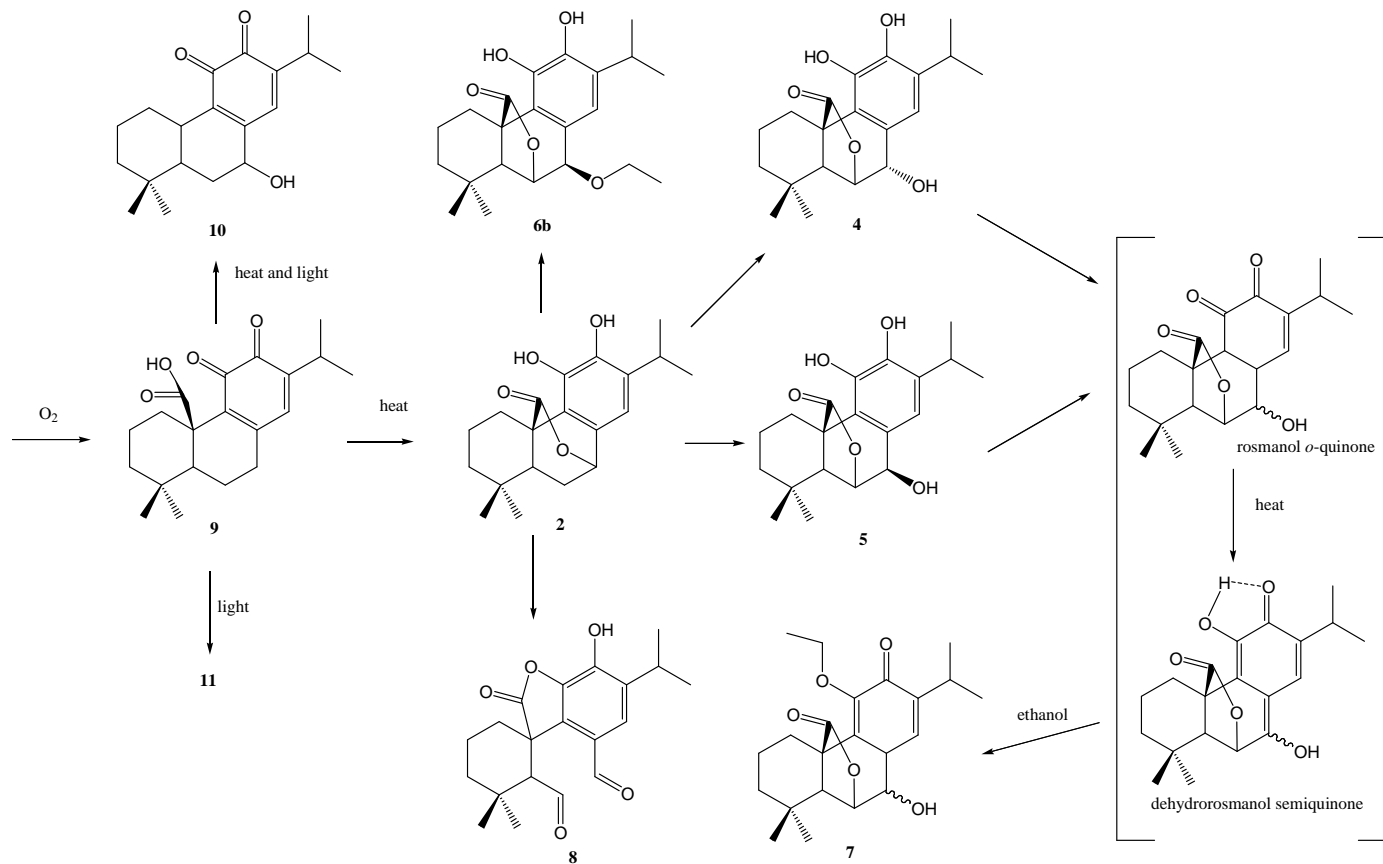


Figure 7.6 The degradation pathway of carnosic acid in ethanol solution.

As seen in Figure 7.5A, there were three small peaks eluted at 11.25, 12.00 and 14.30 min, respectively. The first two peaks only appeared with light exposure. These compounds were not prone to ionization and were not major degradation products in the solutions, thus no further effort was made to identify their structures.

Degradation pathway of carnosic acid

On the basis of the discussion above, a degradation pathway of carnosic acid was postulated and is shown in Figure 7.6. Carnosic acid quinone was likely to be the intermediate in the pathway. It was confirmed that rosmanol, epirosmanol and epirosmanol ethyl ether came from carnosol which is a degradation product of carnosic acid. Also, 5,6,7,10-tetrahydro-7-hydroxy-rosmariquinone and the light induced degradation product, compound **11**, were for the first time reported as degradation products of carnosic acid.

3) Degradation of the mixture

When rosmarinic acid, carnosol and carnosic acid were dissolved in the same solution, similar degradation products were generated as in the individual standard solutions of carnosol and carnosic acid (as shown in Figure 7.7). Rosmarinic acid was stable in both ethanol solutions (see Figure 7. 2A and 2B). Consequently, it is not considered in the following discussion about the degradation behavior of the antioxidants presented in the mixture solution. The rosmanol and epirosmanol peaks were overlapped with the rosmarinic acid peak in Figure 7.7. Their appearance as well as that of epirosmanol ethyl ether indicated the degradation of carnosol. However, the peak area of carnosol in all the chromatograms in Figure 7.7 did not show much change compared to its initial value.

A study of the peak areas of carnosol and epirosmanol ethyl ether in three solutions: 1) carnosol ethanol solution, 2) carnosic acid ethanol solution and 3) the ethanol solution of the three mixed antioxidants was carried out. The peak area values are listed in Table 7.1. The purpose of the study was to see if carnosic acid had protective ability towards carnosol, or

whether the degraded carnosol was simply compensated for by that produced from carnosic acid.

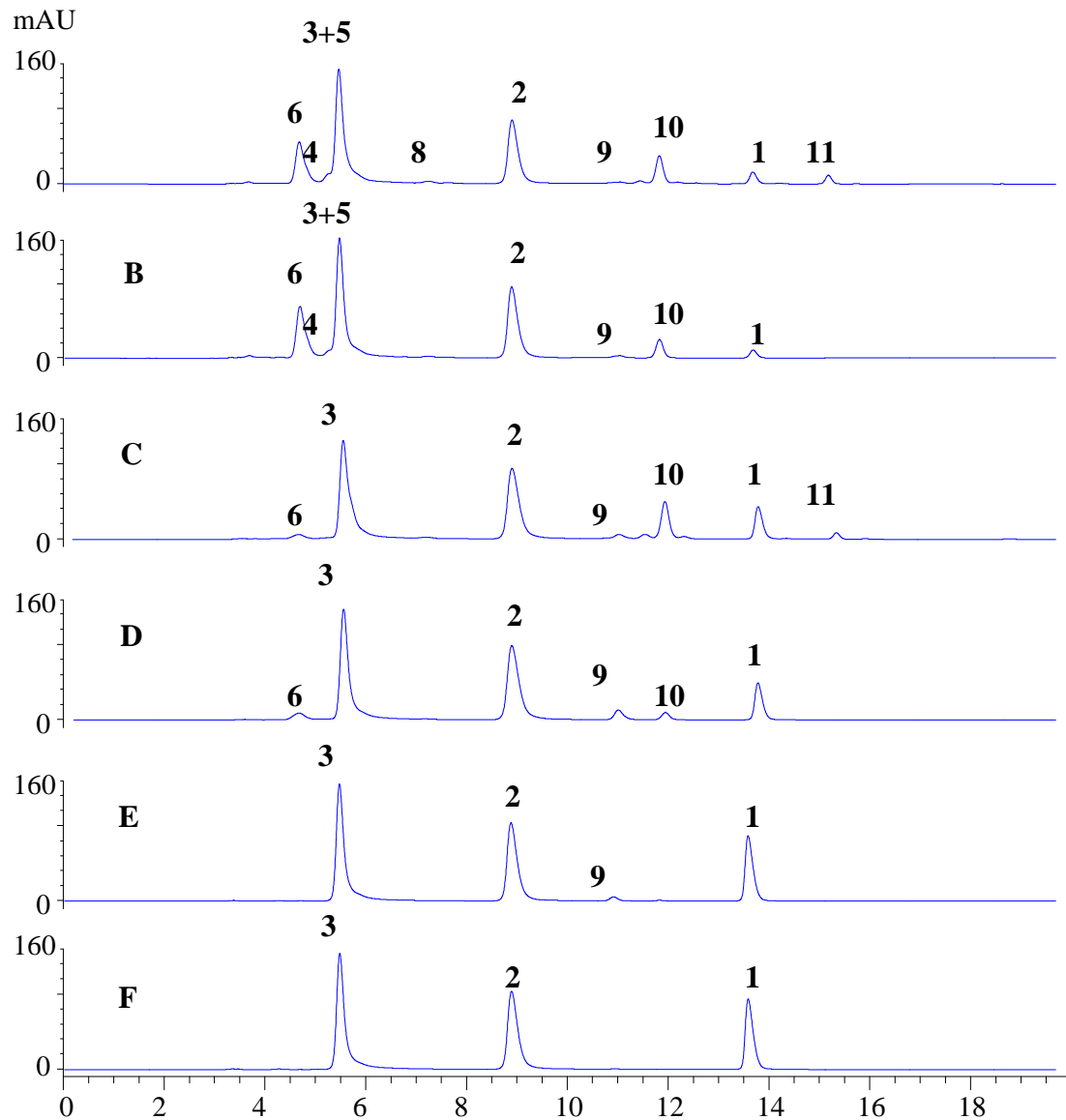


Figure 7.7 HPLC chromatograms of mixed standards stored under different conditions after 14 days. A) 40°C with light exposure, B) 40°C in dark, C) room temperature with light exposure, D) room temperature in dark, E) 4°C in dark, F) -10°C in dark. **1.** carnosic acid, **2.** carnosol, **3.** rosmarinic acid, **4.** rosmanol, **5.** epirosmanol, **6.** epirosmanol ethyl ether **8.** rosmadial, **9.** carnosic acid quinone **10.** 5,6,7,10-tetrahydro-7-hydroxy-rosmariquinone, **11.** the light induced degradation product of carnosic acid.

Table 7.1 The peak areas of epirosmanol ethyl ether and carnosol in carnosol, carnosic acid and mixture solutions

condition	compound	Carnosol solution	Carnosic acid solution	Mixture solution
Initial	epirosmanol ethyl ether	0	0	0
	carnosol	1562.9	0	1556.3
40°C with light ^a	epirosmanol ethyl ether	790.7	290.3	722.1
	carnosol	0	495.0	1222.5
40°C in dark ^a	epirosmanol ethyl ether	897.2	483.8	921.7
	carnosol	0	515.3	1423.0
r. t. with light ^a	epirosmanol ethyl ether	798.0	34.2	80.6
	carnosol	54.4	235.4	1586.2
r. t. in dark ^a	epirosmanol ethyl ether	852.0	54.2	136.1
	carnosol	140.7	316.4	1666.8
4°C in dark ^a	epirosmanol ethyl ether	435.3	0	0
	carnosol	446.7	36.8	1532.6
-10°C in dark ^a	epirosmanol ethyl ether	21.3	0	0
	carnosol	1418.3	0	1525.9

^aAfter 14 days of storage under the conditions.

Epirosmanol ethyl ether was used as an “indicator” for the degradation progress of carnosol since its peak area increased with the degradation of carnosol. The initial concentrations of carnosol and carnosic acid in the individual solutions were the same as those in the mixture solution. If carnosic acid and carnosol degraded independently in the mixture solution without any protective effect, the peak area of carnosol in the mixture solution should be equal to the sum of the peak areas of carnosol in solutions 1 and 2, so should epirosmanol ethyl ether. However, under the same storage conditions, the peak area of epirosmanol ethyl

ether in the mixture solution was much smaller than the sum of its peak areas in solutions 1 and 2. This indicated that the degradation of carnosol was less in mixture. On the other hand, the peak area of carnosol in the mixture solution was significantly larger than the sum of that in solutions 1 and 2. At room temperature, the peak area of carnosol in the mixture solution was even larger than its initial value. Therefore, a portion of carnosol in the mixture solution was produced from the degradation of carnosic acid.

Thus the relative small change in the carnosol concentration in the mixture solution with time was due in part to the protective behavior of carnosic acid towards carnosol and also to the conversion of carnosic acid to carnosol.

7.3.2 Degradation study of rosemary extract in fish oil

Rosemary extracts are often added to polyunsaturated fatty acids (PUFA) as antioxidants and their ability to increase the stability of PUFA has been investigated.^{230, 231} The focus of this study was the stability of the two principal rosemary antioxidants, carnosic acid and carnosol, in fish oil.

The components in rosemary extract can be well separated by the HPLC method developed in this study (see Experimental). As shown in Figure 7.8A, besides carnosic acid and carnosol, cirsimaritin (Figure 7.1-13) was another major component in the rosemary extract. The minor components included acacetin (Figure 7.1-14), chlorogenic acid (Figure 7.1-15) as well as methyl carnosate (Figure 7.1-12), rosmanol, epirosmanol, rosmadial and carnosic acid quinone, which may be derived from carnosic acid and carnosol. These compounds were confirmed by comparing the mass spectra and UV spectra (as shown in Table 7.2) with the literature values.^{278, 279} The structures of the three small peaks eluted between chlorogenic acid and carnosic acid as well as the two small peaks eluted after methyl carnosate were not confirmed due to their low concentration and difficulty in ionization.

When the sample of rosemary extract in fish oil was diluted and directly injected to HPLC, a hump appeared at 11 -15 min as shown in Figure 7.8C. This hump was due to the UV

absorbance of the fish oil (as shown in Figure 7.8B). The concentration of carnosic acid was quantified by subtracting the raised baseline. The concentration of carnosic acid and carnosol in the mixture of rosemary extract and fish oil were 4.2% and 0.60% (weight percent), respectively. Under all storage conditions, the carnosol in fish oil was very stable. The fastest degradation of carnosic acid was observed at 40°C with light exposure. After 50 days at this condition, the concentration of carnosic acid was 3.7%. Less than 12% of carnosic acid degraded. Compared to the degradation behavior of carnosic acid in ethanol solution, the stability of carnosic acid from rosemary extract was greatly enhanced when it was dissolved in fish oil.

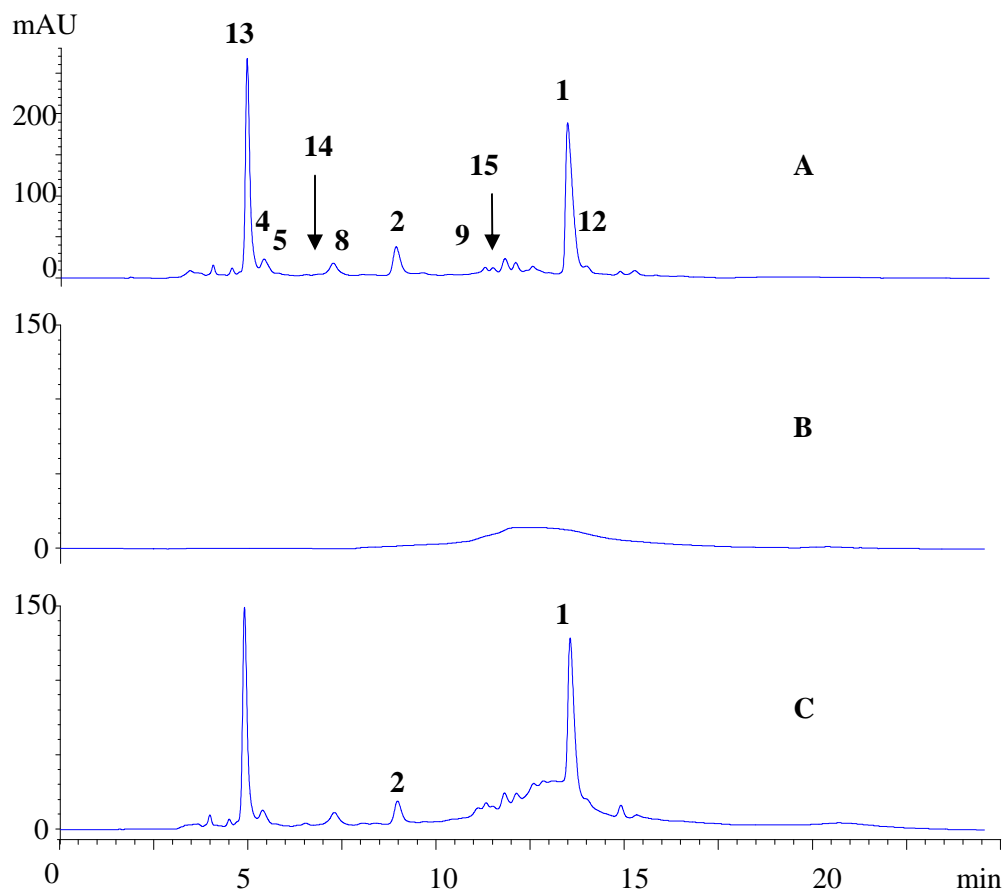


Figure 7.8 HPLC chromatograms A) methanolic rosemary extract, B) fish oil diluted with methanol and C) rosemary extract in fish oil diluted with methanol. The components are: **1.** carnosic acid, **2.** carnosol, **4.** rosmanol, **5.** epirosmanol, **8.** rosmadial, **9.** carnosic acid quinone, **12.** methyl carnosate, **13.** cirsimaritin, **14.** acacetin, **15.** chlorogenic acid.

Table 7.2 Mass spectra and UV spectra data for degradation products of carnosic acids and components in rosemary extracts.

No.	compound name	[M-H] ⁻ m/z	major fragments (intensity) m/z	λ _{max} (nm)
1	carnosic acid	331	287(100%), 244(2%)	284
2	carnosol	329	285(100%)	284
3	Rosmarinic acid	359	315(15%), 223(12%), 197(27%), 179(19%), 161(100%)	330
4	rosmanol	345	301(4%), 283(100%)	288
5	epirosmanol	345	301(5%), 283(100%)	289
6	epirosmanol ethyl ether	373	329(40%), 283(100%)	289
7	11-ethoxy- rosmanol semiquinone	373	N/A	261, 296, 322, 335
8	rosmadial	343	315(34%), 299(100%)	286
9	carnosic acid quinone	329	285(100%)	428
10	5,6,7,10-tetrahydro-7-hydroxy-rosmariquinone,	301	283(42%), 273(15%), 258(100%)	279, 409
11	N/A	N/A	N/A	260
12	methyl carnosate	345	301(100%), 286(6%)	289
13	cirsimaritin	313	298(100%), 283(5%)	333
14	acacetin	283	268(50%)	267, 334
15	chlorogenic acid	353	317(100%), 309(2%)	N/A

7.4 Conclusions

Carnosic acid degraded in a cascade pathway in ethanol solution via an intermediate, carnosic acid quinone. 5,6,7,10-Tetrahydro-7-hydroxy-rosmariquinone was for the first time proposed as a degradation product of carnosic acid. A light induced degradation product compound was also reported. The degradation rates of carnosic acid and carnosol increased with temperature, while light exposure promoted the formation of unique degradation products. When carnosic acid and carnosol were present in the same ethanolic solution, carnosic acid showed a protection capability towards carnosol. When rosemary extract was added to fish oil, the degradation of carnosic acid is greatly reduced.

CHAPTER 8
GENERAL CONCLUSIONS

8.1 Part One (Chapter 1-3)

The development, separation mechanism and application of GC chiral stationary phases based on cyclodextrins have been reviewed. Enantioselective GC is quite complementary to enantioselective HPLC. It can separate analytes that have smaller molecular weight and limited functionality which can sometimes be difficult to separate by HPLC. Also, it is useful for analytes that react with protic solvents and/or have no UV chromophore which can be problematic with HPLC. Enantioselective GC is preferable for quantitative analysis, quality control and volatile molecules.

A series of novel GC chiral selectors has been development based on cyclofructans. PM-CF6 and PM-CF7 have different enantioselectivities when used as chiral selectors in gas chromatography. The hydrogen bonding and dipole-dipole interactions occurring on the pendant fructose moieties of the cyclofructan molecules play an important role in chiral recognition. Also, PM-CF6 or PM-CF7 stationary phases have unique enantioselectivities compared to the synthetic chiral crown ether GC stationary phase. DP-TA-CF6 and DP-PN-CF6 CSPs showed enantioselectivity towards a variety of racemic compounds. The enantiomers separated include derivatized amino acids, amino alcohols, amines, alcohols, tartrates and lactones. Generally, analytes with hydrogen bonding donor groups were better separated on both CSPs than the analytes only having permanent dipole moments. Both DP-TA-CF6 and DP-PN-CF6 CSPs provided best enantioselectivity towards amino acids with alkyl side chains. The thermodynamic parameters indicated that no inclusion complex formation occurs during the chiral recognition process on these cyclofructan-based CSPs. Weak, external associations likely contribute most to the enantioselective retention mechanism.

8.2 Part Two (Chapter 4-6)

A series of trigonal tricationic cationic ionic liquids are synthesized and evaluated as stationary phases in gas chromatography. Due to the rigidity of the cation and the contribution from the core structure, these trigonal tricationic ionic liquids have unique polarities and interaction parameters compared to the monocationic, dicationic and linear tricationic ionic liquids. Many ionic liquids with bis(trifluoromethanesulfonyl)imide anions show peak tailing for alcohols and other H-bond forming analytes, however, the trigonal tricationic ionic liquids containing tri(2-hexanamido)ethylamine core appear to overcome this problem. Alcohol/alkane mixture and Grob test mixtures indicate that the trigonal tricationic ionic liquids are far more polar than either the monocationic or dicationic ionic liquids reported thus far. All these trigonal tricationic ionic liquids were highly thermally stable and were liquids in a wide temperature range.

A rapid, facile GC method has been developed for the quantification of water in extremely diverse solvent samples based on using ionic liquid (IL) columns. Limits of detection using this technique are superior when compared to KFT. Furthermore, the IL-GC methodology requires less sample and is free from other complications associated with KFT. The IL GC method can be used regardless of the chemical nature of the solvent and produces no additional waste products. When compared to other GC methods using commercially available PEG columns, the IL based columns possessed superior selectivity for water in all solvents tested. Further, they show no degradation or chromatographic changes with time. Typical analysis times ranged from <3 min to 7 min.

8.3 Part Three (Chapter 7)

A HPLC method has been developed to separate carnosic acid, carnosol, rosmarinic acid and their degradation products as well as other components in rosemary extracts. A degradation study on carnosic acid and carnosol has been carried out. Carnosic acid degraded in a cascade pathway in ethanol solution via an intermediate, carnosic acid quinone. 5,6,7,10-

Tetrahydro-7-hydroxy-rosmariquinone was for the first time proposed as a degradation product of carnosic acid. A light induced degradation product compound also was reported. The degradation rates of carnosic acid and carnosol increased with temperature, while light exposure promoted the formation of unique degradation products. When carnosic acid and carnosol were present in the same ethanolic solution, carnosic acid showed a protection capability towards carnosol. When rosemary extract was added to fish oil, the degradation of carnosic acid is greatly reduced.

APPENDIX A
PUBLICATION INFORMATION

Chapter 2: A manuscript published in *Analyst*. **Y. Zhang**, Z. S. Breitbach, C. Wang, D. W. Armstrong, *Analyst*, **2010**, 135(5), 1076-1083. Copyright©2010 with permission from Royal Society of Chemistry.

Chapter 3: A manuscript published in *Analyst*. **Y. Zhang**, D. W. Armstrong, *Analyst*, **2011**, 136(14), 2931-2940. Copyright©2011 with permission from Royal Society of Chemistry.

Chapter 5: A manuscript published in *Analytical Chemistry*. T. Payagala, **Y. Zhang**, E. Wanigasekara, K. Huang, Z. S. Breitbach, P. S. Sharma, L. M. Sidisky, D. W. Armstrong, *Analytical Chemistry*, **2009**, 81(1), 160-173. Copyright©2009 with permission from American Chemical Society.

Chapter 6: A manuscript published in *LC-GC Europe*. D. A. Jayawardhana, R. M. Wood, **Y. Zhang**, C. Wang, D. W. Armstrong, *LC-GC Europe*, **2011**, October. Copyright©2011 with permission from Advanstar Communications.

REFERENCES

- 1 E. Gil-Av, B. Feibush and R. Charles-Sigler, *Tetrahedron Lett.*, 1966, 1009-1015.
- 2 V. Schurig, *Ann. Pharm. Fr.*, 2010, **68**, 82-98.
- 3 H. Schlenk, J. L. Gellerman and D. M. Sand, *Anal. Chem.*, 1962, **34**, 1529-1532.
- 4 E. Smolkova-Keulemansova and S. Krysl, *J. Chromatogr.*, 1980, **184**, 347-361.
- 5 E. Smolkova, H. Kralova, S. Krysl and L. Feltl, *J. Chromatogr.*, 1982, **241**, 3-8.
- 6 T. Koscielski, D. Sybilska, L. Feltl and E. Smolkova-Keulemansova, *J. Chromatogr.*, 1984, **286**, 23-30.
- 7 J. Mraz, L. Feltl and E. Smolkova-Keulemansova, *J. Chromatogr.*, 1984, **286**, 17-22.
- 8 S. Krysl and E. Smolkova-Keulemansova, *J. Chromatogr.*, 1985, **349**, 167-176.
- 9 E. Smolkova-Keulemansova, L. Feltl and S. Krysl, *J. Inclusion Phenom.*, 1985, **3**, 183-196.
- 10 E. Smolkova-Keulemansova, E. Neumannova and L. Feltl, *J. Chromatogr.*, 1986, **365**, 279-288.
- 11 T. Koscielski, D. Sybilska and J. Jurczak, *J. Chromatogr.*, 1983, **280**, 131-134.
- 12 Z. Juvancz, G. Alexander and J. Szejtli, *HRC CC, J. High Resolut. Chromatogr. Chromatogr. Commun.*, 1987, **10**, 105-107.
- 13 D. W. Armstrong, W. Li, A. M. Stalcup, H. V. Secor, R. R. Izac and J. I. Seeman, *Anal. Chim. Acta*, 1990, **234**, 365-380.
- 14 W. A. Koenig, S. Lutz, P. Mischnick-Luebbecke, B. Brassat and G. Wenz, *J. Chromatogr.*, 1988, **447**, 193-197.
- 15 W. A. Koenig, S. Lutz, G. Wenz and E. Von der Bey, *HRC CC, J. High Resolut. Chromatogr. Chromatogr. Commun.*, 1988, **11**, 506-509.
- 16 W. A. Koenig, S. Lutz, C. Colberg, N. Schmidt, G. Wenz, E. Von der Bey, A. Mosandl, C. Guenther and A. Kustermann, *HRC CC, J. High Resolut. Chromatogr. Chromatogr. Commun.*, 1988, **11**, 621-625.

- 17 W. Y. Li, H. L. Jin and D. W. Armstrong, *J. Chromatogr.*, 1990, **509**, 303-324.
- 18 V. Schurig and H. P. Nowotny, *J. Chromatogr.*, 1988, **441**, 155-163.
- 19 H. P. Nowotny, D. Schmalzing, D. Wistuba and V. Schurig, *J. High Resolut. Chromatogr.*, 1989, **12**, 383-393.
- 20 A. Berthod, L. He and D. W. Armstrong, *Chromatographia*, 2001, **53**, 63-68.
- 21 K. Huang, X. Zhang and D. W. Armstrong, *J. Chromatogr. , A*, 2010, **1217**, 5261-5273.
- 22 P. Fischer, R. Aichholz, U. Bölz, M. Juza and S. Krimmer, *Angewandte Chemie International Edition in English*, 1990, **29**, 427-429 (DOI:10.1002/anie.199004271).
- 23 V. Schurig, D. Schmalzing, U. Muehleck, M. Jung, M. Schleimer, P. Mussche, C. Duvekot and J. C. Buyten, *J. High Resolut. Chromatogr.*, 1990, **13**, 713-717.
- 24 D. W. Armstrong, Y. Tang, T. Ward and M. Nichols, *Anal. Chem.*, 1993, **65**, 1114-1117.
- 25 V. Schurig, D. Schmalzing and M. Schleimer, *Angew. Chem.*, 1991, **103**, 994-6 (See also *Angew. Chem., Int. Ed. Engl.*, 1991, 30(8), 987-9).
- 26 W. H. Pirkle and C. J. Welch, *J. Chromatogr. , A*, 1996, **731**, 322-326.
- 27 A. Ruderisch, J. Pfeiffer and V. Schurig, *J. Chromatogr. , A*, 2003, **994**, 127-135.
- 28 P. A. Levkin, A. Ruderisch and V. Schurig, *Chirality*, 2005, **18**, 49-63.
- 29 P. A. Levkin, A. Levkina and V. Schurig, *Anal. Chem.*, 2006, **78**, 5143-5148.
- 30 P. A. Levkin, A. Levkina, H. Czesla, S. Nazzi and V. Schurig, *J. Sep. Sci.*, 2007, **30**, 98-103.
- 31 G. Uccello-Barretta, S. Nazzi, F. Balzano, P. A. Levkin, V. Schurig and P. Salvadori, *Eur. J. Org. Chem.*, 2007, , 3219-3226.
- 32 O. Stephany, F. Dron, S. Tisse, A. Martinez, J. Nuzillard, V. Peulon-Agasse, P. Cardinael and J. -. Bouillon, *J. Chromatogr. , A*, 2009, **1216**, 4051-4062.
- 33 P. A. Levkin and V. Schurig, *J. Chromatogr. , A*, 2008, **1184**, 309-322.
- 34 V. Schurig, *J. Chromatogr. , A*, 2001, **906**, 275-299.
- 35 M. L. Bender, M. Komiyama, in , ed. anonymous Springer Verlag, Berlin, 1978,.
- 36 Clifford R. Mitchell, Daniel W. Armstrong, in *in Chiral Separations: Methods and Protocols*, ed. ed. G. Gubitz, M. G. Schmid, 2004, pp.61-112.

- 37 C. Bicchi, G. Artuffo, A. D'Amato, G. M. Nano, A. Galli and M. Galli, *J. High Resolut. Chromatogr.*, 1991, **14**, 301-305.
- 38 D. W. Armstrong, W. Li, C. D. Chang and J. Pitha, *Anal. Chem.*, 1990, **62**, 914-923.
- 39 A. Berthod, W. Li and D. W. Armstrong, *Anal. Chem.*, 1992, **64**, 873-879.
- 40 D. W. Armstrong, F. Nome, L. A. Spino and T. D. Golden, *J. Am. Chem. Soc.*, 1986, **108**, 1418-1421.
- 41 D. W. Armstrong, W. Y. Li and J. Pitha, *Anal. Chem.*, 1990, **62**, 214-217.
- 42 W. A. König, *Journal of High Resolution Chromatography*, 1993, **16**, 569-586 (DOI:10.1002/jhrc.1240161003).
- 43 W. A. König, *Journal of High Resolution Chromatography*, 1993, **16**, 338-352 (DOI:10.1002/jhrc.1240160603).
- 44 A. Dietrich, B. Maas, V. Karl, P. Kreis, D. Lehmann, B. Weber and A. Mosandl, *J. High Resolut. Chromatogr.*, 1992, **15**, 176-179.
- 45 A. Dietrich, B. Maas, W. Messer, G. Bruche, V. Karl, A. Kaunzinger and A. Mosandl, *J. High Resolut. Chromatogr.*, 1992, **15**, 590-593.
- 46 G. Sicoli, F. Pertici, Z. Jiang, L. Jicsinszky and V. Schurig, *Chirality*, 2007, **19**, 391-400.
- 47 D. W. Armstrong, Y. Tang and J. Zukowski, *Anal. Chem.*, 1991, **63**, 2858-2861.
- 48 Ed. G. Eglinton, M. T. J. Murphy, in , ed. nonymous Springer Verlag, New York, 1969,.
- 49 D. W. Armstrong, E. Y. Zhou, J. Zukowski and B. Kosmowska-Ceranowicz, *Chirality*, 1996, **8**, 39-48.
- 50 O. Trapp and V. Schurig, *Enantiomer*, 2001, **6**, 193-194.
- 51 K. Huang and D. W. Armstrong, *Org. Geochem.*, 2009, **40**, 283-286.
- 52 G. Sicoli, D. Kreidler, H. Czesla, H. Hopf and V. Schurig, *Chirality*, 2008, **21**, 183-198.
- 53 M. Lindstrom, *J. High Resolut. Chromatogr.*, 1991, **14**, 765-767.
- 54 V. Schurig, M. Jung, S. Mayer, M. Fluck, S. Negura and H. Jakubetz, *J. Chromatogr. , A*, 1995, **694**, 119-128.
- 55 D. W. Armstrong, J. T. Lee and L. W. Chang, *Tetrahedron: Asymmetry*, 1998, **9**, 2043-2064.

- 56 D. W. Armstrong, L. He, T. Yu, J. T. Lee and Y. Liu, *Tetrahedron: Asymmetry*, 1999, **10**, 37-60.
- 57 K. Huang, Z. S. Breitbach and D. W. Armstrong, *Tetrahedron: Asymmetry*, 2006, **17**, 2821-2832.
- 58 M. Kawamura, T. Uchiyama, T. Kuramoto, Y. Tamura and K. Mizutani, *Carbohydr. Res.*, 1989, **192**, 83-90.
- 59 S. Immel, G. E. Schmitt and F. W. Lichtenthaler, *Carbohydr. Res.*, 1998, **313**, 91-105.
- 60 D. W. Armstrong, *J. Liq. Chromatogr.*, 1980, **3**, 895-900.
- 61 D. W. Armstrong and G. Y. Stine, *J. Am. Chem. Soc.*, 1983, **105**, 2962-2964.
- 62 W. Saenger, *Biochem Soc Trans*, 1983, **11**, 136-139.
- 63 D. W. Armstrong and W. DeMond, *J. Chromatogr. Sci.*, 1984, **22**, 411-415.
- 64 M. Shizuma, Y. Takai, M. Kawamura, T. Takeda and M. Sawada, *J. Chem. Soc. , Perkin Trans. 2*, 2001, , 1306-1314.
- 65 J. C. Reijenga, T. P. E. M. Verheggen and M. Chiari, *J. Chromatogr. , A*, 1999, **838**, 111-119.
- 66 Y. Takai, Y. Okumura, T. Tanaka, M. Sawada, S. Takahashi, M. Shiro, M. Kawamura and T. Uchiyama, *J. Org. Chem.*, 1994, **59**, 2967-2975.
- 67 M. Sawada, Y. Takai, M. Shizuma, Y. Takai, T. Takeda, H. Adachi and T. Uchiyama, *Chem. Commun. (Cambridge)*, 1998, 1453-1454.
- 68 M. Shizuma, H. Adachi, Y. Takai, M. Hayashi, J. Tanaka, T. Takeda and M. Sawada, *Carbohydr. Res.*, 2001, **335**, 275-281.
- 69 M. Shizuma, H. Adachi, M. Kawamura, Y. Takai, T. Takeda and M. Sawada, *J. Chem. Soc. , Perkin Trans. 2*, 2001, 592-601.
- 70 K. Huang, D. W. Armstrong, E. Forro, F. Fulop and A. Peter, *Chromatographia*, 2008, **69**, 331-337.
- 71 S. Abdalla, E. Bayer and H. Frank, *Chromatographia*, 1987, **23**, 83-85.
- 72 M. Sawada, T. Tanaka, Y. Takai, T. Hanafusa, K. Hirotsu, T. Higuchi, M. Kawamura and T. Uchiyama, *Chem. Lett.*, 1990, 2011-2014.

- 73 M. Sawada, T. Tanaka, Y. Takai, T. Hanafusa, T. Taniguchi, M. Kawamura and T. Uchiyama, *Carbohydr. Res.*, 1991, **217**, 7-17.
- 74 X. Zhou, H. Yan, Y. Chen, C. Wu and X. Lu, *J. Chromatogr. , A*, 1996, **753**, 269-277.
- 75 K. A. Bode and J. Applequist, *J. Phys. Chem.*, 1996, **100**, 17820-17824.
- 76 J. E. True, T. D. Thomas, R. W. Winter and G. L. Gard, *Inorg. Chem.*, 2003, **42**, 4437-4441.
- 77 M. N. Rudaya, V. I. Saloutin and K. I. Pashkevich, *Izv. Akad. Nauk SSSR, Ser. Khim.*, 1984, , 1807-1809.
- 78 A. L. McClellan, in , ed. nonymous Freeman, San Francisco, California, 1963,.
- 79 M. Li, J. Huang and T. Li, *J. Chromatogr. , A*, 2008, **1191**, 199-204.
- 80 V. Schurig, *J. Chromatogr. , A*, 2001, **906**, 275-299.
- 81 E. Gil-Av and B. Feibush, *Tetrahedron Lett.*, 1967, , 3345-3347.
- 82 R. Charles, U. Beitler, B. Feibush and E. Gil-Av, *J. Chromatogr.*, 1975, **112**, 121-133.
- 83 U. Beitler and B. Feibush, *J Chromatogr*, 1976, **123**, 149-166.
- 84 H. Frank, G. J. Nicholson and E. Bayer, *J Chromatogr Sci*, 1977, **15**, 174-176.
- 85 R. Charles and E. Gil-Av, *J. Chromatogr.*, 1980, **195**, 317-327.
- 86 S. C. Chang, R. Charles and E. Gil-Av, *J. Chromatogr.*, 1982, **238**, 29-39.
- 87 S. C. Chang, R. Charles and E. Gil-Av, *J. Chromatogr.*, 1982, **235**, 87-108.
- 88 V. Schurig, *Angew. Chem.*, 1984, **96**, 733-752.
- 89 V. Schurig, *Chromatographia*, 1980, **13**, 263-270.
- 90 V. Schurig, *Angew. Chem.*, 1977, **89**, 113-114.
- 91 V. Schurig, H. P. Nowotny, M. Schleimer and D. Schmalzing, *J. High Resolut. Chromatogr.*, 1989, **12**, 549-551.
- 92 Z. Jin and H. L. Jin, *Chromatographia*, 1994, **38**, 22-28.
- 93 I. Spanik, J. Krupcik, I. Skacani, P. Sandra and D. W. Armstrong, *J. Chromatogr. , A*, 2005, **1071**, 59-66.

- 94 J. Ding, T. Welton and D. W. Armstrong, *Anal. Chem.*, 2004, **76**, 6819-6822.
- 95 P. Sun, C. Wang, Z. S. Breitbach, Y. Zhang and D. W. Armstrong, *Anal. Chem. (Washington, DC, U. S.)*, 2009, **81**, 10215-10226.
- 96 P. Sun, C. Wang, N. L. T. Padivitage, Y. S. Nanayakkara, S. Perera, H. Qiu, Y. Zhang and D. W. Armstrong, *Analyst (Cambridge, U. K.)*, 2011, **136**, 787-800.
- 97 P. Sun and D. W. Armstrong, *J. Chromatogr. , A*, 2010, **1217**, 4904-4918.
- 98 K. Kalikova, L. Janeckova, D. W. Armstrong and E. Tesarova, *J. Chromatogr. , A*, 2011, **1218**, 1393-1398.
- 99 Y. Zhang, Z. S. Breitbach, C. Wang and D. W. Armstrong, *Analyst (Cambridge, U. K.)*, 2010, **135**, 1076-1083.
- 100 C. Jiang, M. Tong, Z. S. Breitbach and D. W. Armstrong, *Electrophoresis*, 2009, **30**, 3897-3909.
- 101 M. Sawada, T. Tanaka, Y. Takai, T. Hanafusa, T. Taniguchi, M. Kawamura and T. Uchiyama, *Carbohydr. Res.*, 1991, **217**, 7-17.
- 102 S. Immel, G. E. Schmitt and F. W. Lichtenthaler, *Carbohydr. Res.*, 1998, **313**, 91-105.
- 104 K. Kalikova, L. Janeckova, D. W. Armstrong and E. Tesarova, *J. Chromatogr. , A*, 2011, **1218**, 1393-1398.
- 105 D. W. Armstrong, J. R. Faulkner and S. M. Han, *J Chromatogr*, 1988, **452**, 323-330.
- 106 V. Pino, A. W. Lantz, J. L. Anderson, A. Berthod and D. W. Armstrong, *Anal. Chem.*, 2006, **78**, 113-119.
- 107 I. Spanik, J. Krupcik and V. Schurig, *J. Chromatogr. , A*, 1999, **843**, 123-128.
- 108 L. D. Garner-O'Neale, A. F. Bonamy, T. L. Meek and B. G. Patrick, *J. Mol. Struct. : THEOCHEM*, 2003, **639**, 151-156.
- 109 S. G. Bratsch, *J. Chem. Educ.*, 1985, **62**, 101-103.
- 110 A. Berthod, W. Li and D. W. Armstrong, *Anal. Chem.*, 1992, **64**, 873-879.
- 111 P. Walden, *Bull. Acad. Imp. Sci. St. -Petersbourg*, 1914, , 405-422.
- 112 J. S. Wilkes and M. J. Zaworotko, *J. Chem. Soc. , Chem. Commun.*, 1992, , 965-967.
- 113 X. Han and D. W. Armstrong, *Acc. Chem. Res.*, 2007, **40**, 1079-1086.

- 114 J. Plaquevent, Y. Genisson and F. Guillen, *Tech. Ing. , Constantes Phys. -Chim.*, 2008, **51**, K1230/1-K1230/17.
- 115 M. Opallo and A. Lesniewski, *J. Electroanal. Chem.*, 2011, **656**, 2-16.
- 116 J. L. Anderson, R. Ding, A. Ellern and D. W. Armstrong, *J. Am. Chem. Soc.*, 2005, **127**, 593-604.
- 117 T. Payagala, J. Huang, Z. S. Breitbach, P. S. Sharma and D. W. Armstrong, *Chem. Mater.*, 2007, **19**, 5848-5850.
- 118 K. Huang, X. Han, X. Zhang and D. W. Armstrong, *Anal. Bioanal. Chem.*, 2007, **389**, 2265-2275.
- 119 E. Wanigasekara, X. Zhang, Y. Nanayakkara, T. Payagala, H. Moon and D. W. Armstrong, *ACS Appl. Mater. Interfaces*, 2009, **1**, 2126-2133.
- 120 *Pat.*, WO; 2011068944, 0609; Patent Application Date: 20101202.; Priority Application Date: 20091204.
- 121 P. S. Sharma, T. Payagala, E. Wanigasekara, A. B. Wijeratne, J. Huang and D. W. Armstrong, *Chem. Mater.*, 2008, **20**, 4182-4184.
- 122 T. Payagala, Y. Zhang, E. Wanigasekara, K. Huang, Z. S. Breitbach, P. S. Sharma, L. M. Sidisky and D. W. Armstrong, *Anal. Chem. (Washington, DC, U. S.)*, 2009, **81**, 160-173.
- 123 D. W. Armstrong, L. He and Y. Liu, *Anal. Chem.*, 1999, **71**, 3873-3876.
- 124 J. L. Anderson, J. Ding, T. Welton and D. W. Armstrong, *J. Am. Chem. Soc.*, 2002, **124**, 14247-14254.
- 125 J. L. Anderson and D. W. Armstrong, *Anal. Chem.*, 2003, **75**, 4851-4858.
- 126 D. W. Armstrong, L. Zhang, L. He and M. L. Gross, *Anal. Chem.*, 2001, **73**, 3679-3686.
- 127 M. H. Abraham, *Chem. Soc. Rev.*, 1993, **22**, 73-83.
- 128 J. L. Anderson and D. W. Armstrong, *Anal. Chem.*, 2005, **77**, 6453-6462.
- 129 K. R. Seddon, *J. Chem. Technol. Biotechnol.*, 1997, **68**, 351-356.
- 130 M. J. Earle, P. B. McCormac and K. R. Seddon, *Green Chem.*, 1999, **1**, 23-25.
- 131 P. J. Dyson, D. J. Ellis, T. Welton and D. G. Parker, *Chem. Commun. (Cambridge)*, 1999, , 25-26.

- 132 T. Welton, *Chem. Rev. (Washington, D. C.)*, 1999, **99**, 2071-2083.
- 133 A. C. Cole, J. L. Jensen, I. Ntai, K. L. T. Tran, K. J. Weaver, D. C. Forbes and J. H. Davis Jr, *J. Am. Chem. Soc.*, 2002, **124**, 5962-5963.
- 134 R. A. Sheldon, R. M. Lau, M. J. Sorgedragar, F. van Rantwijk and K. R. Seddon, *Green Chem.*, 2002, **4**, 147-151.
- 135 J. Ding, V. Desikan, X. Han, T. L. Xiao, R. Ding, W. S. Jenks and D. W. Armstrong, *Org. Lett.*, 2005, **7**, 335-337.
- 136 S. T. Handy and M. Okello, *J. Org. Chem.*, 2005, **70**, 2874-2877.
- 137 A. R. Khosropour, M. M. Khodaei, M. Beygzadeh and M. Jokar, *Heterocycles*, 2005, **65**, 767-773.
- 138 X. Han and D. W. Armstrong, *Org. Lett.*, 2005, **7**, 4205-4208.
- 139 Y. Xia, H. Wu, Y. Zhang, Y. Fang, S. Sun and Y. Shi, *Huaxue Jinzhan*, 2006, **18**, 1660-1667.
- 140 V. Rumbau, R. Marcilla, E. Ochoteco, J. A. Pomposo and D. Mecerreyes, *Macromolecules*, 2006, **39**, 8547-8549.
- 141 P. U. Naik, S. J. Nara, J. R. Harjani and M. M. Salunkhe, *J. Mol. Catal. B: Enzym.*, 2007, **44**, 93-98.
- 142 M. Paljevac, M. Habulin and Z. Knez, *Chem. Ind. Chem. Eng. Q.*, 2006, **12**, 181-186.
- 143 E. V. Dickinson, M. E. Williams, S. M. Hendrickson, H. Masui and R. W. Murray, *J. Am. Chem. Soc.*, 1999, **121**, 613-616.
- 144 M. Ue and M. Takeda, *J. Korean Electrochem. Soc.*, 2002, **5**, 192-196.
- 145 C. Lagrost, D. Carrie, M. Vaultier and P. Hapiot, *J. Phys. Chem. A*, 2003, **107**, 745-752.
- 146 K. P. Doyle, C. M. Lang, K. Kim and P. A. Kohl, *J. Electrochem. Soc.*, 2006, **153**, A1353-A1357.
- 147 C. Y. Wang, V. Mottaghitalab, C. O. Too, G. M. Spinks and G. G. Wallace, *J. Power Sources*, 2007, **163**, 1105-1109.
- 148 A. Jimenez and M. Bermudez, *Tribol. Lett.*, 2007, **26**, 53-60.
- 149 Y. Xia, S. Sasaki, T. Murakami, M. Nakano, L. Shi and H. Wang, *Wear*, 2007, **262**, 765-771.

- 150 S. Chun, S. V. Dzyuba and R. A. Bartsch, *Anal. Chem.*, 2001, **73**, 3737-3741.
- 151 S. Carda-Broch, A. Berthod and D. W. Armstrong, *Anal. Bioanal. Chem.*, 2003, **375**, 191-199.
- 152 C. Li, B. Xin, W. Xu and Q. Zhang, *J. Chem. Technol. Biotechnol.*, 2007, **82**, 196-204.
- 153 R. Germani, M. V. Mancini, G. Savelli and N. Spreti, *Tetrahedron Lett.*, 2007, **48**, 1767-1769.
- 154 S. Carda-Broch, A. Berthod and D. W. Armstrong, *Rapid Commun. Mass Spectrom.*, 2003, **17**, 553-560.
- 155 A. Tholey and E. Heinzle, *Anal. Bioanal. Chem.*, 2006, **386**, 24-37.
- 156 T. N. Laremore, F. Zhang and R. J. Linhardt, *Anal. Chem.*, 2007, **79**, 1604-1610.
- 157 J. E. Gordon, J. E. Selwyn and R. L. Thorne, *J. Org. Chem.*, 1966, **31**, 1925-1930.
- 158 F. Pacholec, H. T. Butler and C. F. Poole, *Anal. Chem.*, 1982, **54**, 1938-1941.
- 159 F. Pacholec and C. F. Poole, *Chromatographia*, 1983, **17**, 370-374.
- 160 A. Heintz and S. P. Verevkin, *J. Chem. Eng. Data*, 2005, **50**, 1515-1519.
- 161 I. A. Sumartschenkowa, S. P. Verevkin, T. V. Vasil'tsova, E. Bich, A. Heintz, M. P. Shevelyova and G. J. Kabo, *J. Chem. Eng. Data*, 2006, **51**, 2138-2144.
- 162 J. L. Anderson, D. W. Armstrong and G. Wei, *Anal. Chem.*, 2006, **78**, 2893-2902.
- 163 A. Heintz, S. P. Verevkin and D. Ondo, *J. Chem. Eng. Data*, 2006, **51**, 434-437.
- 164 J. Pernak, A. Skrzypczak, G. Lota and E. Frackowiak, *Chem. --Eur. J.*, 2007, **13**, 3106-3112.
- 165 P. Bonhote, A. Dias, N. Papageorgiou, K. Kalyanasundaram and M. Graetzel, *Inorg. Chem.*, 1996, **35**, 1168-1178.
- 166 W. O. McReynolds, *J. Chromatogr. Sci.*, 1970, **8**, 685-691.
- 167 A. J. Carmichael and K. R. Seddon, *J. Phys. Org. Chem.*, 2000, **13**, 591-595.
- 168 M. J. Muldoon, C. M. Gordon and I. R. Dunkin, *J. Chem. Soc. , Perkin Trans. 2*, 2001, , 433-435.

- 169 S. N. V. K. Aki, J. F. Brennecke and A. Samanta, *Chem. Commun. (Cambridge, U. K.)*, 2001, , 413-414.
- 170 J. L. Reynolds, K. R. Erdner and P. B. Jones, *Org. Lett.*, 2002, **4**, 917-919.
- 171 L. Rohrschneider, *J. Chromatogr.*, 1966, **22**, 6-22.
- 172 M. H. Abraham, G. S. Whiting, R. M. Doherty and W. J. Shuely, *J. Chromatogr.*, 1990, **518**, 329-348.
- 173 M. H. Abraham, G. S. Whiting, J. Andonian-Haftvan, J. W. Steed and J. W. Grate, *J. Chromatogr.*, 1991, **588**, 361-364.
- 174 M. H. Abraham, G. S. Whiting, R. M. Doherty and W. J. Shuely, *J. Chromatogr.*, 1991, **587**, 213-228.
- 175 M. H. Abraham, C. F. Poole and S. K. Poole, *J. Chromatogr. , A*, 1999, **842**, 79-114.
- 176 W. Kiridena, W. W. Koziol and C. F. Poole, *J. Chromatogr. , A*, 2001, **932**, 171-177.
- 177 M. Vitha and P. W. Carr, *J. Chromatogr. , A*, 2006, **1126**, 143-194.
- 178 K. Grob Jr., G. Grob and K. Grob, *J. Chromatogr.*, 1978, **156**, 1-20.
- 179 K. Grob, G. Grob and K. Grob Jr, *J. Chromatogr.*, 1981, **219**, 13-20.
- 180 M. Celik, C. Tureli, M. Celik, Y. Yanar, U. Erdem and A. Kucukgulmez, *Food Chem.*, 2004, **88**, 271-273.
- 181 Z. S. Breitbach and D. W. Armstrong, *Anal. Bioanal. Chem.*, 2008, **390**, 1605-1617.
- 182 D. Brodnjak-Voncina, Z. C. Kodba and M. Novic, *Chemom. Intell. Lab. Syst.*, 2005, **75**, 31-43.
- 183 J. Harynuk, P. M. Wynne and P. J. Marriott, *Chromatographia*, 2006, **63**, S61-S66.
- 184 G. M. de Jong, J. R. Huizenga, B. G. Wolthers, H. G. Jansen, D. R. Uges, F. R. Hindriks and C. H. Gips, *Clin. Chim. Acta*, 1987, **166**, 187-194.
- 185 K. Fischer, *Angew. Chem.*, 1935, **48**, 394-396.
- 186 E. Scholz, *Anal. Chem.*, 1985, **57**, 2965-2971.
- 187 H. G. Streim, E. A. Boyce and J. R. Smith, *Anal. Chem.*, 1961, **33**, 85-89.
- 188 H. S. Knight and F. T. Weiss, *Anal. Chem.*, 1962, **34**, 749-751.

- 189 E. R. Quiram, *Anal. Chem.*, 1963, **35**, 593-595.
- 190 J. M. Hogan, R. A. Engel and H. F. Stevenson, *Anal. Chem.*, 1970, **42**, 249-252.
- 191 J. C. MacDonald and C. A. Brady, *Anal. Chem.*, 1975, **47**, 947-948.
- 192 T. E. Houston, *Met Finish*, 1997, **95**, 36-38.
- 193 J. Jalbert, R. Gilbert and P. Tetreault, *Anal. Chem.*, 1999, **71**, 3283-3291.
- 194 R. Nussbaum, D. Lischke, H. Paxmann and B. Wolf, *Chromatographia*, 2000, **51**, 119-121.
- 195 P. F. Vornheder and W. J. Brabbs, *Anal. Chem.*, 1970, **42**, 1454-1456.
- 196 M. Li and G. E. Pacey, *Talanta*, 1997, **44**, 1949-1958.
- 197 X. Zhou, P. A. Hines, K. C. White and M. W. Borer, *Anal. Chem.*, 1998, **70**, 390-394.
- 198 C. Pinheiro, J. C. Lima and A. J. Parola, *Sens. Actuators, B*, 2006, **B114**, 978-983.
- 199 H. Sun, B. Wang and S. G. DiMagno, *Org. Lett.*, 2008, **10**, 4413-4416.
- 200 E. Jamin, R. Guerin, M. Retif, M. Lees and G. J. Martin, *J. Agric. Food Chem.*, 2003, **51**, 5202-5206.
- 201 EMD Chemicals AQUASTAR Tech Notes
- 202 <http://www.jmscience.com/AQ-300-Karl-Fischer-Coulometric-Titrator.htm>
- 203 <http://www.jmscience.com/AQ-2200/AQ-2200.htm>
- 204 E. Scholz, *Karl Fisher Titration. Determination of water.*, Springer-Verlag, New York, 1984.
- 205 H. D. Isengard and U. Striffler, *Fresenius J. Anal. Chem.*, 1992, **342**, 287-291.
- 206 W. K. O'Keefe, F. T. T. Ng and G. L. Rempel, *J. Chromatogr. , A*, 2008, **1182**, 113-118.
- 207 H. S. Knight, *Anal. Chem.*, 1958, **30**, 2030-2032.
- 208 P. Sun and D. W. Armstrong, *Anal. Chim. Acta*, 2010, **661**, 1-16.
- 209 Center for Drug Evaluation and Research (CDER), US Food and Drug Administration (FDA), *Reviewer Guidance: Validation of Chromatographic Methods*, Center for Drug Evaluation and Research (CDER), US Food and Drug Administration (FDA), 1994.

- 210 Center for Drug Evaluation and Research (CDER), US Food and Drug Administration (FDA), *Guidance for Industry, Q2B Validation of Analytical Methods Protocol: Methodology*, Center for Drug Evaluation and Research (CDER), US Food and Drug Administration (FDA), USA, 1996.
- 211 N. V. Yanishlieva, E. Marinova and J. Pokorny, *Eur. J. Lipid Sci. Technol.*, 2006, **108**, 776-793.
- 212 J. R. Chipault, G. R. Mizuno, J. M. Hawkins and W. O. Lundberg, *Food Res.*, 1952, **17**, 46-55.
- 213 J. R. Chipault, G. R. Mizuno and W. O. Lundberg, *Food Res.*, 1955, **20**, 443-448.
- 214 J. R. Chipault, G. R. Mizuno and W. O. Lundberg, *Food Technol. (Chicago, IL, U. S.)*, 1956, **10**, 209-211.
- 215 E. Wenkert, A. Fuchs and J. D. McChesney, *J. Org. Chem.*, 1965, **30**, 2931-2934.
- 216 U. Bracco, J. Loliger and J. L. Viret, *JAOCS, J. Am. Oil Chem. Soc.*, 1981, **58**, 686-690.
- 217 A. Akgul, *Doga: Turk Tarim Ormancilik Derg.*, 1989, **13**, 11-25.
- 218 G. W. Plumb, S. J. Chambers, N. Lambert, B. Bartolome, R. K. Heaney, S. Wanigatunga, O. I. Aruoma, B. Halliwell and G. Williamson, *J. Food Lipids*, 1996, **3**, 171-188.
- 219 J. Pokorny, Z. Reblova, L. Trojakova, H. T. T. Nguyen, J. Korczak and W. Janitz, *Proc. World Conf. Oilseed Edible Oils Process.*, 1998, **2**, 265-269.
- 220 W. Ternes and E. Bigge, *Riv. Ital. EPPOS*, 1998, 252-259.
- 221 N. V. Yanishlieva and E. M. Marinova, *Recent Res. Dev. Oil Chem.*, 1998, **2**, 1-14.
- 222 C. Hall III, *Oily Press Lipid Libr.*, 2003, **13**, 73-112.
- 223 M. Rac and B. Ostric, *Rev. Fr. Corps Gras*, 1955, **2**, 796-803.
- 224 S. S. Chang, B. Ostric-Matijasevic, O. A. L. Hsieh and C. Huang, *J. Food Sci.*, 1977, **42**, 1102-1106.
- 225 K. Nozaki, *New Food Ind.*, 1989, **31**, 27-31.
- 226 H. Basaga, C. Tekkaya and F. Acikel, *Food Sci. Technol. (London)*, 1997, **30**, 105-108.
- 227 M. Lacroix, W. Smoragiewicz, L. Pazdernik, M. I. Kone and K. Krzystyniak, *Food Res. Int.*, 1998, **30**, 457-462.

- 228 Z. Zegarska, R. Rafalowski, R. Amarowicz, M. Karamac and F. Shahidi, *Z. Lebensm. - Unters. Forsch. A*, 1998, **206**, 99-102.
- 229 S. C. Etter, *J. Herbs, Spices Med. Plants*, 2004, **11**, 121-159.
- 230 H. Wang, F. Liu, L. Yang, Y. Zu, H. Wang, S. Qu and Y. Zhang, *Food Chem.*, 2011, **128**, 93-99.
- 231 I. Medina, M. J. Gonzalez, M. Pazos, D. Della Medaglia, R. Sacchi and J. M. Gallardo, *Eur. Food Res. Technol.*, 2003, **217**, 301-307.
- 232 V. C. Ramalho and N. Jorge, *Rev. Inst. Adolfo Lutz*, 2006, **65**, 15-20.
- 233 C. Hall III, S. Cuppett, D. Wheeler and X. Fu, *J. Am. Oil Chem. Soc.*, 1994, **71**, 533-535.
- 234 A. R. Hras, M. Hadolin, Z. Knez and D. Bauman, *Food Chem.*, 2000, **71**, 229-233.
- 235 L. Trojakova, Z. Reblova, H. T. T. Nguyen and J. Pokorny, *J. Food Lipids*, 2001, **8**, 1-13.
- 236 A. Palitzsch, H. Schulze, F. Metzler and H. Baas, *Fleischwirtschaft*, 1969, **49**, 1349-52, 1354.
- 237 H. Schulze, H. Baas, A. Palitzsch and G. Lotter, *Fleischwirtschaft*, 1971, **51**, 303-306.
- 238 A. Palitzsch, H. Schulze, G. Lotter and A. Steichele, *Fleischwirtschaft*, 1974, **54**, 63-68.
- 239 M. Huisman, H. L. Madsen, L. H. Skibsted and G. Bertelsen, *Z. Lebensm. -Unters. Forsch.*, 1994, **198**, 57-59.
- 240 U. Gerhardt and T. Boehm, *Fleischwirtschaft*, 1980, **60**, 1523-1526.
- 241 F. Shahidi, R. B. Pegg and Z. O. Saleemi, *J. Food Lipids*, 1995, **2**, 145-153.
- 242 M. Karpinska, J. Borowski and M. Danowska-Oziewicz, *Nahrung*, 2000, **44**, 38-41.
- 243 S. L. Richeimer, M. W. Bernart, G. A. King, M. C. Kent and D. T. Bailey, *J. Am. Oil Chem. Soc.*, 1996, **73**, 507-514.
- 244 S. Munne-Bosch, K. Schwarz and L. Alegre, *Free Radical Res.*, 1999, **31**, S107-S112.
- 245 A. Kirca and E. Arslan, *Int. J. Food Sci. Technol.*, 2008, **43**, 2038-2046.
- 246 J. Pokorny, *EJEAFChe, Electron. J. Environ. , Agric. Food Chem.*, 2008, **7**, 3320-3324.
- 247 C. H. Brieskorn and H. J. Doemling, *Z. Lebensm. -Unters. -Forsch.*, 1969, **141**, 10-16.
- 248 N. Nakatani and R. Inatani, *Agric. Biol. Chem.*, 1981, **45**, 2385-2386.

- 249 S. Samman, B. Sandstrom, M. B. Toft, K. Bukhave, M. Jensen, S. S. Sorensen and M. Hansen, *Am. J. Clin. Nutr.*, 2001, **73**, 607-612.
- 250 J. Del Campo and M. Amiot, *J. Food Prot.*, 2000, **63**, 1359-1368.
- 251 M. S. Bandara, K. K. Tanino and S. N. Acharya, *Adv. Med. Plant Res.*, 2007, , 173-194.
- 252 J. J. Johnson, *Cancer Lett. (N. Y. , NY, U. S.)*, 2011, **305**, 1-7.
- 253 O. I. Aruoma, J. P. E. Spencer, R. Rossi, R. Aeschbach, A. Khan, N. Mahmood, A. Munoz, A. Murcia, J. Butler and B. Halliwell, *Food Chem. Toxicol.*, 1996, **34**, 449-456.
- 254 O. Folin and V. Ciocalteu, *J. Biol. Chem.*, 1927, **73**, 627-650.
- 255 O. H. Lowry, N. J. Rosebrough, A. L. Farr and R. J. Randall, *J. Biol. Chem.*, 1951, **193**, 265-275.
- 256 M. Cuvelier, C. Berset and H. Richard, *Sci. Aliments*, 1994, **14**, 811-815.
- 257 N. Okamura, Y. Fujimoto, S. Kuwabara and A. Yagi, *J. Chromatogr. , A*, 1994, **679**, 381-386.
- 258 P. J. Hidalgo, J. L. Ubera, M. T. Tena and M. Valcarcel, *J. Agric. Food Chem.*, 1998, **46**, 2624-2627.
- 259 M. Herrero, M. Plaza, A. Cifuentes and E. Ibáñez, *Journal of Chromatography A*, 2010, **1217**, 2512-2520 (DOI:DOI: 10.1016/j.chroma.2009.11.032).
- 260 C. Bicchi, A. Binello and P. Rubiolo, *Phytochem. Anal.*, 2000, **11**, 236-242.
- 261 P. Ramirez, F. J. Senorans, E. Ibanez and G. Reglero, *J. Chromatogr. , A*, 2004, **1057**, 241-245.
- 262 P. Ramirez, M. R. Garcia-Risco, S. Santoyo, F. J. Senorans, E. Ibanez and G. Reglero, *J. Pharm. Biomed. Anal.*, 2006, **41**, 1606-1613.
- 263 P. Ramirez, T. Fornari, F. J. Senorans, E. Ibanez and G. Reglero, *J. Supercrit. Fluids*, 2005, **35**, 128-132.
- 264 P. Ramirez, S. Santoyo, M. R. Garcia-Risco, F. J. Senorans, E. Ibanez and G. Reglero, *J. Chromatogr. , A*, 2007, **1143**, 234-242.
- 265 R. Saenz-Lopez, P. Fernandez-Zurbano and M. T. Tena, *J Chromatogr A*, 2002, **953**, 251-256.
- 266 M. Bonoli, M. Pelillo and G. Lercker, *Chromatographia*, 2003, **57**, 505-512.

- 267 M. Bonoli, T. Gallina Toschi and G. Lercker, *Prog. Nutr.*, 2005, **7**, 31-35.
- 268 A. L. Crego, E. Ibanez, E. Garcia, R. Rodriguez de Pablos, F. J. Senorans, G. Reglero and A. Cifuentes, *Eur. Food Res. Technol.*, 2004, **219**, 549-555.
- 269 D. W. Armstrong, J. R. Faulkner Jr. and S. M. Han, *J. Chromatogr.*, 1988, **452**, 323-330.
- 270 A. M. Stalcup, S. C. Chang, D. W. Armstrong and J. Pitha, *J. Chromatogr.*, 1990, **513**, 181-194.
- 271 E. H. A. Doolaee, K. Raes, K. Smet, M. Andjelkovic, C. Van Poucke, S. De Smet and R. Verhe, *J. Agric. Food Chem.*, 2007, **55**, 7283-7287.
- 272 S. A. Coronado, G. R. Trout, F. R. Dunshea and N. P. Shah, *Meat Sci.*, 2002, **62**, 217-224.
- 273 E. N. Frankel, S. Huang, E. Prior and R. Aeschbach, *J. Sci. Food Agric.*, 1996, **72**, 201-208.
- 274 K. Schwarz and W. Ternes, *Z. Lebensm. -Unters. Forsch.*, 1992, **195**, 99-103.
- 275 K. Schwarz, W. Ternes and E. Schmauderer, *Z. Lebensm. -Unters. Forsch.*, 1992, **195**, 104-107.
- 276 S. Irmak, K. Solakyildirim, A. Hesenov and O. Erbatur, *J. Anal. Chem.*, 2010, **65**, 899-906.
- 277 M. Jose del Bano, O. Benavente-Garcia, P. M. Marin, A. M. Marin and J. Castillo, *Nutrafoods*, 2006, **5**, 41-48.
- 278 M. B. Hossain, D. K. Rai, N. P. Brunton, A. B. Martin-Diana and C. Barry-Ryan, *J. Agric. Food Chem.*, 2010, **58**, 10576-10581.
- 279 L. Almela, B. Sanchez-Munoz, J. A. Fernandez-Lopez, M. J. Roca and V. Rabe, *J. Chromatogr. , A*, 2006, **1120**, 221-229.
- 280 S. L. Richhelmer, D. T. Beiley, M. W. Bernart, M. Kent, J. V. Vininski and L. D. Anderson, *Recent Res. Dev. Oil Chem.*, 1999, **3**, 45-58.
- 281 E. Pretsch, P. Buhlmann and C. Affolter, *Structure Determination of Organic Compounds: Tables of Spectral Data*, Springer-Verlag, Berlin, 2000.
- 282 T. Masuda, Y. Inaba and Y. Takeda, *J. Agric. Food Chem.*, 2001, **49**, 5560-5565.
- 283 S. Nagakura and A. Kuboyama, *J. Am. Chem. Soc.*, 1954, **76**, 1003-1005.
- 284 A. G. González, L. S. Andrés, Z. E. Aguiar and J. G. Luis, *Phytochemistry*, 1992, **31**, 1297-1305 (DOI:10.1016/0031-9422(92)80282-J).

285 T. Masuda, Y. Inaba, T. Maekawa, Y. Takeda, H. Tamura and H. Yamaguchi, *J. Agric. Food Chem.*, 2002, **50**, 5863-5869.

286 C. M. Houlihan, C. T. Ho and S. S. Chang, *JAOCs, J. Am. Oil Chem. Soc.*, 1985, **62**, 96-98.

BIOGRAPHICAL INFORMATION

Ying Zhang obtained her Bachelor of Science from Chongqing University in 2003 and her Master of Science from Chongqing University in 2006. She joined Dr. Armstrong's group and received her Doctor of Philosophy from University of Texas at Arlington in November 2011. Her research is focused on development of chiral GC and HPLC stationary phases and ionic liquid GC stationary phases, as well as separations of small chiral/achiral molecules on HPLC, GC and GC/MS.